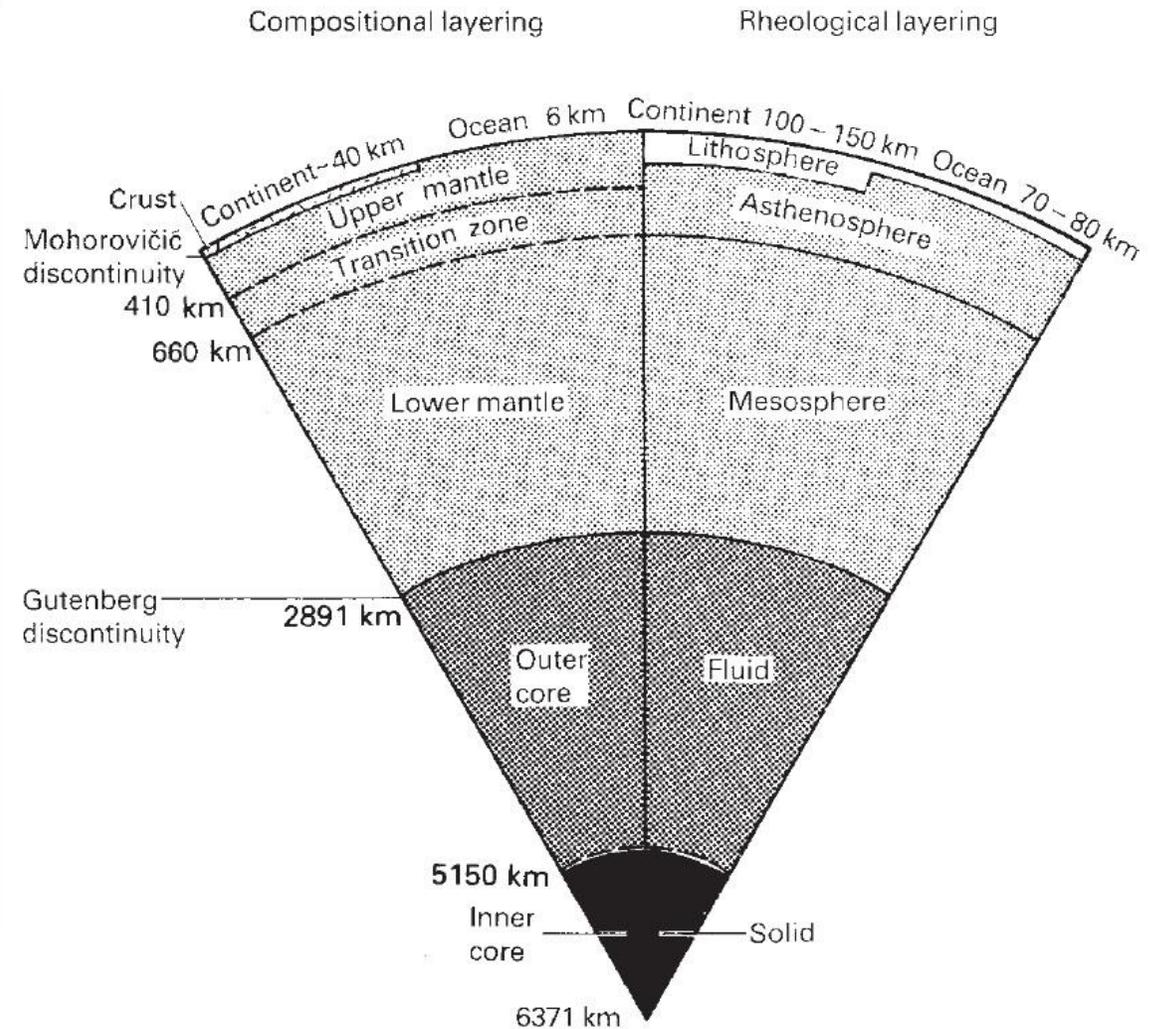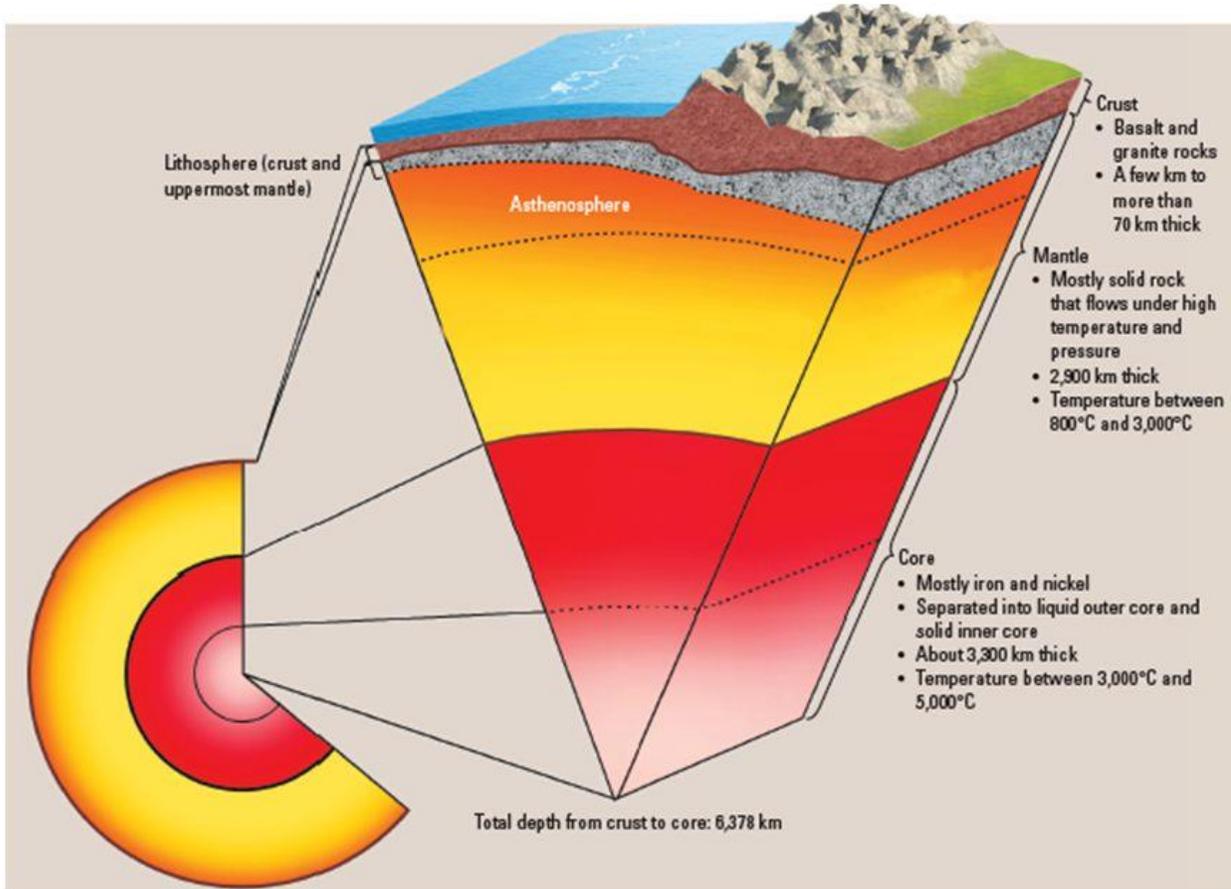# Course of Geodynamics

Prof. Magdala Tesauro

Course Outline:

1. **Thermo-physical structure of the continental and oceanic crust**
2. Thermo-physical structure of the continental lithosphere
3. Thermo-physical structure of the oceanic lithosphere and oceanic ridges
4. Rheology and mechanics of the lithosphere
5. Plate tectonics and boundary forces
6. Hot spots, plumes, and convection
7. Subduction zones systems
8. Orogens formation and evolution
9. Sedimentary basins formation and evolution

Earth's Structure

What is the internal structure of the earth?

Lithosphere (crust and uppermost mantle)

Asthenosphere

Crust
- Basalt and granite rocks
- A few km to more than 70 km thick

Mantle
- Mostly solid rock that flows under high temperature and pressure
- 2,900 km thick
- Temperature between 800°C and 3,000°C

Core
- Mostly iron and nickel
- Separated into liquid outer core and solid inner core
- About 3,300 km thick
- Temperature between 3,000°C and 5,000°C

Total depth from crust to core: 6,378 km

Compositional layering

Rheological layering

Ocean 6 km Continent 100 – 150 km Ocean 70 – 80 km

Continent ~40 km

Crust

Mohorovičić discontinuity
410 km
660 km

Upper mantle

Transition zone

Lithosphere

Asthenosphere

Lower mantle

Mesosphere

Gutenberg discontinuity

2891 km

Outer core

Fluid

5150 km

Inner core

Solid

6371 km

Mantle Structure

o At least 90% of the **mantle** by mass can be represented in terms of the oxides FeO, MgO, and SiO_2, and a further 5–10% is made up of CaO, Al_2O_3, and Na_2O. These oxides form minerals, such as olivine (~50 % or more), piroxenes (~30%), and garnet (15% or less).

o The two major velocity discontinuities at 410 km and 660 km, marking the top and bottom of the **mantle transition zone**, are due to phase of the olivine into spinel and perovskite, respectively.

o The other components of mantle peridotite, pyroxene, and garnet, also undergo phase changes in this depth range but they are gradual and do not produce discontinuities in the variation of seismic velocity with depth.

o The low velocity zone (**asthenosphere**) is characterized by low seismic velocities, high seismic attenuation, and a high electrical conductivity, likely due to the presence of molten material (~ 1% or less).

Phase transformations of olivine that are thought to define the upper mantle transition zone (after Helffrich & Wood, 2001).

Depth	Pressure	
410 km	13–14 GPa	$(Mg,Fe)_2SiO_4 = (Mg,Fe)_2SiO_4$ Olivine Wadsleyite (β-spinel structure)
520 km	18 GPa	$(Mg,Fe)_2SiO_4 = (Mg,Fe)_2SiO_4$ Wadsleyite Ringwoodite (γ-spinel structure)
660 km	23 GPa	$(Mg,Fe)_2SiO_4 = (Mg,Fe)SiO_3 + (Mg,Fe)O$ Ringwoodite Perovskite Magnesiowüstite

Mantle and Core Structure

o The **lower mantle** represents almost 50% of the mass of the entire Earth. It is assumed relatively homogeneous in its mineralogy, having mostly a perovskite structure, but the penetration of subducted oceanic lithosphere through the 660 km discontinuity may make it compositionally heterogeneous.

o The lowest 200–300 km of the mantle, Layer D" is characterized by a change in seismic velocity, it is very heterogeneous , suggesting that the liquid iron of the core reacts with mantle silicates in Layer D", with the production of metallic alloys and nonmetallic silicates from perovskite.

o The **outer core**, at a depth of 2891–5150 km, does not transmit S waves and thus must be fluid. The convective motions responsible for the geomagnetic field involve velocities of $\sim 10^4$ m yr^{-1}, five orders of magnitude larger than convection in the mantle.

o The **inner core** is solid, indeed both S and P-waves propagate within it and the amplitude of a phase reflected off the inner core also suggests that it must have a finite rigidity.

o This iron–nickel mixture provides a composition for the outer core, while the inner core has a seismic velocity and density consistent with a composition of pure iron.

o Other light elements present in the outer core, which include silicon, sulfur, oxygen, and potassium.

Physical properties of the crust and mantle lithosphere
Why do we want to study them?

Schematic cross-section of plate tectonics
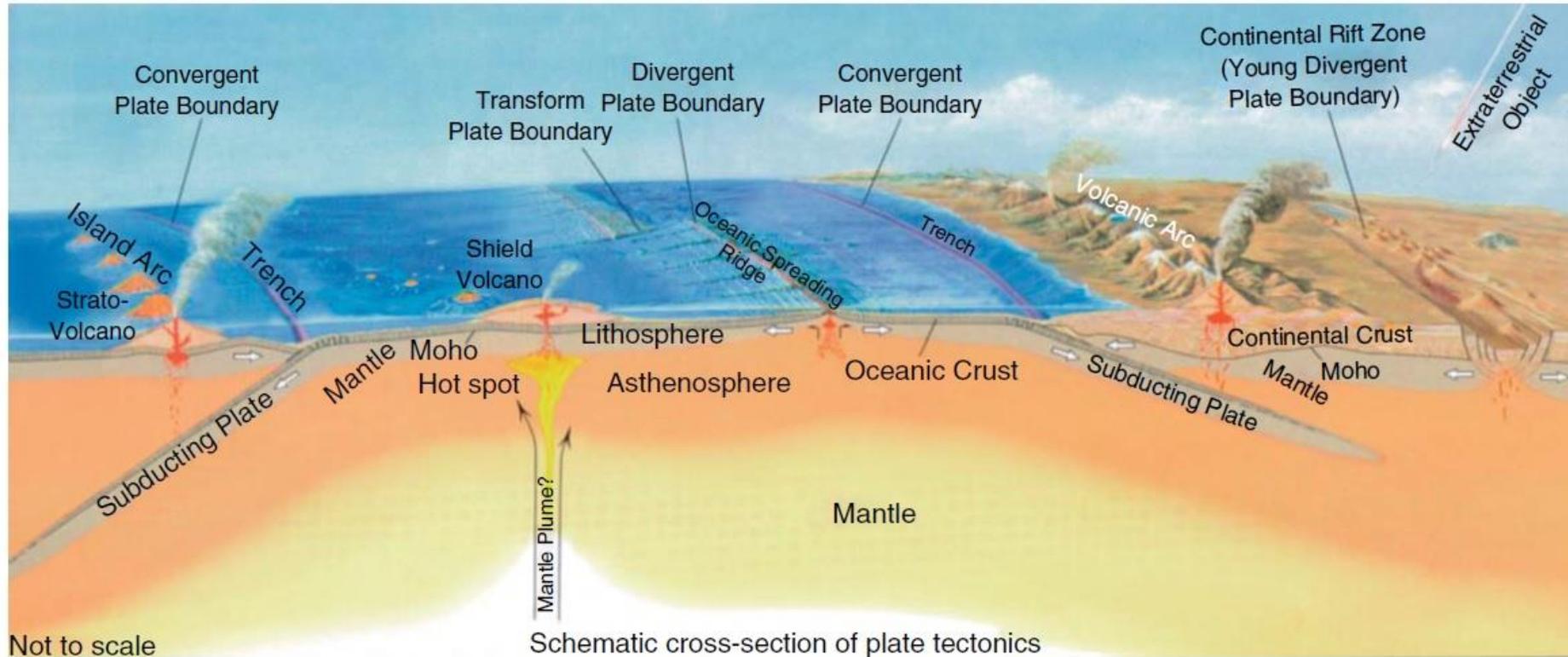
- Modulate the rate at which heat is released to the Earth's surface
- Regulate mantle convection
- Determine the location of earthquakes and volcanoes
- Define the rules for plate tectonic processes

Seismological techniques to explore the crust

## Active-source data (utilize man-made sources):

- <u>Seismic refraction</u>: reliable information about the distribution of seismic velocities within the crust and Moho depth.

- <u>Seismic reflection</u>: detailed structural image of the crust (resolution=50 m), allows correlation of the reflectivity patterns (due to composition, metamorphic layering, fault zones and lenses of partial melt) with distinct geologic settings, but weak constraints on deep crustal velocities.

Passive-source data (derived from naturally occurring seismicity):

- <u>Seismic tomography:</u> Local and distant (teleseismic) earthquake data can be used to determine crustal and mantle structure, by examining the arrival times of many criss-crossing paths between the earthquakes and seismometers.

- <u>Surface waves</u>: They are generated by the earthquakes. Vertical resolution of the obtained V_S models is generally lower if compared to a V_P tomography. However, the coverage is higher and more homogeneous.

<u>Receiver functions (RF)</u>: It is based on the analysis of converted P and S phases at seismic discontinuities beneath seismic stations.
- The amplitudes of the arrivals in RF depend on the incidence angle of the impinging wave and on the velocity contrast across the seismic converter.
- The RF method does not determine absolute velocity, but it is particularly suitable for detecting sharp layer boundaries, such as Moho depth, corresponding to a positive polarity of the converted phase (P-wave receiver functions) and lithosphere-asthenosphere boundary, corresponding to a negative polarity of the converted phase (S-wave receiver functions).
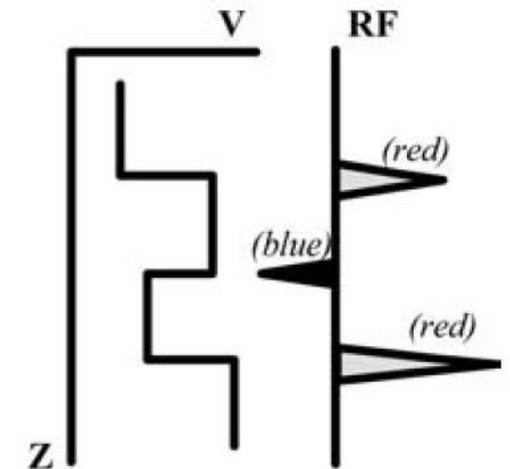
Other geophysical techniques to explore the crust

- <u>Gravity anomalies</u>: reveal rock density variations, with the amplitude of the anomaly proportional to the density contrast and thickness of the anomalous body. Short-wavelength (<250 km) gravity anomalies are usually correlated with crustal structures, while long wavelength (<1000km) gravity anomalies are correlated with lateral variations of mantle densities.

- <u>Aeromagnetics</u>: rocks commonly retain magnetism that originates from the time of their formation. The remnant magnetization of a mineral is fixed in the direction of the Earth's magnetic field when the mineral is cooled below the Curie temperature (about 580 °C) and removed when heated above this temperature. An example is given by a series of magnetic stripes, originating from the mid-ocean ridge.

- <u>Geoelectrical measurements</u>: At intermediate depths, conductivity depends on water content and composition (particularly graphite and sulfide content). At great depths, where temperatures rise to at least 500 °C, conductivity is mainly a function of electron and ion mobility. The magneto-telluric method relies on measurements of five separate components of the time-varying electromagnetic field at the surface of the Earth.

- <u>Heat flow data</u>: The highest heat flow values are found at mid-ocean ridges and within geothermal zones and active volcanoes. Heat flow data reflect radiogenic heat production in the crust and heat transferred from the convecting mantle.

- <u>Borehole data</u>: provide direct sampling of the composition of the upper crust, as well as measurements of *in situ* seismic velocities, density, temperature, state of stress, rock porosity, and the fluid pressure to depths of 3-5 km.

How old is the Earth?
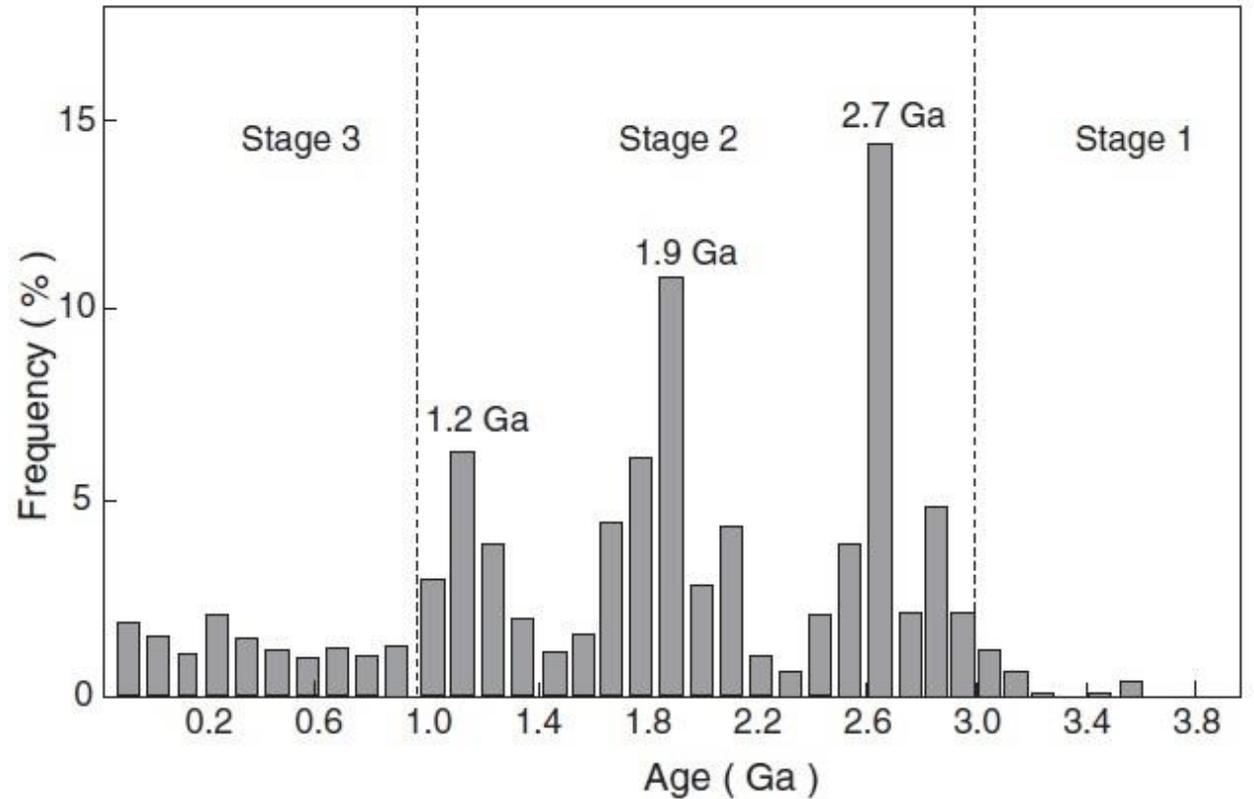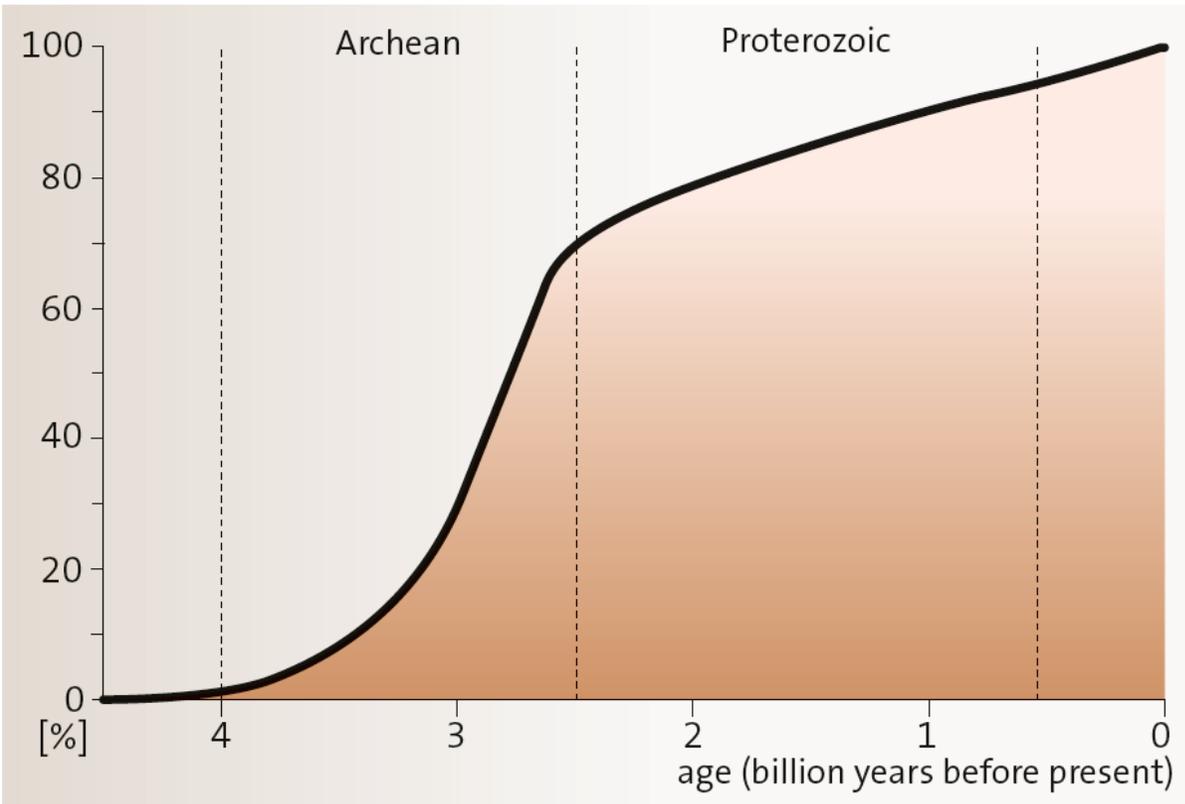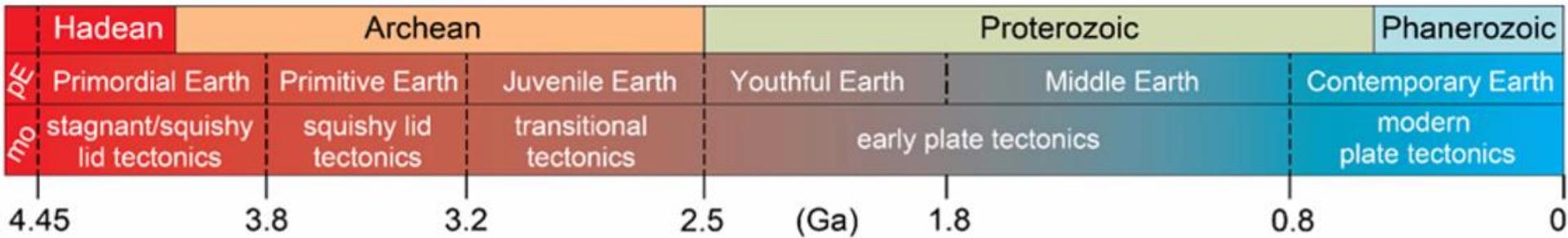
Secular Evolution of Earth

ao, accretionary orogen; co, collisional orogen; GOE, great oxidation event; LLSVP, large low-shear velocity provinces; NOE, Neoproterozoic oxidation event; pE, Proto-Earth; mo, magma ocean.

Cawood et al., 2022, Rev. Geophys, 60

Crustal Growth

- Enormous crustal growth occurred in the second half of the Archean era (before only small, unstable continents), between 3.2 and 2.5 Gyr. This is due to the considerably more efficient production of rocks constituting continental crust above subduction zones since ca. 3.2 Gyr.

- Measurements of Nb/Th and Nb/U ratios could define the net production rate of continental crust since 3.8 Gyr (the different ratios potentially provide information on the extent of the chemical depletion and the amount of continental crust that was present on Earth at different times).

- These results and on those of isotopic age determinations suggest that crust production was episodic with rapid net growth at 2.7, 1.9, and 1.2 Gyr (with pulses of ≤ 100 Myr) and slower growth afterwards.

- Previous studies suggested that: 39% of the continental crust formed in the Archean, 31% in the Early Proterozoic, 12% in the Middle–Late Proterozoic, and 18% in the Phanerozoic.

Secular Evolution of Continental Crust

Hadean	Archean			Proterozoic		Phanerozoic
Primordial Earth	Primitive Earth	Juvenile Earth	Youthful Earth	Middle Earth		Contemporary Earth
stagnant/squishy lid tectonics	squishy lid tectonics	transitional tectonics	early plate tectonics			modern plate tectonics

4.45   3.8   3.2   2.5   (Ga)   1.8   0.8   0

- \> 4.45 Ga – Proto-Earth – magma ocean & Earth-Moon forming impact
- 4.45-3.8 Ga – Primordial Earth – mainly mineral archive – crustal reworking, limited juvenile crust
- 3.8-3.2 Ga – Primitive Earth – juvenile crustal addition – craton formation
- 3.2-2.5 Ga – Juvenile Earth – craton stabilization, potassic felsic magmatism
- < 2.5 Ga – Youthful to Contemporary Earth – rigid lithosphere, focused zones of deformation

- Link to tectonic mode
- Multi-modal & transitional switches in mode
- Stagnant to active lid
- Early active lid – broad deformation & non-rigid lithosphere

Cawood et al., 2022, Rev. Geophys, 60

Crustal Evolution
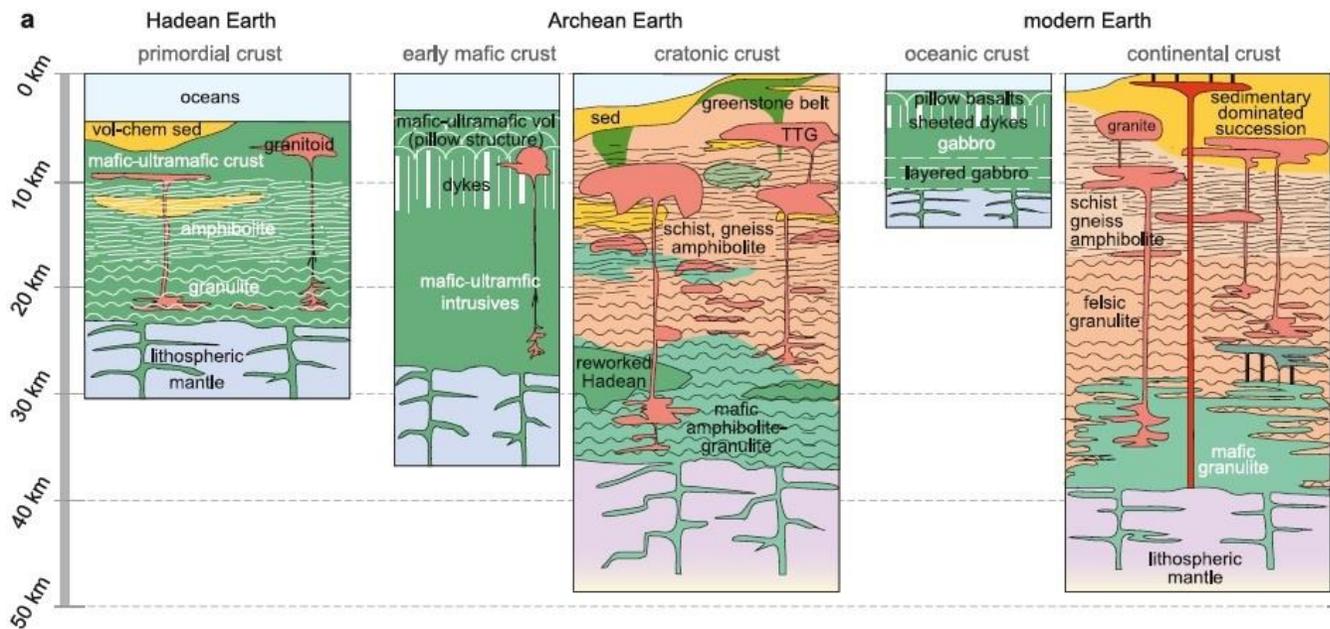
Cawood et al., 2022, Rev. Geophys, 60
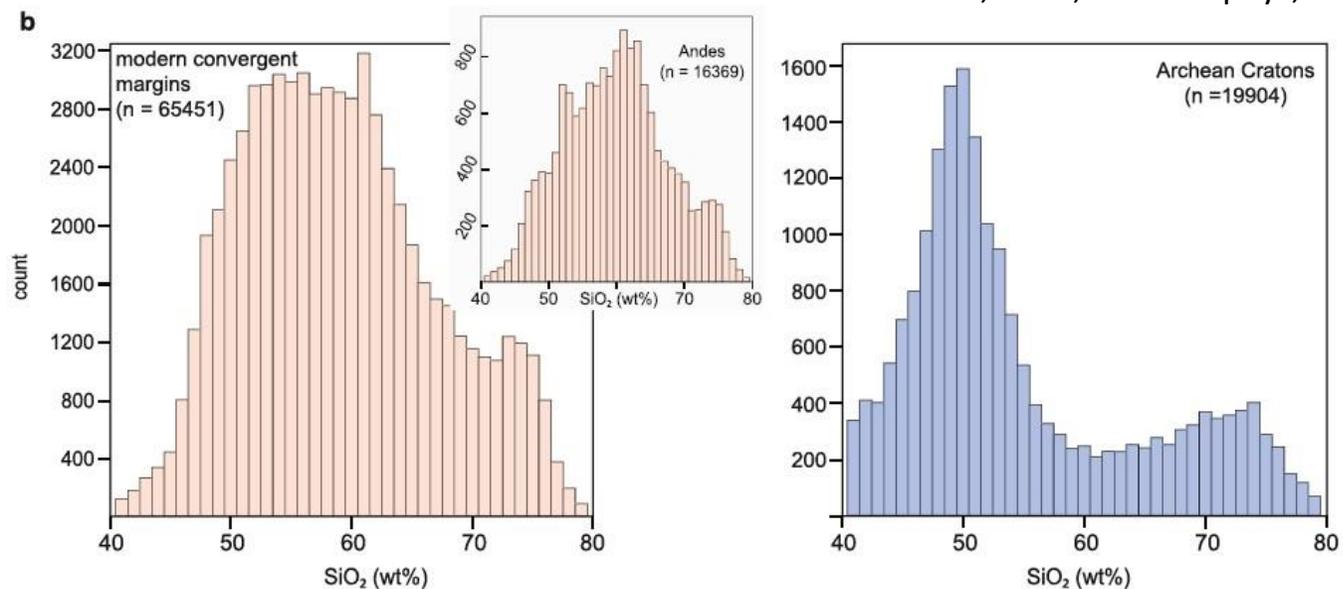
Composition of the continental crust

Comparison of the upper, middle, lower and total continental crust compositions

Element	Upper crust	Middle crust	Lower crust	Total crust
SiO_2	66.6	63.5	53.4	60.6
TiO_2	0.64	0.69	0.82	0.72
Al_2O_3	15.4	15.0	16.9	15.9
FeO_T	5.04	6.02	8.57	6.71
MnO	0.10	0.10	0.10	0.10
MgO	2.48	3.59	7.24	4.66
CaO	3.59	5.25	9.59	6.41
Na_2O	3.27	3.39	2.65	3.07
K_2O	2.80	2.30	0.61	1.81
P_2O_5	0.15	0.15	0.10	0.13
Total	100.05	100.00	100.00	100.12
Mg#	46.7	51.5	60.1	55.3

FeO_T = Total Fe as FeO
Mg#=(Mg/Mg+Fe)x100

Rudnick and Gao, 2003, Treatise on Geochemistry, Vol. 3

Crustal Types

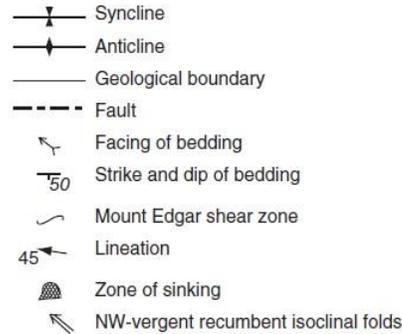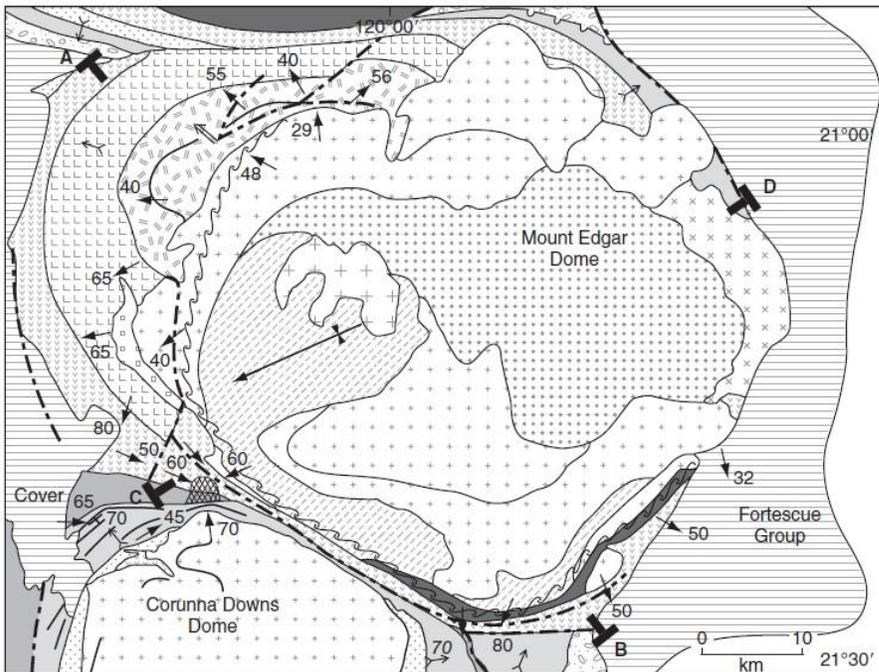**A progressive change in the bulk composition of the crust through time has been observed:**

- During the Early Archean, basaltic rocks were most abundant, later, the partial melting of these rocks produced large volumes of tonalites-granitoids suite (granite-greenstone belts).
- By 3.2 Gyr granites first appeared in the geologic record and were produced in large quantities after 2.6 Gyr.
- This compositional trend from basalt to tonalite to granite is attributed to an increase in the importance of subduction and crustal recycling during the transition from Late Archean to Early Proterozoic times.
- The appearance and preservation of thick sequences of sedimentary rock (e.g., evaporites and red beds deposits) has been interpreted to reflect the stabilization of Precambrian continental crust during Proterozoic times.
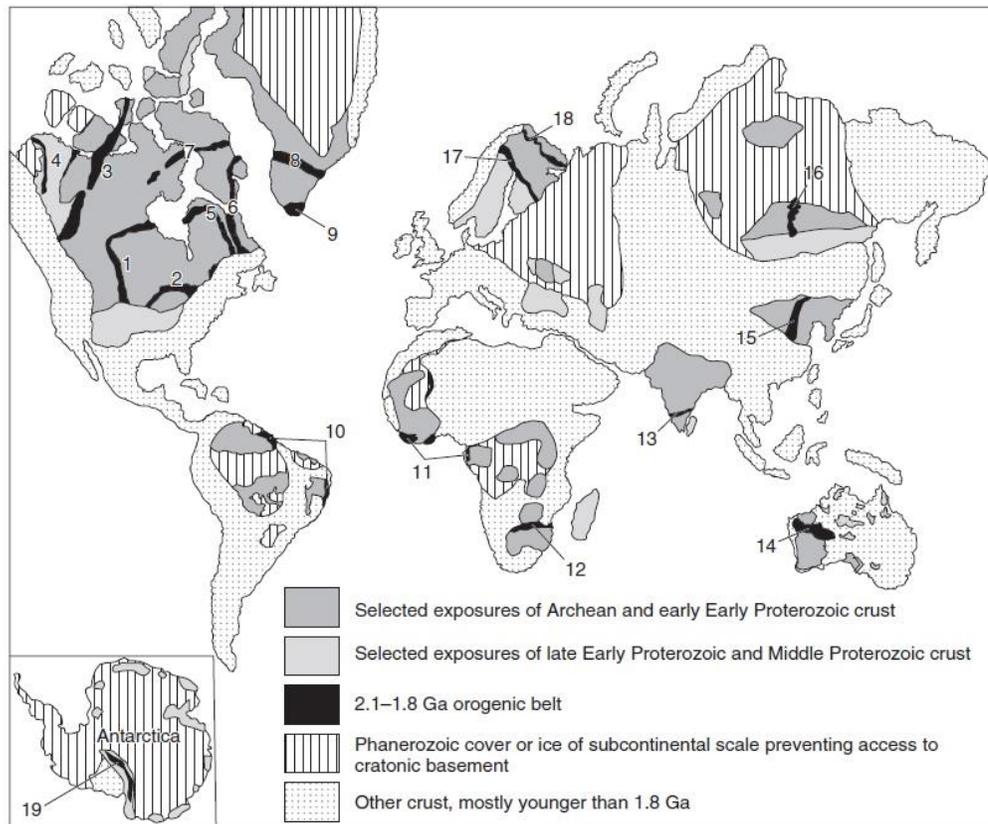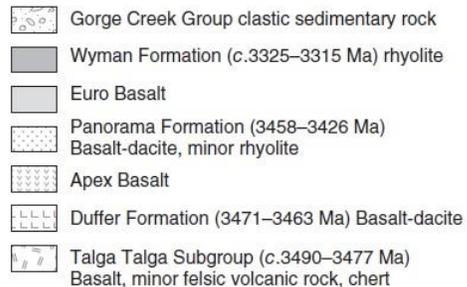

Orogens labeled as follows: 1, Trans-Hudson; 2, Penokean; 3, Taltson-Thelon; 4, Wopmay; 5, Cape Smith–New Quebec; 6, Torngat; 7, Foxe; 8, Nagssugtoqidian; 9, Makkovikian–Ketilidian; 10, Transamazonian; 11, Eburnian; 12, Limpopo; 13, Moyar; 14, Capricorn; 15, Trans-North China; 16, Central Aldan; 17, Svecofennian; 18, Kola-Karelian; 19, Transantarctic.

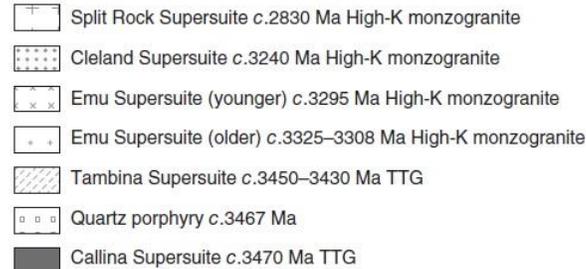# Precambrian Crust: Granite-greenstone belts

Eastern Pilbara Craton (Western Australia)

Legend (map symbols):
- ⊥ Syncline
- ⊕ Anticline
- — Geological boundary
- - - - Fault
- Facing of bedding
- 50 Strike and dip of bedding
- Mount Edgar shear zone
- 45 Lineation
- Zone of sinking
- NW-vergent recumbent isoclinal folds

Greenstones
- Gorge Creek Group clastic sedimentary rock
- Wyman Formation (c.3325–3315 Ma) rhyolite
- Euro Basalt
- Panorama Formation (3458–3426 Ma) Basalt-dacite, minor rhyolite
- Apex Basalt
- Duffer Formation (3471–3463 Ma) Basalt-dacite
- Talga Talga Subgroup (c.3490–3477 Ma) Basalt, minor felsic volcanic rock, chert

Granitic rocks
- Split Rock Supersuite c.2830 Ma High-K monzogranite
- Cleland Supersuite c.3240 Ma High-K monzogranite
- Emu Supersuite (younger) c.3295 Ma High-K monzogranite
- Emu Supersuite (older) c.3325–3308 Ma High-K monzogranite
- Tambina Supersuite c.3450–3430 Ma TTG
- Quartz porphyry c.3467 Ma
- Callina Supersuite c.3470 Ma TTG

- The greenstones consist of metavolcanic and metasedimentary rocks that exhibit a low pressure (200–500 MPa), low temperature (350–500°C) regional metamorphism of the greenschist facies (tholeiitic and komatiitic lavas, felsic volcanic rocks, clastic sediments, gneisses, and amphibolite/granulite rocks).

- The granitoids that intrude the greenstones and high-grade gneisses form a compositionally distinctive group known as *tonalite-trondhjemite-granodiorite*, or *TTG*, suites.

- The greenstones often consist of domes contains remnants of 3.50–3.43 Gyr TTG suite granitoids that are intruded by younger (3.33–2.83 Gyr) more potassic igneous suites (e.g., Eastern Pilbara Craton).

- The domes display compositional zonations and variable degrees of deformation, with the youngest bodies located in the cores of the domes and older, more deformed granitoids at the margins (reflecting the emplacement of many magmatic intrusions).

- The formation of the greenstones of Eastern Pilbara Craton were affected by one or more periods of horizontal contraction (Early Archean collision and terrane accretion) and extension, leading to the emplacement of the granitoid domes.

Archean Crustal evolution

(a) Oceanic crust was too thick to be subducted as a unit, and so its lowermost parts (piroxenites) delaminated and melted, favoring the formation of basaltic melts.

(b) As the oceanic crust cooled and became thinner (in the Late Archean) the entire crust could subduct, amphibolite was introduced into subduction zones and led to the widespread formation of the TTG suites.
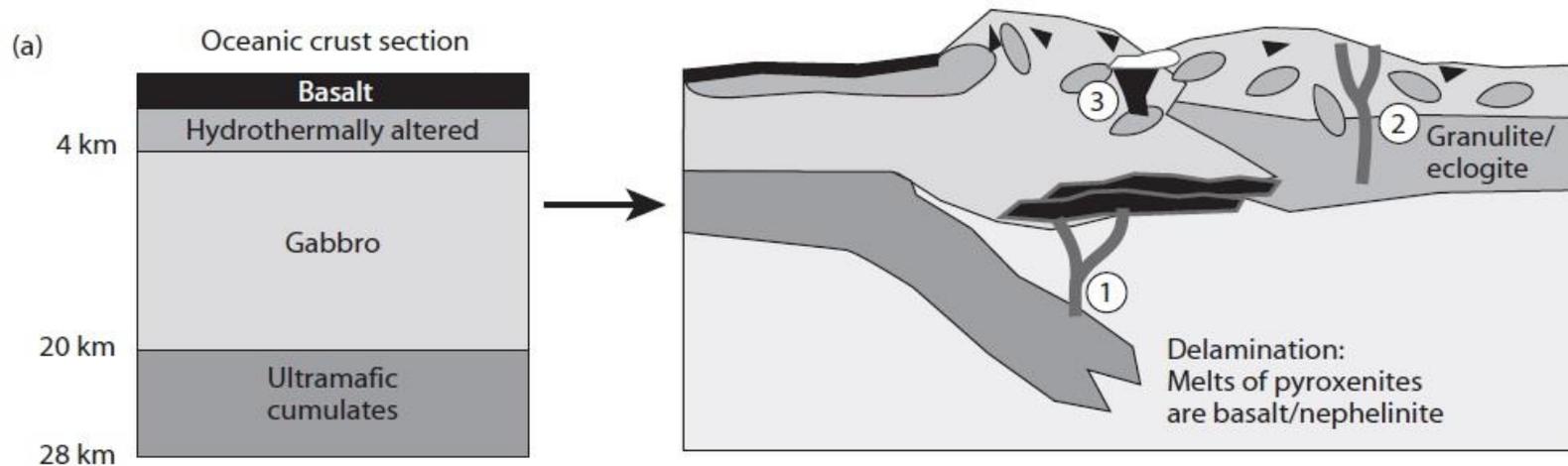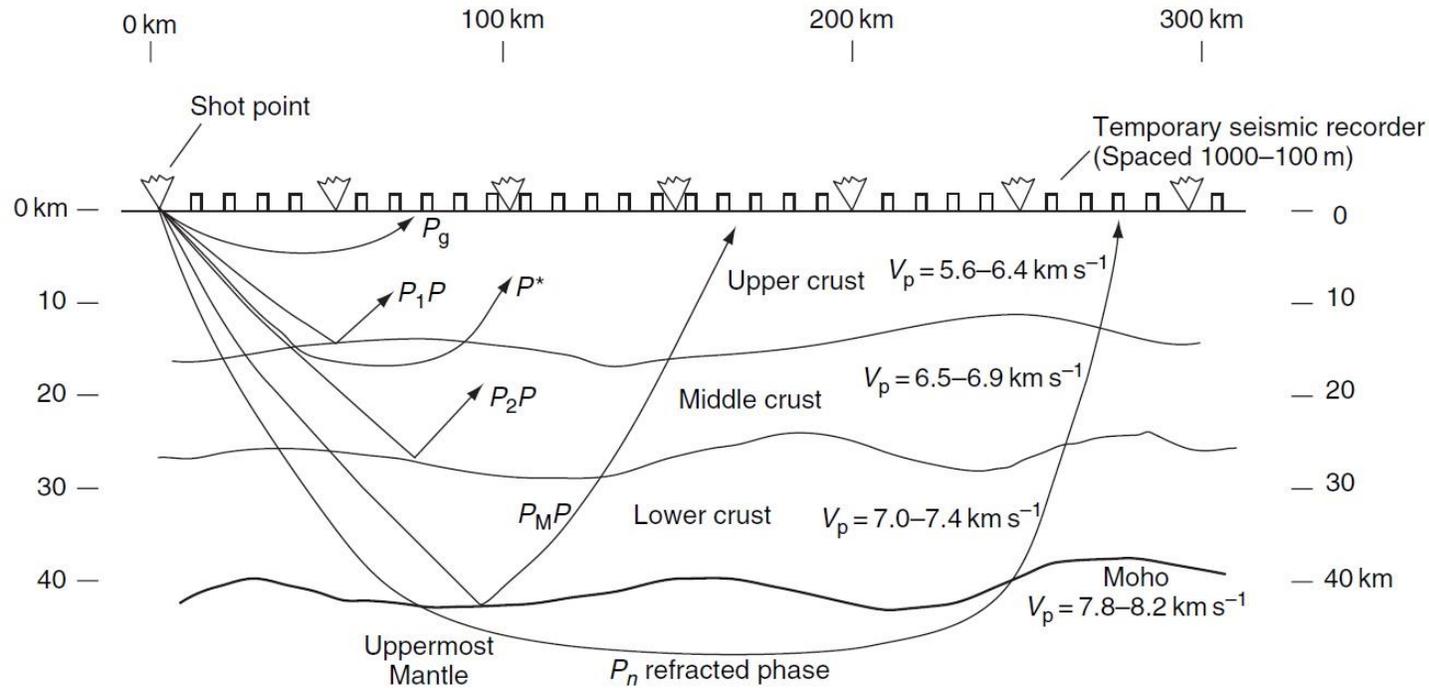

(1). Local melting of lower crust (2) and garnet amphibolite (3) may also occur to produce small volumes of felsic magma.
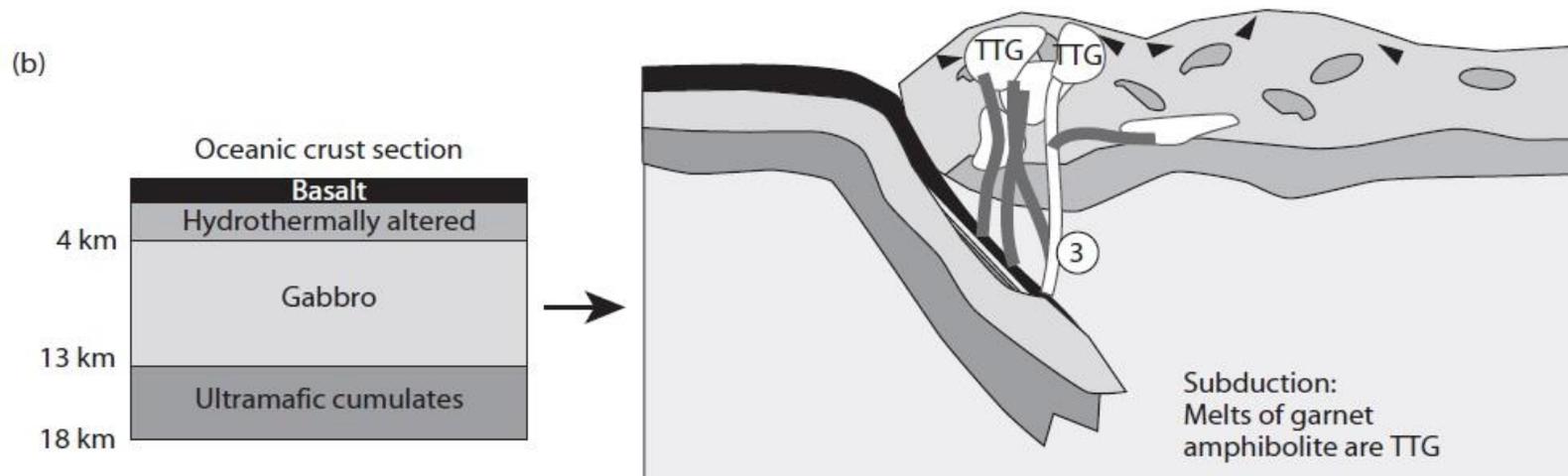
Crustal seismic velocities

- Mineralogical composition
- Confining pressure (from depth of burial)
- Temperature (from heat flow data)
- Anisotropy
- Pore fluid pressure

Velocity *vs* Depth

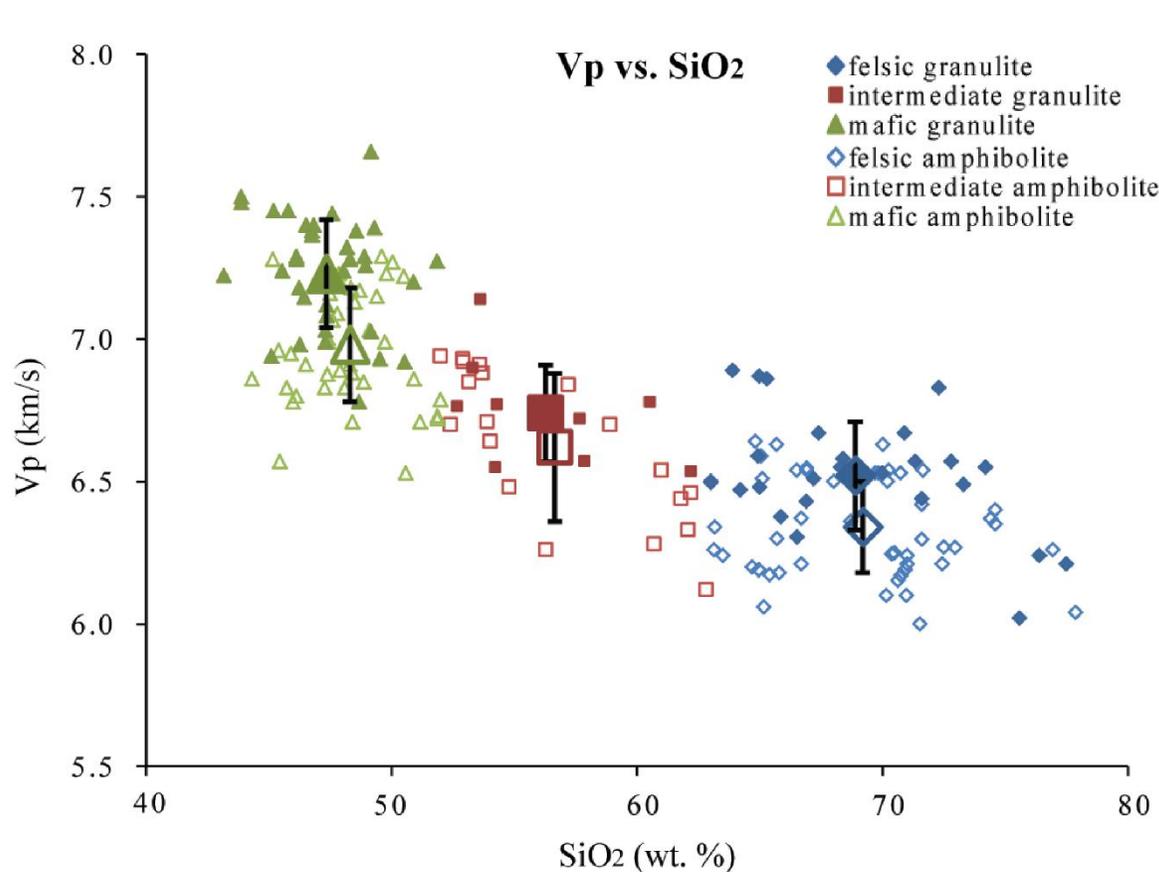Christensen and Mooney, 1995, JGR, 100
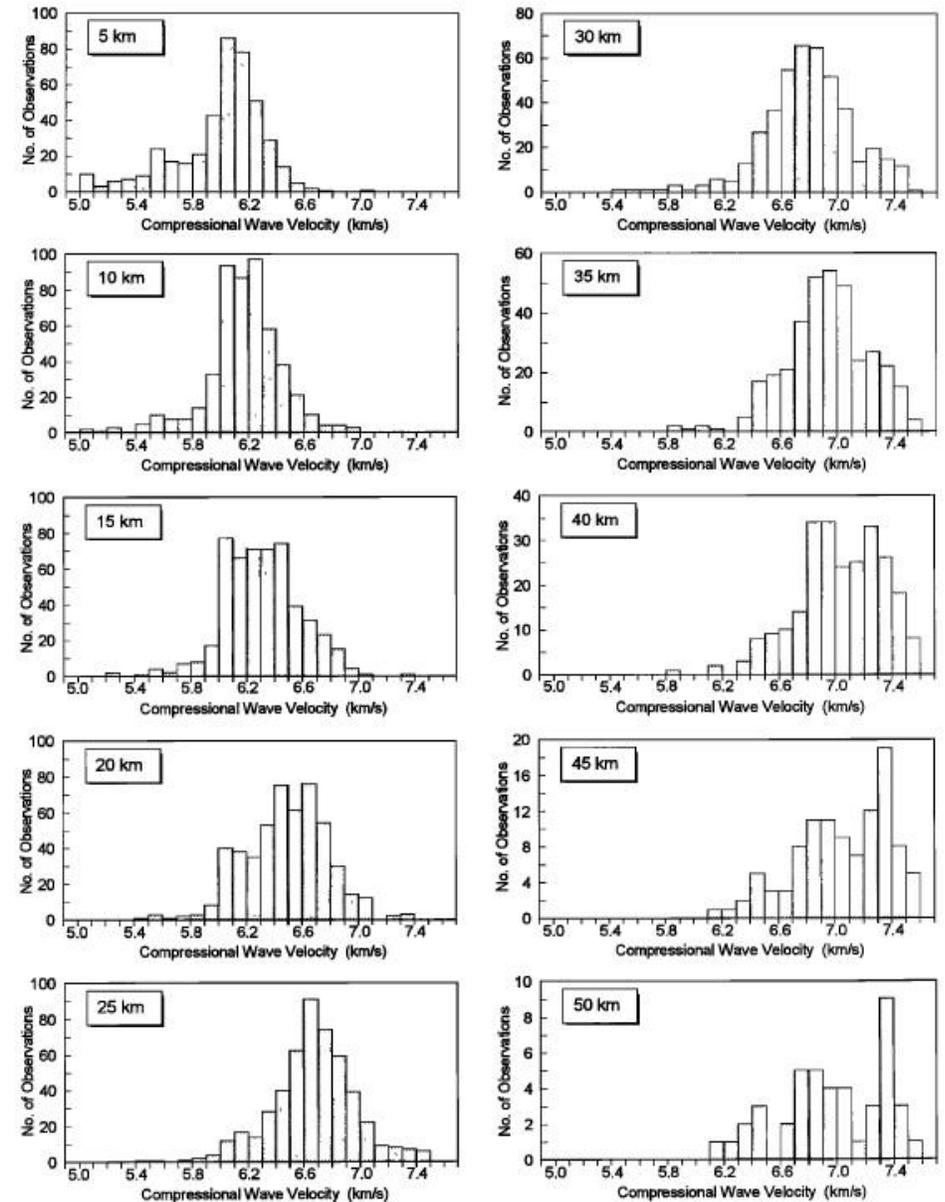
Crustal seismic velocities
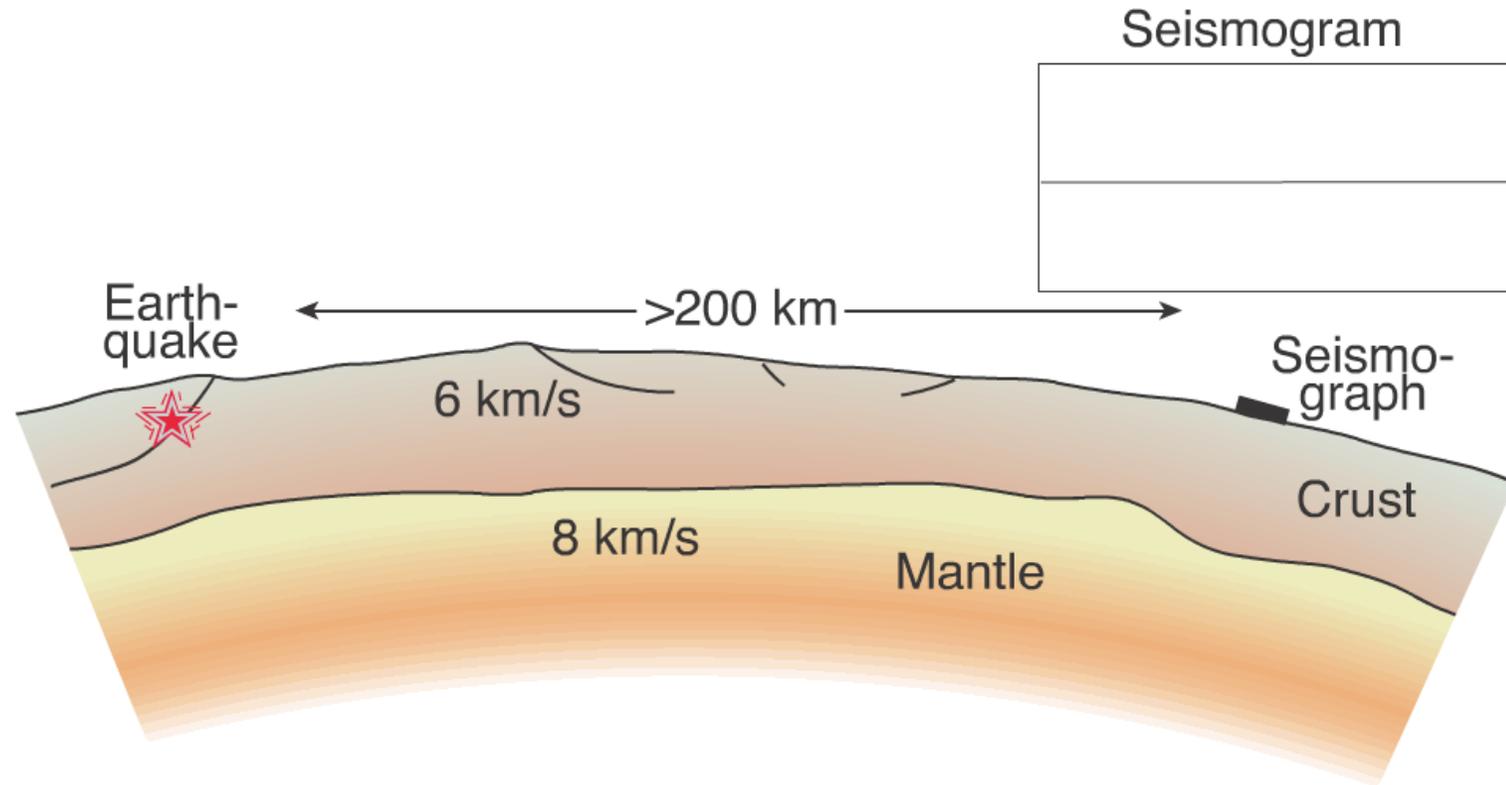
Seismic paths through and under the crust. Above some minimum distance, waves traveling along the longest path arrive first
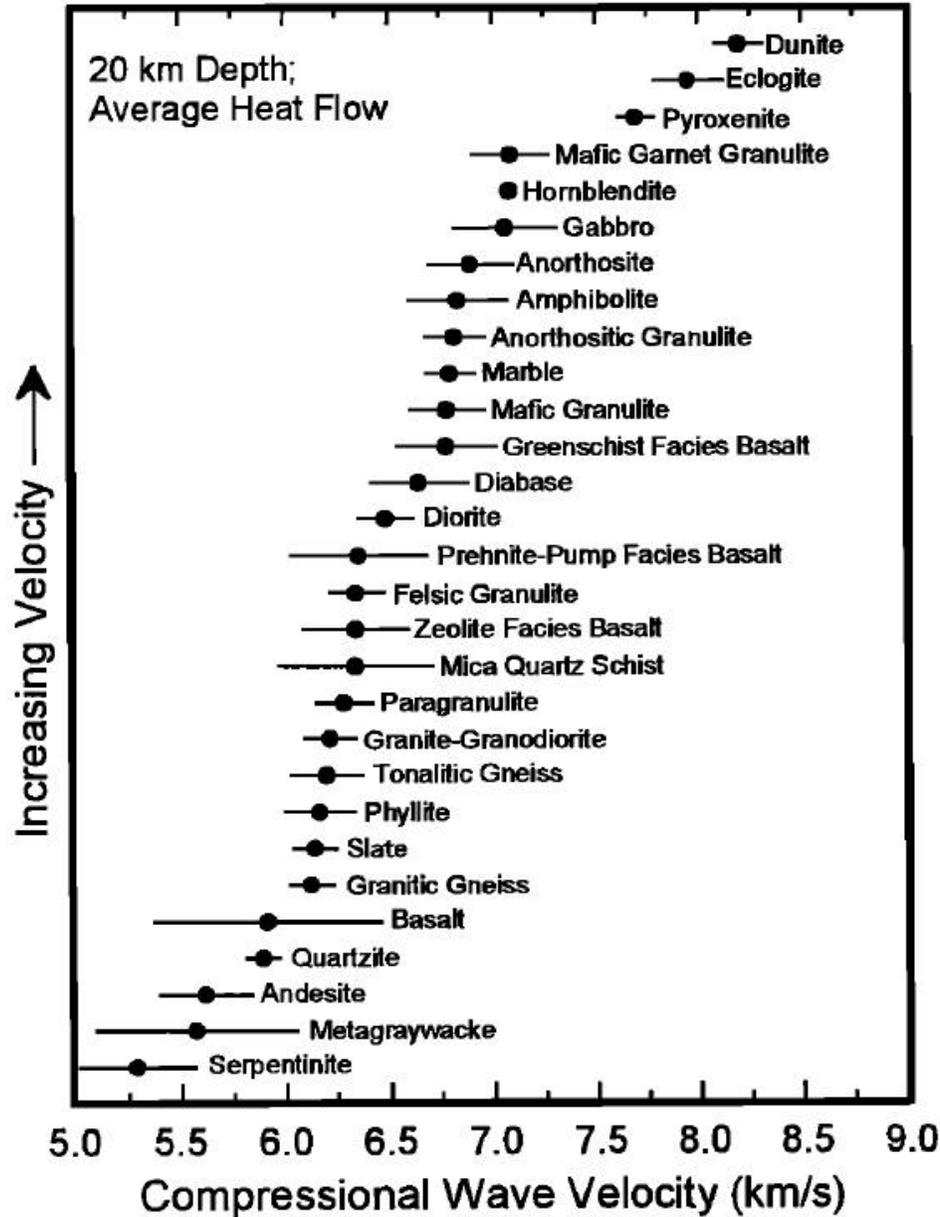
P-wave and *S-wave* velocity correlates with bulk composition
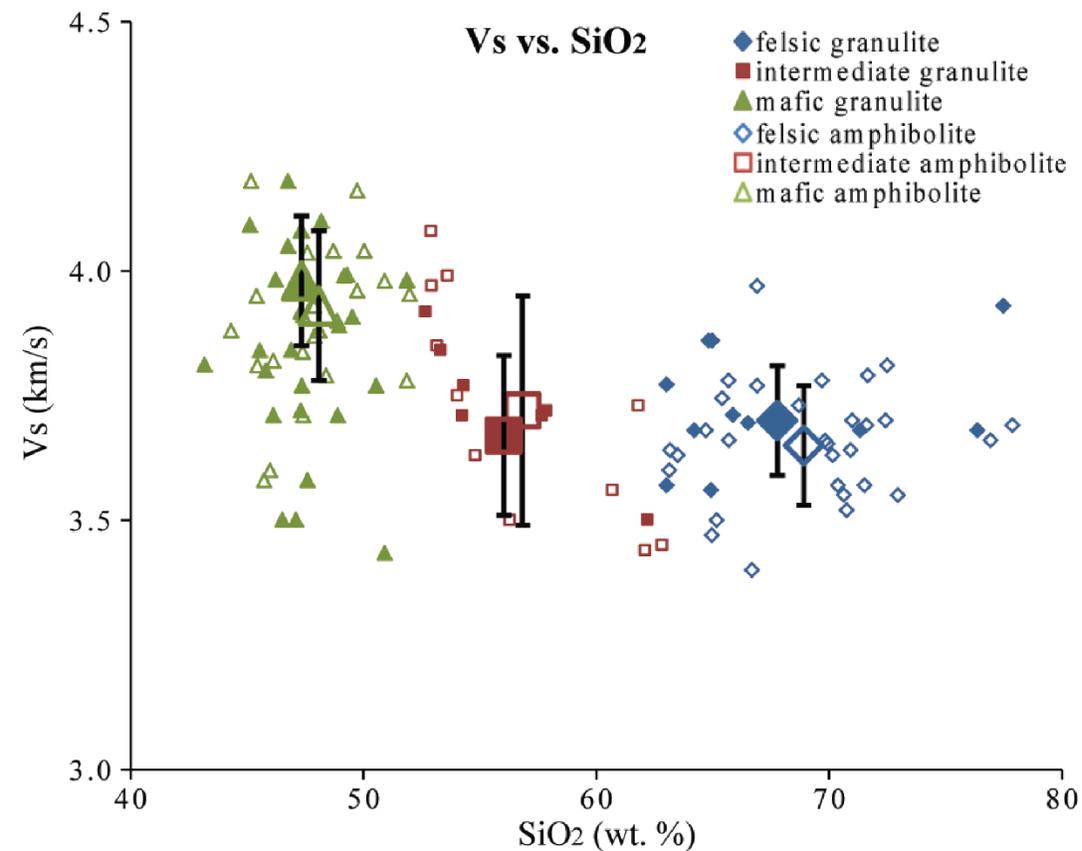
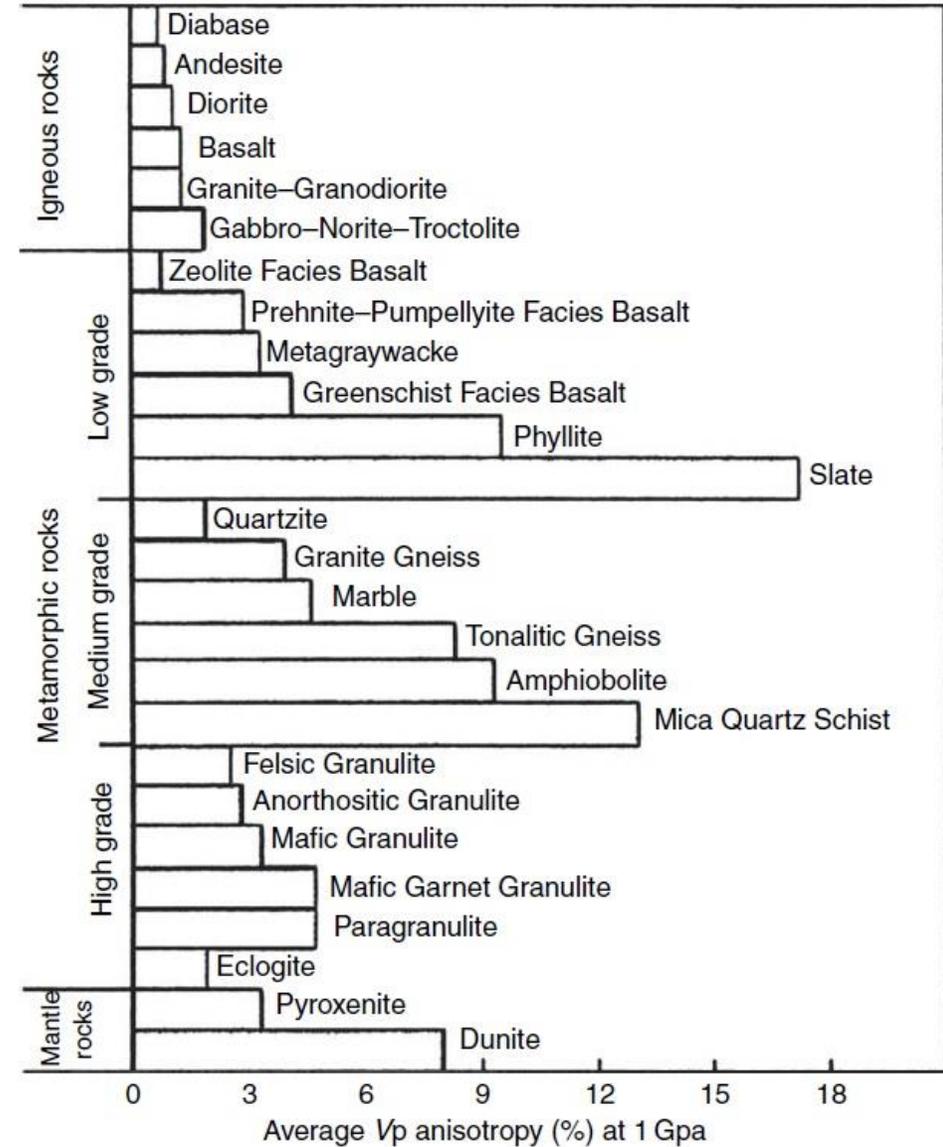Ultrasonic velocities at 0.6 GPa, room T
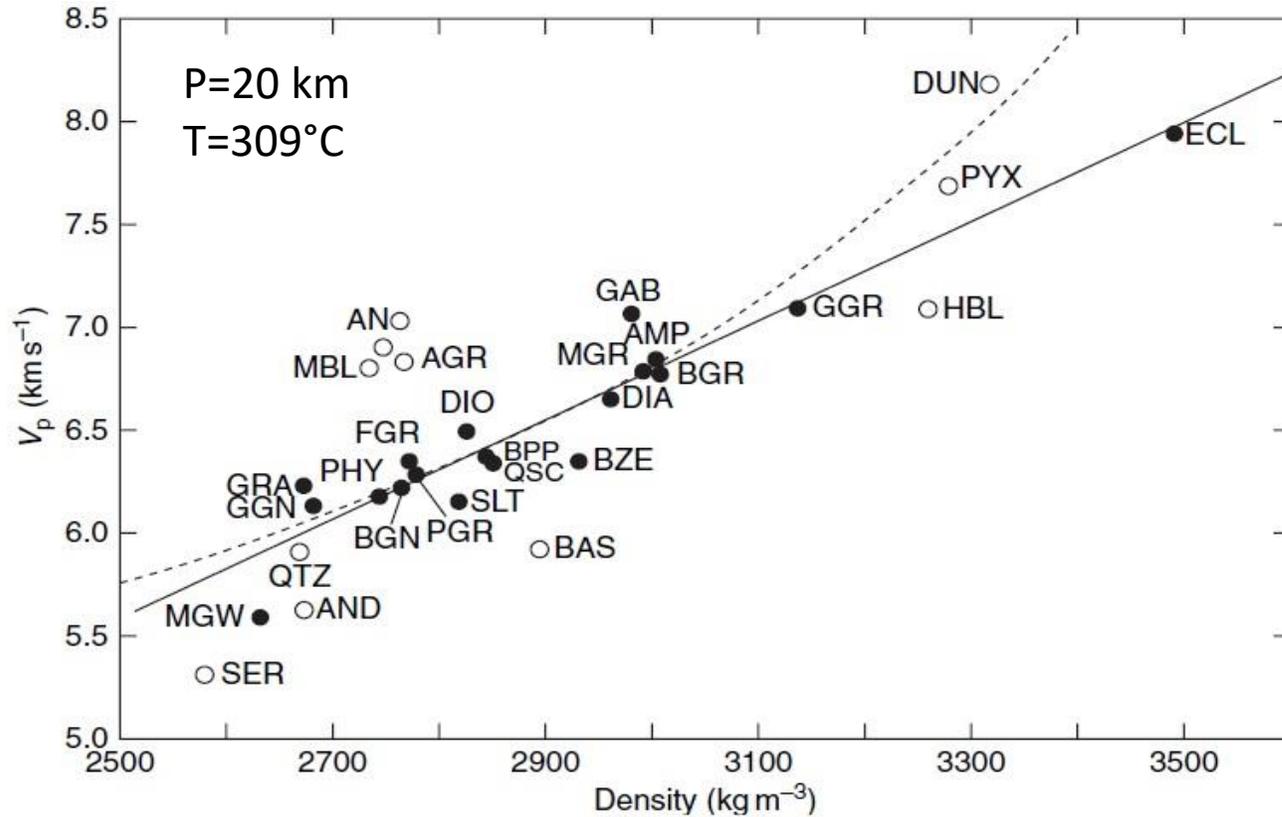
Huang et al., 2013

Rocks' P-wave velocity

Average Anisotropy 100x (Vmax-Vmin)/Vavg

Elastic waves show a directional dependence in wave speed in many minerlas

Christensen and Mooney, 1995, JGR, 100

Velocity vs Density

P=20 km
T=309°C

Linear Velocity-Density Regression Line Parameters

	ρ = a + bVp				Vp = a + bρ			
Depth, km	a, kg m⁻³	b, kg m⁻³/km s⁻¹	S(ρ, Vp), kg m⁻³	r², %	a, km s⁻¹	b, km s⁻¹/kg m⁻³	S(Vp, ρ), km s⁻¹	r², %
All Rocks								
10	989.3	289.1	116.3	75	-0.924	0.00259	0.348	75
20	947.3	296.6	113.3	76	-0.836	0.00256	0.333	76
30	946.6	299.7	112.5	76	-0.802	0.00252	0.326	76
40	964.5	300.5	113.3	75	-0.764	0.00249	0.326	75
50	1078.3	299.0	120.3	71	-0.775	0.00238	0.339	71
All Rocks Except Volcanic Rocks and Monomineralic Rocks								
10	540.6	360.1	70.2	88	-0.566	0.00245	0.183	88
20	444.1	375.4	62.8	91	-0.454	0.00241	0.159	91
30	381.2	388.0	57.8	92	-0.377	0.00237	0.143	92
40	333.4	398.8	53.8	93	-0.318	0.00232	0.130	93
50	257.1	431.4	49.1	94	-0.192	0.00218	0.110	94

Nonlinear Velocity-Density Regression Line Parameters

	ρ = a + b/Vp				Vp⁻¹ = a + bρ³			
Depth, km	a, kg m⁻³	b, kg m⁻³/km s⁻¹	S(ρ, Vp), kg m⁻³	r², %	a, km/s⁻¹	b, -	S(Vp, ρ), km s⁻¹	r², %
10	4929	-13294	69.30	87	0.2124	-2.4315×10⁻¹²	0.19	91
20	5055	-14094	62.20	90	0.2110	-2.3691×10⁻¹²	0.17	92
30	5141	-14539	57.36	91	0.2115	-2.3387×10⁻¹²	0.15	93
40	5212	-14863	53.63	92	0.2123	-2.3155×10⁻¹²	0.14	94
50	5281	-15174	50.51	93	0.2130	-2.2884×10⁻¹²	0.13	95

Vp is compressional wave velocity; ρ, density; $S(ρ, Vp)$, standard error of estimate of ρ on Vp; $S(Vp, ρ)$, standard error of estimate of Vp on ρ; r², coefficient of determination.

Rock abbreviations are as follows: **AGR**, anorthositic granulite; **AMP**, amphibolite; **AND**, andesite; **BAS**, basalt; **BGN**, biotite (tondite) gneiss; **BGR**, greenschist facies basalt; **BPP**, prehnite–pumpelliyite facies basalt; **BZE**, Zeolite facies basalt; **DIA**, diabase; **DIO**, dionite; **DUN**, Dunite; **ECL**, mafic eclogite; **FGR**, felsic granulite; **GAB**, gabbro–norite–troctolite; **GGN**, granite gneiss; **GGR**, mafic garnet granulite; **GRA**, granite–granodiorite; **HBL**, hornblendite; **MBL**, calcite marble; **MGR**, mafic granulite; **MGW**, metagraywacke; **PGR**, paragranulite; **PHY**, phyllite; **PYX**, Pyroxenite; **QCC**, mica quartz schist; **QTZ**, quartzite; **SER**, serpentinite; **SLT**, slate.

Christensen and Mooney, 1995, JGR, 100

Vp/Vs and Poisson's ratio (σ=0.23-0.32)

Poisson's ratio (ν or σ) is the ratio of transverse strain to corresponding axial strain on a material (rock) stressed along one axis

Table 1. Compressional (V_p) and Shear (V_s) Wave Velocity Ratios and Poisson's Ratios for Rock-Forming Minerals

Mineral	Symmetry[a]	Density, (kg/m³)	R	HS⁻	VRH	HS⁺	V	R	HS⁻	VRH	HS⁺	V	Reference
					V_p/V_s					Poisson's Ratio			
Framework silicates													
Feldspars													
Microcline[b]	T	2561	1.856	1.857	1.838	1.844	1.822	0.296	0.296	0.290	0.292	0.285	Ryzhova and Alexandrov [1965]
Plagioclase(An₆)	T	2610	1.819	1.819	1.817	1.819	1.816	0.283	0.284	0.283	0.283	0.282	Ryzhova [1964]
Plagioclase(An₂₄)	T	2640	1.840	1.835	1.832	1.831	1.823	0.291	0.289	0.288	0.288	0.285	Ryzhova [1964]
Plagioclase(An₂₉)	T	2640	1.841	1.835	1.830	1.830	1.820	0.291	0.289	0.287	0.287	0.284	Ryzhova [1964]
Plagioclase(An₅₃)	T	2680	1.875	1.863	1.858	1.856	1.842	0.301	0.298	0.296	0.295	0.291	Ryzhova [1964]
Plagioclase(An₅₆)	T	2690	1.872	1.859	1.853	1.851	1.836	0.300	0.296	0.295	0.294	0.289	Ryzhova [1964]
Quartz	TR	2649	1.498	1.482	1.477	1.475	1.458	0.098	0.082	0.077	0.074	0.056	McSkimin et al. [1965]
Natrolite	O	2250	1.737	1.733	1.733	1.731	1.728	0.252	0.250	0.250	0.249	0.248	Ryzhova et al. [1966]
Sheet silicates													
Muscovite	M	2844	1.760	1.740	1.729	1.721	1.704	0.261	0.253	0.249	0.245	0.237	Vaughan and Guggenheim [1986]
Biotite	M	3050	2.155	1.948	1.831	1.719	1.656	0.363	0.321	0.288	0.244	0.213	Alexandrov and Ryzhova [1961a]
Phlogopite	M	2810	2.177	1.988	1.872	1.769	1.696	0.366	0.331	0.300	0.265	0.234	Alexandrov and Ryzhova [1961a]
Chain silicates													
Amphibole													
Hornblende	M	3120	1.835	1.832	1.831	1.831	1.828	0.289	0.288	0.287	0.288	0.286	Alexandrov and Ryzhova [1961b]
Pyroxenes													
Enstatite	O	3272	1.648	1.648	1.648	1.648	1.649	0.208	0.209	0.209	0.209	0.209	Duffy and Vaughan [1988]
Bronzite	O	3380	1.739	1.737	1.737	1.737	1.735	0.253	0.252	0.252	0.252	0.251	Ryzhova et al. [1966]
Orthoferrosilite	O	4002	1.807	1.810	1.809	1.810	1.812	0.279	0.280	0.280	0.280	0.281	Bass and Weidner [1984]
Diopside	M	3270	1.745	1.755	1.756	1.760	1.767	0.255	0.260	0.260	0.262	0.264	Levien et al. [1979]
Jadeite	M	3400	1.743	1.739	1.738	1.737	1.732	0.255	0.253	0.252	0.252	0.250	Kandelin and Weidner [1988a]
Hedenbergite	M	3640	1.804	1.809	1.810	1.811	1.815	0.278	0.280	0.280	0.281	0.282	Kandelin and Weidner [1988b]
Augite	M	3320	1.717	1.727	1.727	1.731	1.737	0.243	0.248	0.248	0.249	0.252	Alexandrov et al. [1964]
Diallage	M	3300	1.650	1.649	1.648	1.648	1.646	0.210	0.209	0.209	0.209	0.208	Alexandrov et al. [1964]
Aegirine-augite	M	3420	1.850	1.869	1.869	1.876	1.886	0.294	0.299	0.299	0.302	0.305	Alexandrov et al. [1964]
Aegirine	M	3500	1.801	1.800	1.799	1.799	1.797	0.277	0.277	0.276	0.276	0.276	Alexandrov et al. [1964]
Orthosilicates and ring silicates													
Olivine group													
Forsterite	O	3224	1.712	1.710	1.710	1.709	1.708	0.241	0.240	0.240	0.240	0.239	Kumazawa and Anderson [1969]
Olivine(Fo₉₃)	O	3311	1.725	1.724	1.724	1.724	1.722	0.247	0.247	0.246	0.246	0.246	Kumazawa and Anderson [1969]
Fayalite(Fe₂SiO₄)	O	4400	2.029	2.014	2.011	2.007	1.994	0.340	0.336	0.336	0.335	0.332	Sumino [1979]
Garnet group													
Spessartite-almandine	C	4249	1.784	1.784	1.784	1.784	1.784	0.271	0.271	0.271	0.271	0.271	Wang and Simmons [1974]
Almandine	C	4160	1.792	1.792	1.792	1.792	1.792	0.274	0.274	0.274	0.274	0.274	Soga [1967]
Grossularite	C	3617	1.725	1.725	1.725	1.725	1.724	0.247	0.247	0.247	0.247	0.247	Halleck [1973]
Staurolite	M	3369	1.606	1.618	1.627	1.628	1.646	0.183	0.191	0.196	0.197	0.208	Alexandrov and Ryzhova [1961c]
Sillimanite	O	3241	1.791	1.784	1.783	1.781	1.776	0.273	0.271	0.271	0.270	0.268	Vaughan and Weidner [1978]
Andalusite	O	3145	1.718	1.723	1.723	1.724	1.728	0.244	0.246	0.246	0.247	0.248	Vaughan and Weidner [1978]
Epidote	M	3400	1.778	1.755	1.752	1.746	1.728	0.269	0.260	0.258	0.256	0.248	Ryzhova et al. [1966]
Beryl	H	2680	1.756	1.750	1.750	1.749	1.745	0.260	0.258	0.258	0.257	0.255	Hearmon [1956]
Tourmaline	TR	3050	1.659	1.659	1.657	1.658	1.656	0.215	0.214	0.214	0.214	0.213	Hearmon [1956]
Nonsilicates													
Chromite	C	4450	1.813	1.809	1.809	1.808	1.804	0.281	0.280	0.280	0.280	0.278	Hearmon [1956]
Magnetite	C	5180	1.763	1.761	1.761	1.761	1.760	0.263	0.262	0.262	0.262	0.262	Alexandrov and Ryzhova [1961c]
Pyrite	C	5013	1.582	1.574	1.572	1.555	1.583	0.167	0.162	0.160	0.147	0.168	Alexandrov and Ryzhova [1961d]
Calcite	TR	2712	2.027	1.972	1.944	1.931	1.874	0.339	0.327	0.320	0.317	0.301	Peselnick and Robie [1963]
Aragonite	O	2930	1.598	1.595	1.597	1.594	1.595	0.178	0.176	0.177	0.176	0.176	Hearmon [1956]

R is Reuss average; HS⁻, Hashin Shtrikman lower bound; VRH, Voigt Reuss Hill average; HS⁺, Hashin Shtrikman upper bound; V, Voigt average.
[a] Cubic(C), hexagonal(H), trigonal(TR), orthorhombic(O), monoclinic(M), triclinic(T).

Christensen, 1996, JGR, 101

$$\langle M \rangle = \frac{1}{2}\left(M^{voigt} + M^{reuss} \right) \qquad M^{voigt} = \Sigma \lambda_i M_i \; ; \; M^{reuss} = \left(\Sigma \frac{\lambda_i}{M_i} \right)^{-1}$$

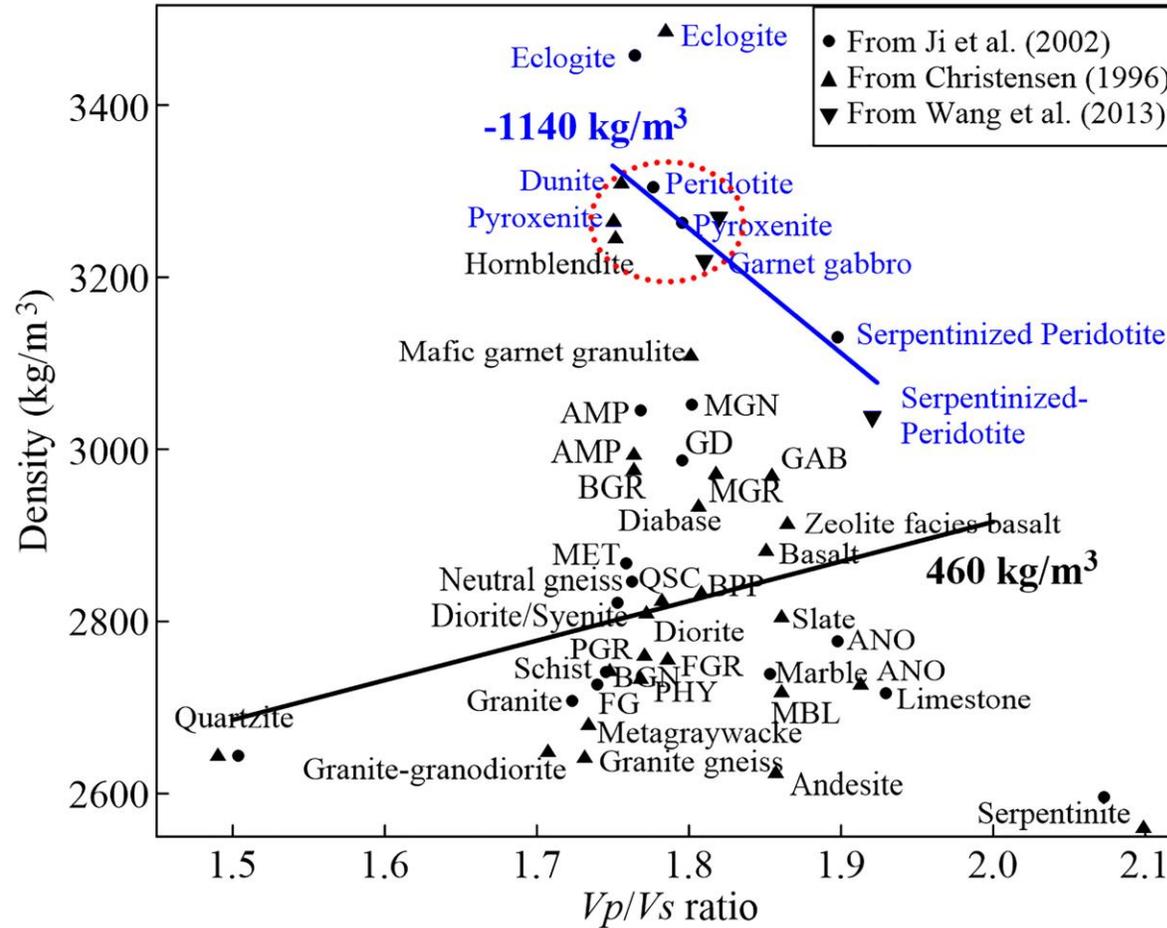λ_i=**volumetric proportion of mineral** *i*, *M*=**elastic parameter**
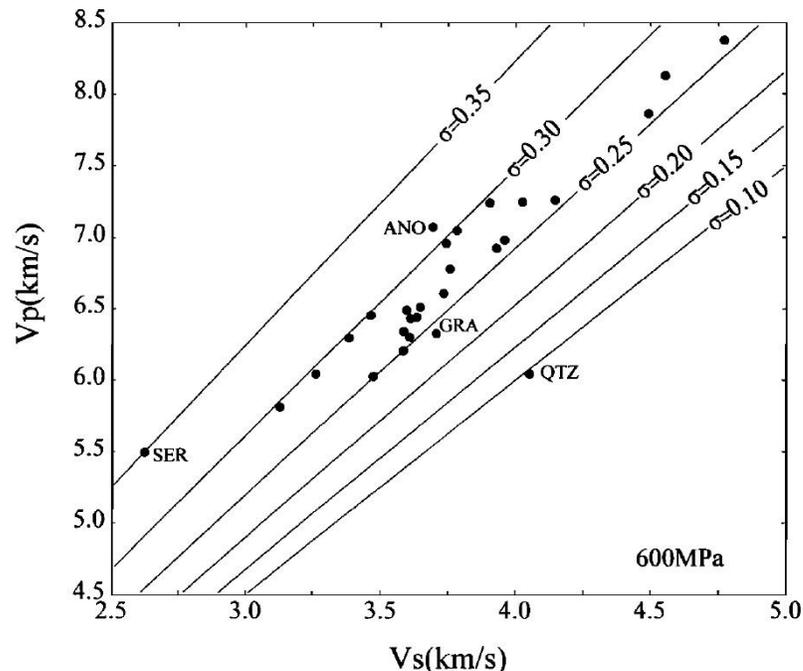
$$\sigma = \frac{1}{2}\left[1 - \frac{1}{(V_p/V_s)^2 - 1} \right]$$

Four lithologies (serpentinite (SER), anorthosite (ANO), granite-granodiorite (GRA), and quartzite (QTZ)) fall outside the area bounded by Poisson's ratios between 0.25 and 0.30.

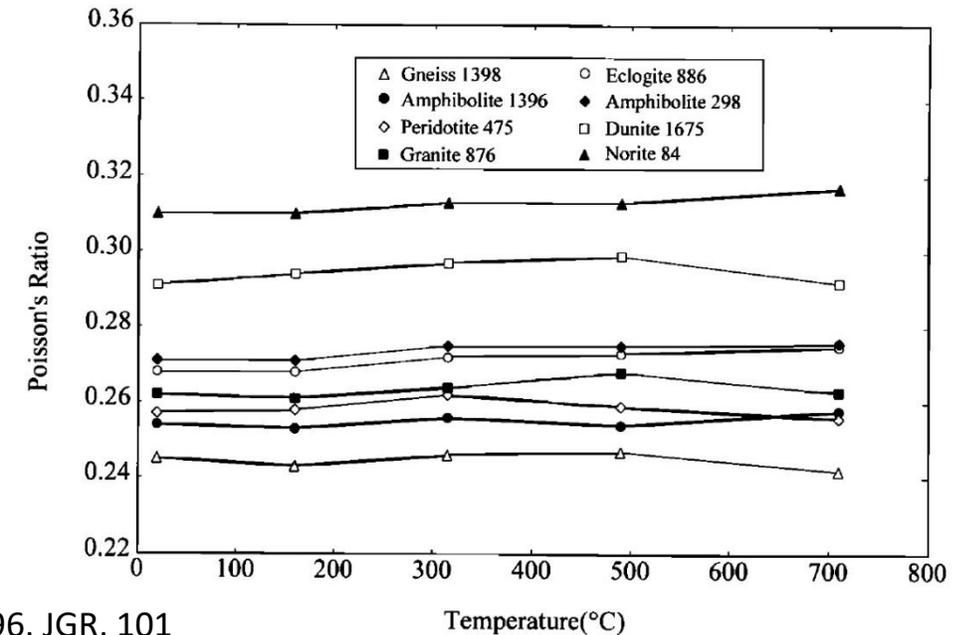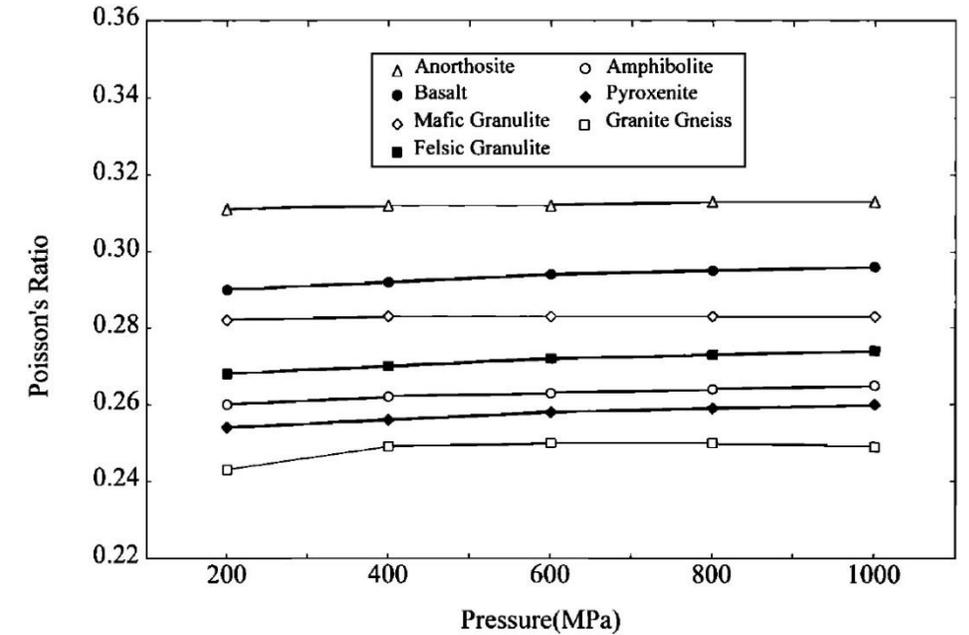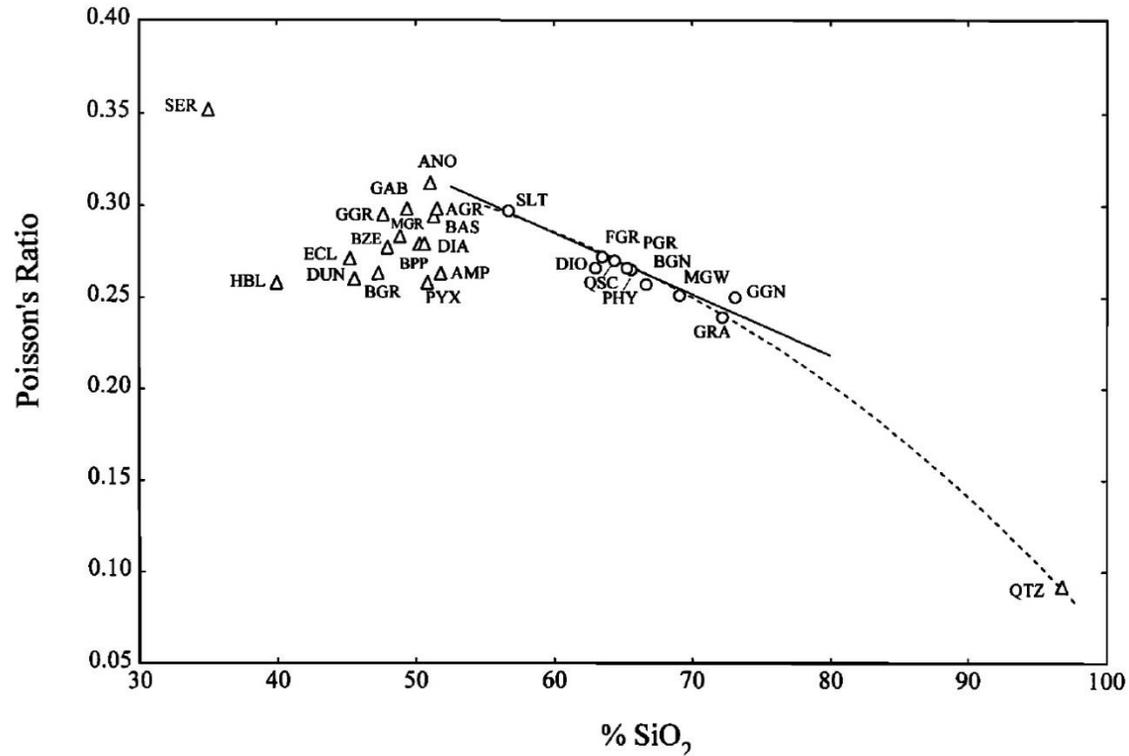Average Crustal Velocities (V_p, V_s), Velocity Ratios (V_p/V_s), and Poisson's Ratios (σ)

Crustal Type	V_p, km s⁻¹	V_s, km s⁻¹	V_p/V_s	σ	Reference
Oceanic crust, Samail Ophiolite, Oman	6.464	3.440	1.879	0.302	Christensen and Smewing [1981]
Oceanic crust, Bay of Islands Ophiolite, Newfoundland	6.608	3.494	1.891	0.306	Christensen and Salisbury [1982]
Arc crust, Kohistan, Pakistan	6.691	3.780	1.770	0.266	Miller and Christensen [1994]
Average continental crust	6.454	3.650	1.768	0.265	Christensen and Mooney [1995]

Vp/Vs and Density

Zhang et al., 2020, JGR, 125

Poisson's ratio dependance (SIO₂, P, T)

- Rocks with SiO_2 contents between 55% and 75% show a linear decrease in Poisson's ratio with increasing weight percent SiO_2.

Rock abbreviations are as follows: **AGR**, anorthositic granulite; **AMP**, amphibolite; **AND**, andesite; **ANO**, Anorthosite; **BAS**, basalt; **BGN**, biotite (tondite) gneiss; **BGR**, greenschist facies basalt; **BPP**, prehnite–pumpelliyite facies basalt; **BZE**, Zeolite facies basalt; **DIA**, diabase; **DIO**, dionite; **DUN**, Dunite; **ECL**, mafic eclogite; **FGR**, felsic granulite; **GAB**, gabbro–norite–troctolite; **GGN**, granite gneiss; **GGR**, mafic garnet granulite; **GRA**, granite–granodiorite; **HBL**, hornblendite; **MBL**, calcite marble; **MGR**, mafic granulite; **MGW**, metagraywacke; **PGR**, paragranulite; **PHY**, phyllite; **PYX**, Pyroxenite; **QCC**, mica quartz schist; **QTZ**, quartzite; **SER**, serpentinite; **SLT**, slate. Christensen (1996).

Other empirical relations

Brocher et al., 2005
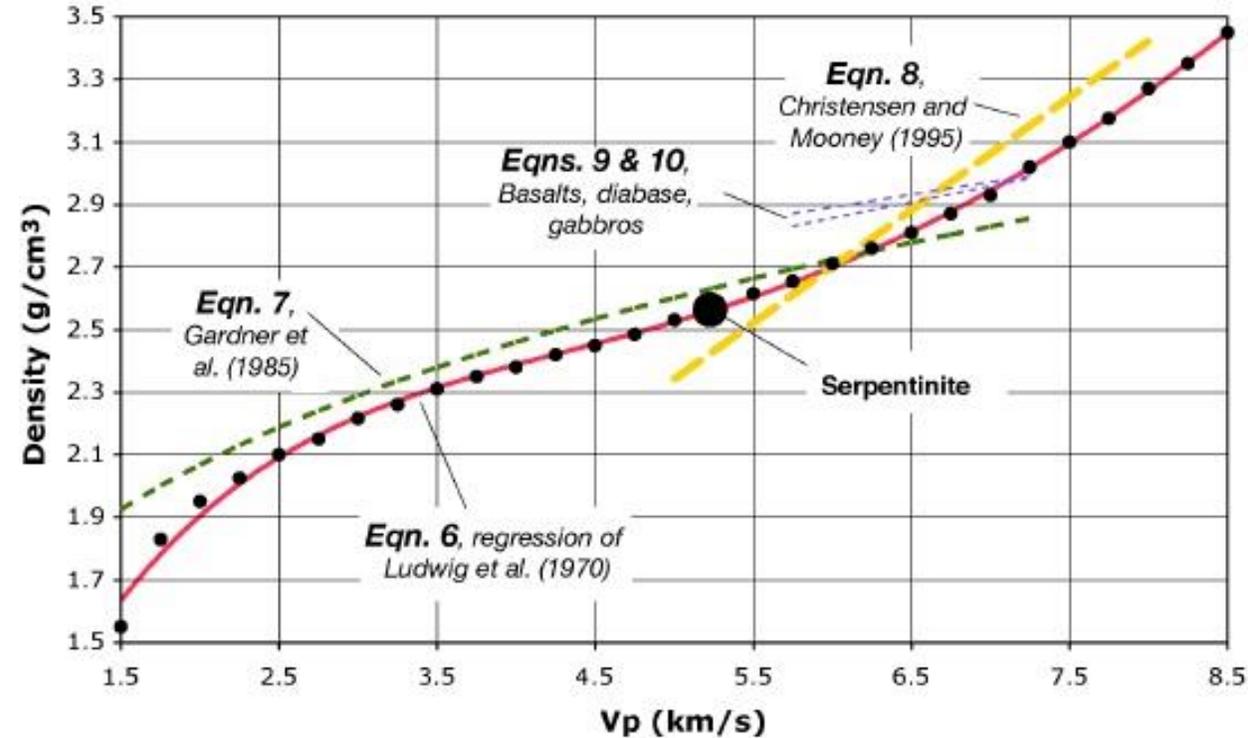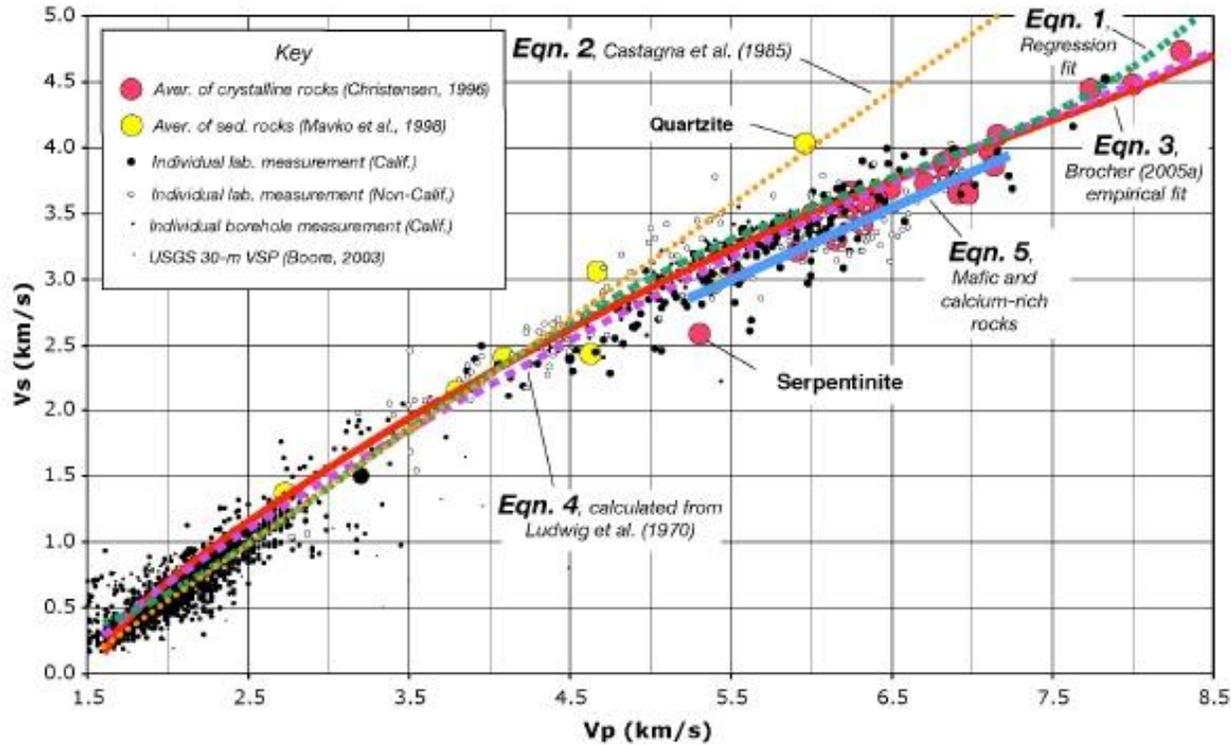
[eqn. 6] ρ (g/cm³) = 1.6612Vp − 0.4721Vp² + 0.0671Vp³ − 0.0043Vp⁴ + 0.000106Vp⁵

[eqn. 1] Vs (km/s) = 0.7858 − 1.2344Vp + 0.7949Vp² − 0.1238Vp³ + 0.0064Vp⁴

[eqn. 7] ρ (g/cm³) = 1.74Vp^{0.25}

[eqn. 3] σ = 0.8835 − 0.315Vp + 0.0491Vp² − 0.0024Vp³

[eqn. 8] ρ (g/cm³) = 0.541 + 0.3601Vp

[eqn. 4] σ = 0.769 − 0.226Vp + 0.0316Vp² − 0.0014Vp³.

[eqn. 9] ρ (g/cm³) = 2.4372 + 0.0761Vp

[eqn. 5] Vs (km/s) = 2.88 + 0.52(Vp−5.25)

[eqn. 10] ρ (g/cm³) = 2.2428 + 0.1052Vp

Rocks' Density vs *T* and *P*

Densities and Compressional Wave Velocities as Functions of Temperature and Depth

Name	5 km					10 km					15 km					20 km					25 km				
Specimens (S)	ρ,	Room	Low	Avg	High	ρ,	Room	Low	Avg	High	ρ,	Room	Low	Avg	High	ρ,	Room	Low	Avg	High	ρ,	Room	Low	Avg	High
Rocks (R)	kg/m³	20°C	64°C	84°C	138°C	kg/m³	20°C	116°C	157°C	263°C	kg/m³	20°C	160°C	225°C	381°C	kg/m³	20°C	200°C	309°C	501°C	kg/m³	20°C	247°C	389°C	645°C
Andesite (AND)																									
S=30 Avg	2627	5.429	5.393	5.381	5.351	2630	5.627	5.561	5.538	5.477	2633	5.731	5.640	5.603	5.514	2635	5.800	5.686	5.623	5.514	2638	5.851	5.710	5.629	5.483
R=10 S.D.	71	0.280	0.280	0.280	0.280	70	0.239	0.239	0.239	0.239	70	0.227	0.227	0.227	0.227	70	0.224	0.224	0.224	0.224	69	0.224	0.224	0.224	0.224
Basalt (BAS)																									
S=415 Avg	2878	5.877	5.852	5.845	5.823	2883	5.954	5.908	5.892	5.851	2889	6.003	5.940	5.915	5.854	2894	6.039	5.961	5.918	5.843	2899	6.067	5.971	5.915	5.815
R=149 S.D.	144	0.547	0.547	0.547	0.547	144	0.543	0.543	0.543	0.543	144	0.542	0.542	0.542	0.542	144	0.541	0.541	0.541	0.541	144	0.540	0.540	0.540	0.540
Diabase (DIA)																									
S=54 Avg	2946	6.673	6.648	6.640	6.619	2952	6.719	6.674	6.658	6.617	2957	6.747	6.685	6.659	6.599	2962	6.765	6.687	6.645	6.570	2967	6.779	6.683	6.628	6.528
R=18 S.D.	85	0.253	0.253	0.253	0.253	85	0.245	0.245	0.245	0.245	85	0.239	0.239	0.239	0.239	85	0.235	0.235	0.235	0.235	85	0.232	0.232	0.232	0.232
Granite-Granodiorite (GRA)																									
S=134 Avg	2654	6.215	6.179	6.182	6.161	2661	6.287	6.221	6.226	6.184	2667	6.321	6.230	6.234	6.173	2673	6.344	6.230	6.224	6.149	2679	6.361	6.220	6.209	6.110
R=52 S.D.	24	0.135	0.135	0.135	0.135	24	0.125	0.125	0.125	0.125	24	0.124	0.124	0.124	0.124	24	0.124	0.124	0.124	0.124	24	0.125	0.125	0.125	0.125
Diorite (DIO)																									
S=24 Avg	2810	6.443	6.418	6.410	6.389	2815	6.528	6.483	6.467	6.426	2820	6.575	6.513	6.487	6.427	2825	6.608	6.530	6.487	6.412	2831	6.633	6.536	6.481	6.381
R=8 S.D.	85	0.167	0.167	0.167	0.167	85	0.155	0.155	0.155	0.155	85	0.144	0.144	0.144	0.144	85	0.134	0.134	0.134	0.134	85	0.126	0.126	0.126	0.126
Gabbro-Norite-Troctolite (GAB)																									
S=187 Avg	2966	7.096	7.060	7.048	7.018	2971	7.167	7.101	7.078	7.017	2975	7.210	7.118	7.081	6.992	2981	7.240	7.126	7.063	6.954	2985	7.262	7.122	7.041	6.895
R=69 S.D.	71	0.246	0.246	0.246	0.246	70	0.247	0.247	0.247	0.247	70	0.248	0.248	0.248	0.248	69	0.250	0.250	0.250	0.250	68	0.251	0.251	0.251	0.251
Metagraywacke (MGW)																									
S=87 Avg	2615	5.369	5.344	5.336	5.315	2621	5.522	5.477	5.461	5.420	2627	5.624	5.561	5.536	5.475	2632	5.701	5.623	5.580	5.505	2638	5.764	5.668	5.613	5.513
R=29 S.D.	112	0.615	0.615	0.615	0.615	112	0.564	0.564	0.564	0.564	112	0.519	0.519	0.519	0.519	112	0.479	0.479	0.479	0.479	112	0.443	0.443	0.443	0.443
Slate (SLT)																									
S=30 Avg	2801	6.098	6.073	6.065	6.044	2807	6.172	6.127	6.111	6.070	2813	6.227	6.164	6.139	6.078	2818	6.268	6.190	6.148	6.073	2824	6.302	6.206	6.151	6.051
R=10 S.D.	28	0.131	0.131	0.131	0.131	28	0.124	0.124	0.124	0.124	28	0.117	0.117	0.117	0.117	28	0.110	0.110	0.110	0.110	28	0.103	0.103	0.103	0.103
Phyllite (PHY)																									
S=144 Avg	2728	6.105	6.080	6.073	6.052	2734	6.210	6.164	6.148	6.107	2740	6.260	6.197	6.172	6.111	2745	6.292	6.214	6.171	6.096	2751	6.316	6.220	6.165	6.065
R=48 S.D.	58	0.258	0.258	0.258	0.258	58	0.206	0.206	0.206	0.206	58	0.183	0.183	0.183	0.183	58	0.168	0.168	0.168	0.168	58	0.158	0.158	0.158	0.158
Zeolite Facies Basalt (BZE)																									
S=57 Avg	2916	6.277	6.253	6.245	6.224	2922	6.368	6.323	6.307	6.266	2927	6.425	6.363	6.337	6.277	2932	6.465	6.387	6.344	6.269	2937	6.495	6.399	6.344	6.244
R=19 S.D.	81	0.269	0.269	0.269	0.269	81	0.261	0.261	0.261	0.261	81	0.257	0.257	0.257	0.257	81	0.254	0.254	0.254	0.254	81	0.252	0.252	0.252	0.252

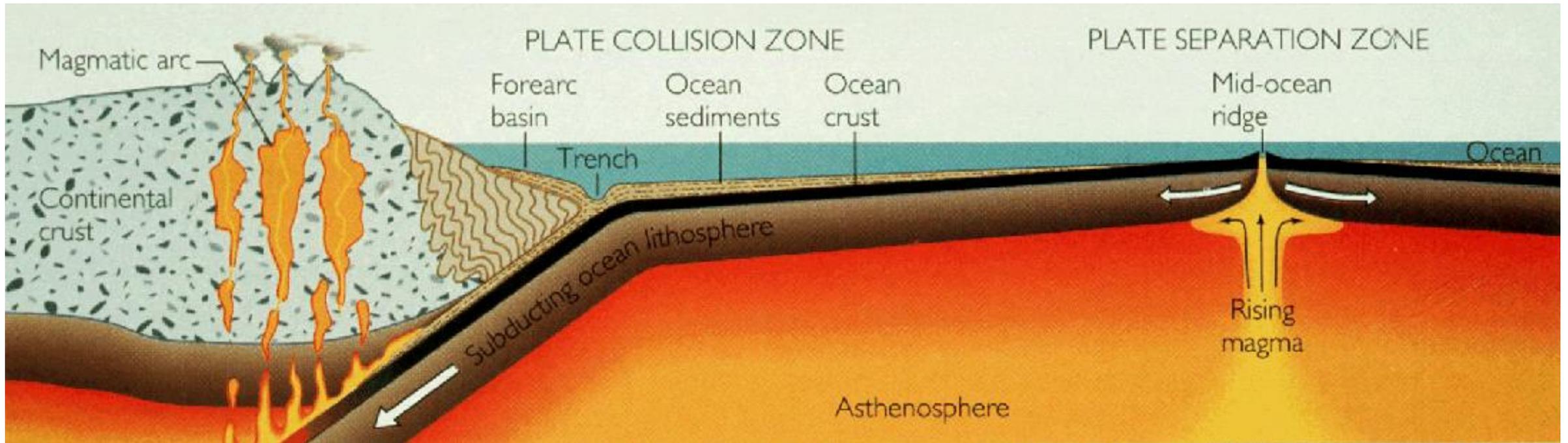Christensen and Mooney, 1995, JGR, 100

Earth Velocity
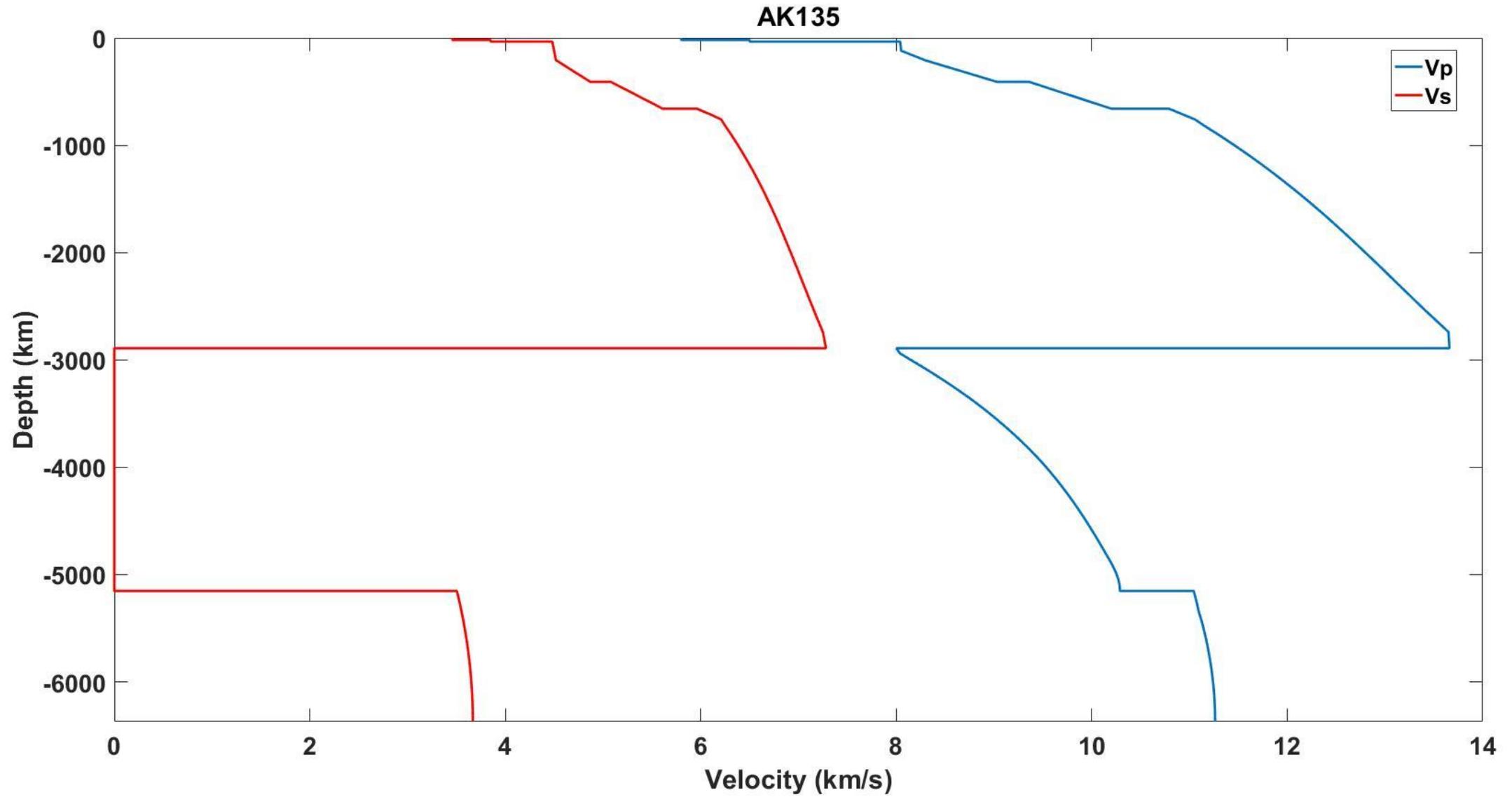
Earth Density
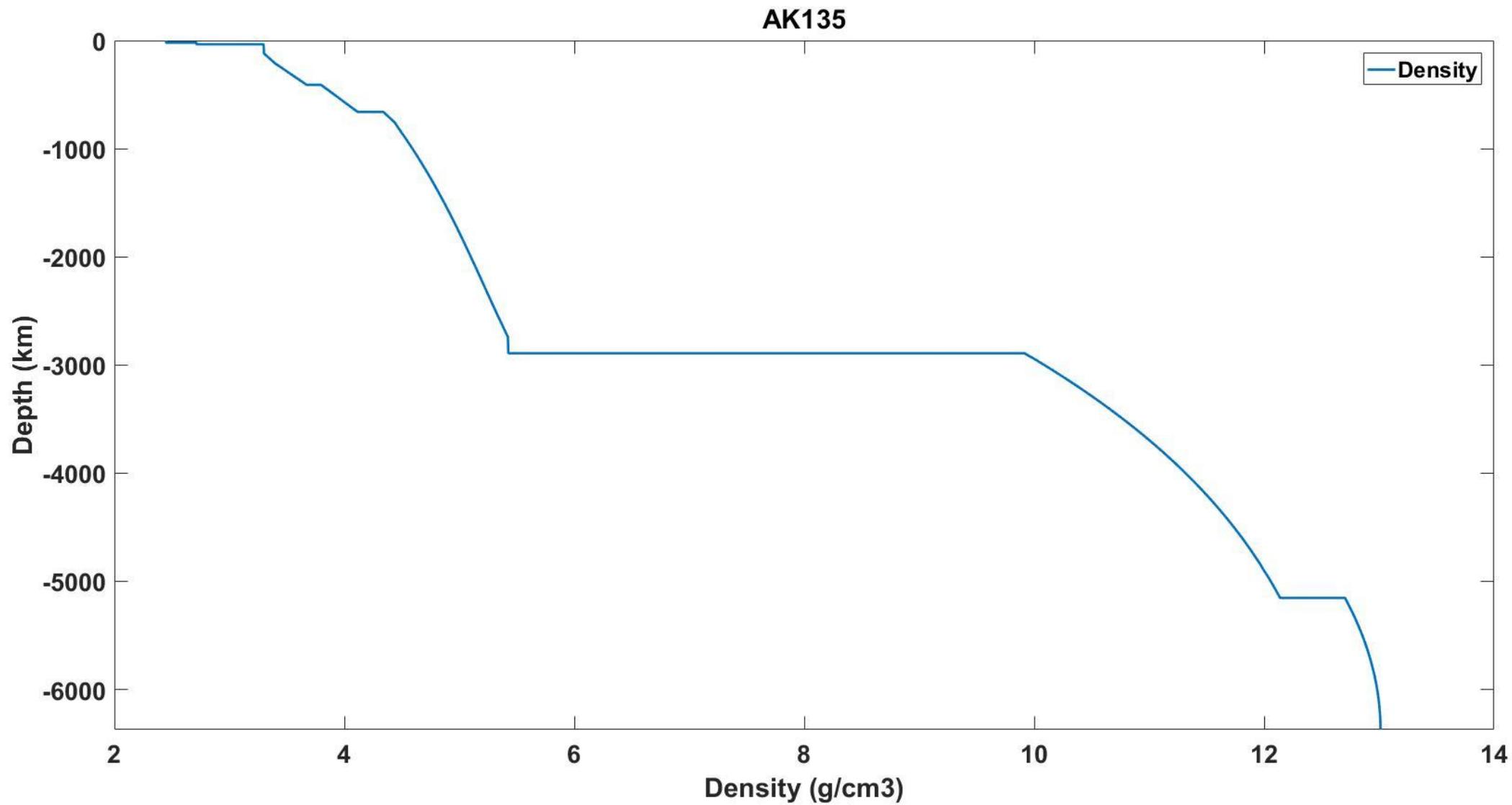
# Oceanic and continental crust

- Oceanic and continental lithosphere differ fundamentally in terms of geometry, composition, and thermal structure
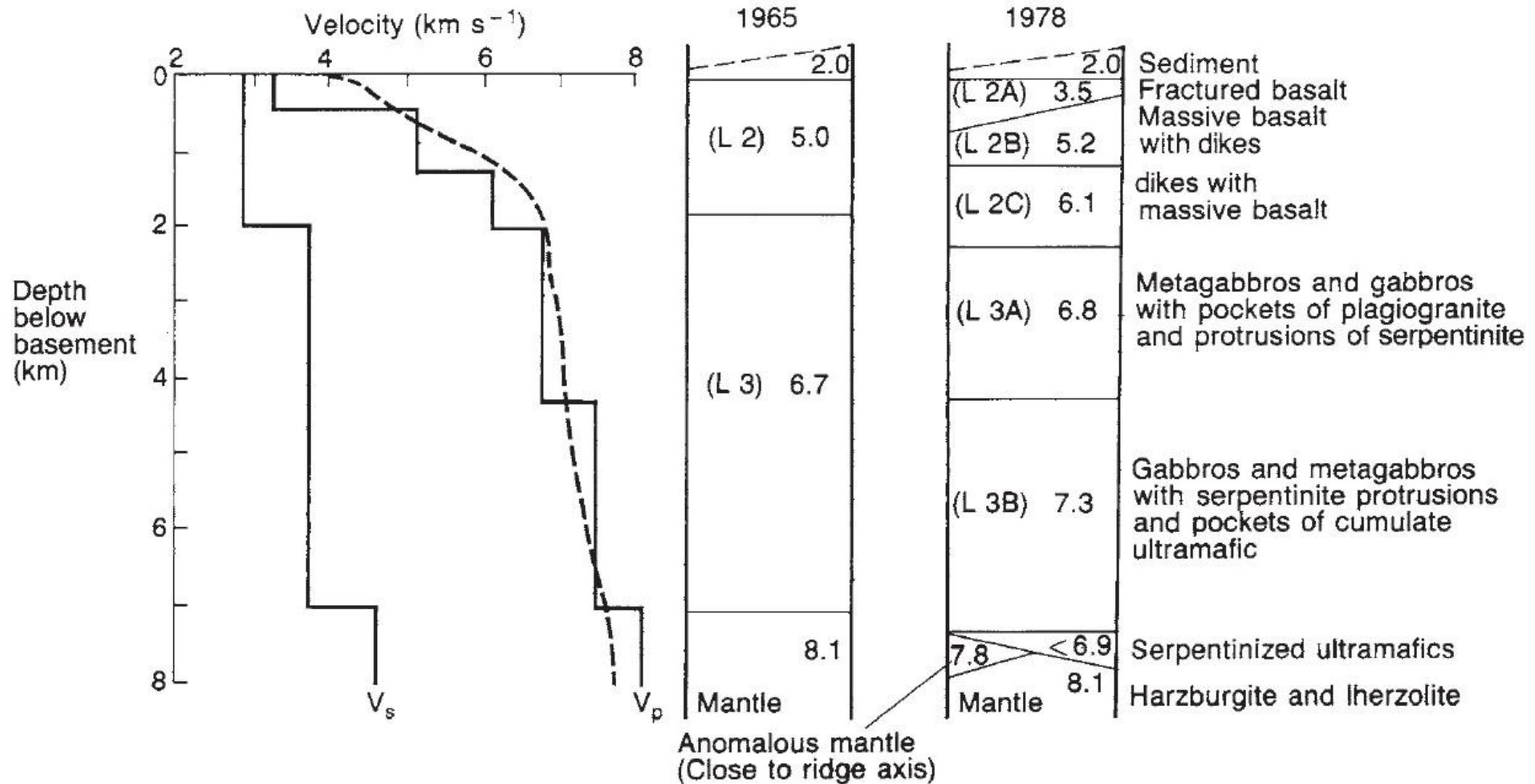
Compositional Model of Oceanic Crust

(1) 0.5 km of soft sediments (layer 1), P-wave velocity 2.0 km/s
(2) a 1–3-km-thick upper layer (layer 2) P-wave velocity 2.5–6.4 km/s
(3) 4–5-km thick lower crustal layer (layer 3), with a velocity of 6.5–7.3 km/s.
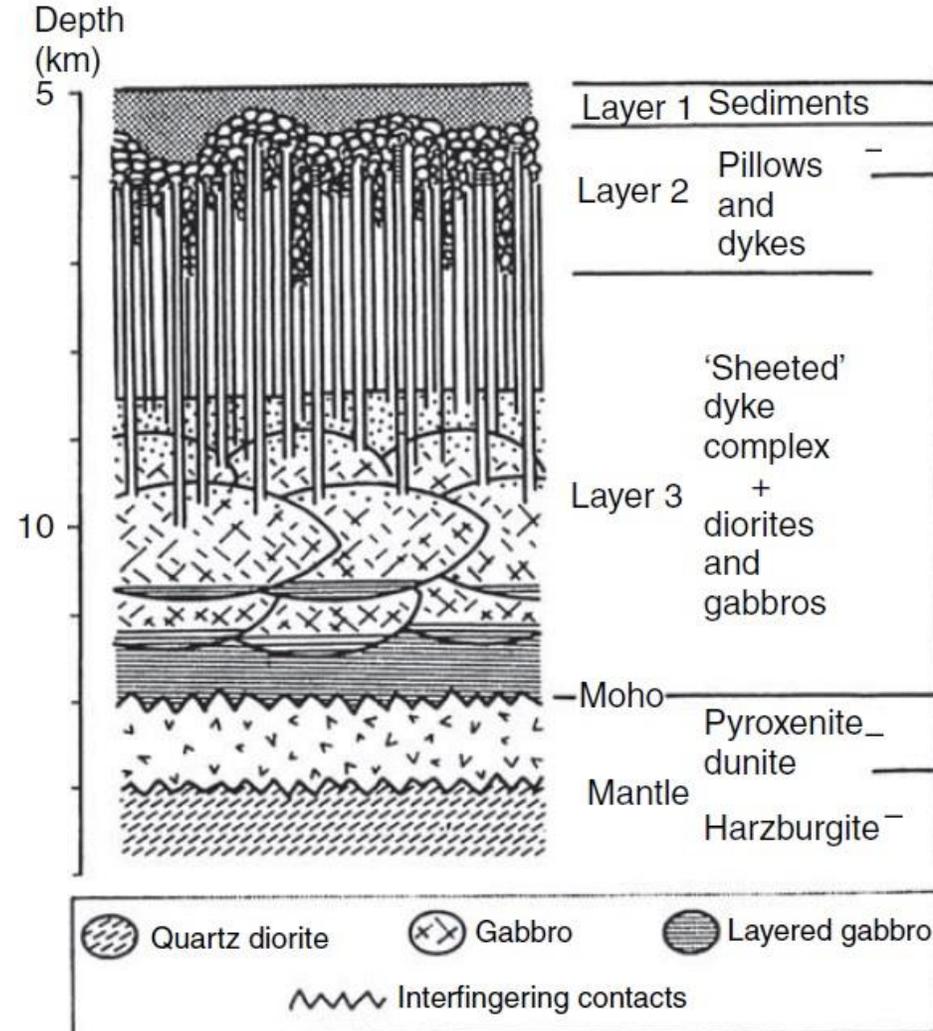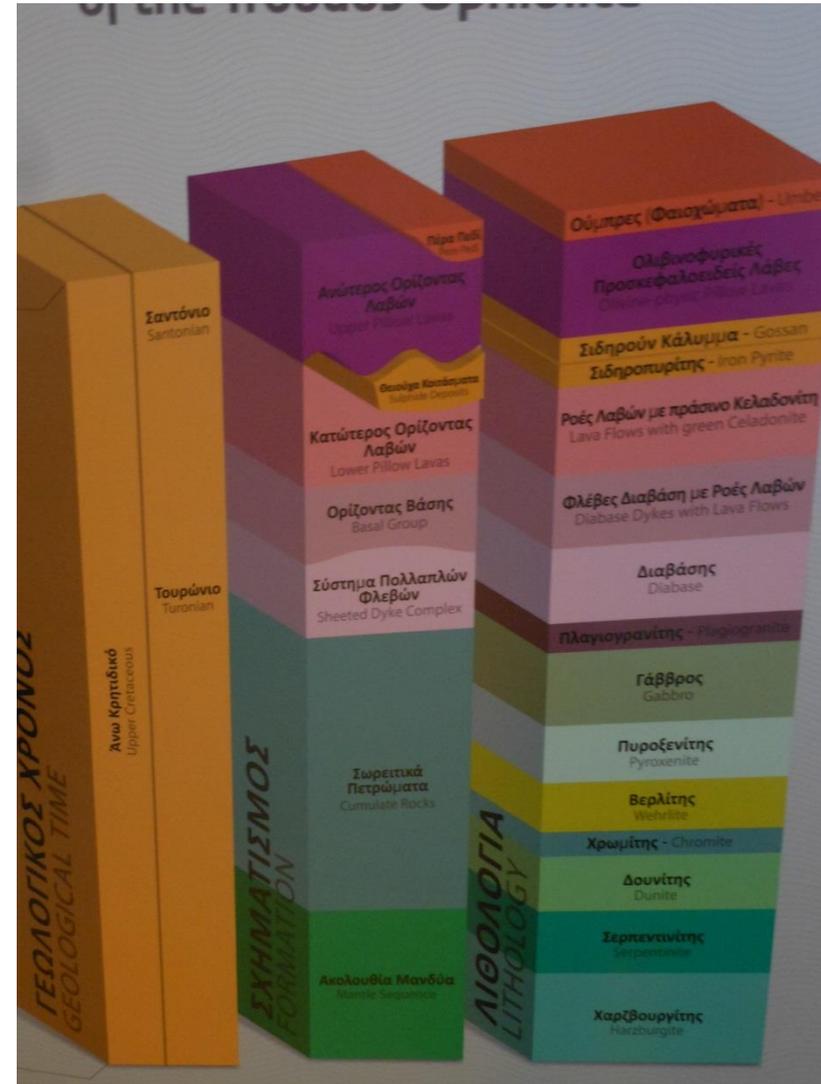
Compositional Model of Oceanic Crust

Ophiolites

Ophiolites usually occur in collisional orogens and their association of deep-sea sediments, basalts, gabbros, and ultramafic rocks suggests that they originated as oceanic lithosphere.

Correlation of ophiolite stratigraphy with the oceanic lithosphere

Stratigraphy of the Troodos (Cyprus) ophiolite

Global Ophiolite Distribution by Age

Key
Eocene
Jurassic-Cretaceous
Devonian-E. Permian
Ordovician
Neoproterozoic-Cambrian

c.448 Ma: SS [58]
c.498 Ma: Shet. [63]
c.478 Ma: Ball. [61]
c.480 Ma: ThM [60]
c.485 Ma: Bol [62]
c.392 Ma: Liz. [55]
c.395 Ma: Car. [57]
c.151 Ma: Jos. [17]
c.476 Ma: MHM [60]
c.477 Ma: BM [59]
c.392 Ma: Mor. [56]
c.440 Ma: Ac. [10]
c.93 Ma: Kut. [49]
c.91 Ma: Kiz. [46]
c.171 Ma: Vou. [51]
c.91 Ma: Tau. [47]
c.285 Ma: Yak. [54]
c.102 Ma: Fuj.
c.168,158 Ma: Alb. [20,52]
c.169 Ma: Oth. [51]
c.93 Ma: Mer. [48]
c.94 Ma: Sam. [18]
c.71,65 Ma:
c.165 Ma: Pin. [51]
c.278 Ma: DnM. [53]

Oceanic Ridge

Fast-spreading ridges (spreading rate = 8–16 cm/yr)
Intermediate (spreading rate = 4–8 cm/yr)
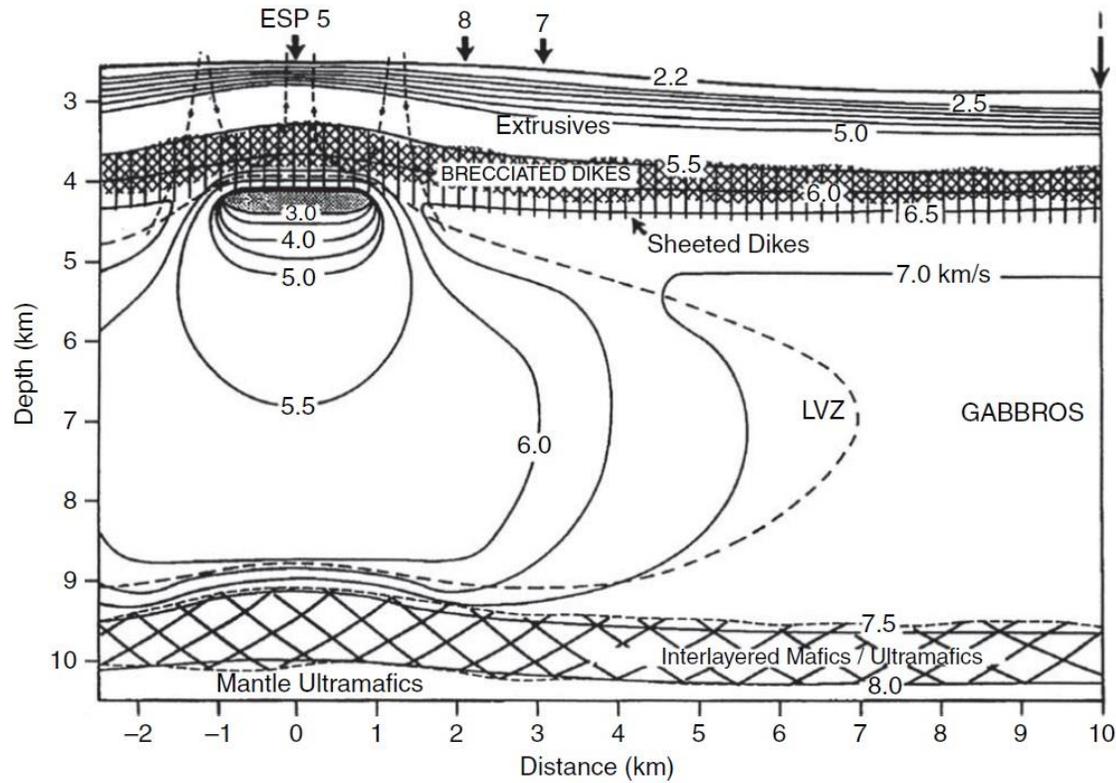
slow-spreading ridges (spreading rate = 1–4 cm/yr)
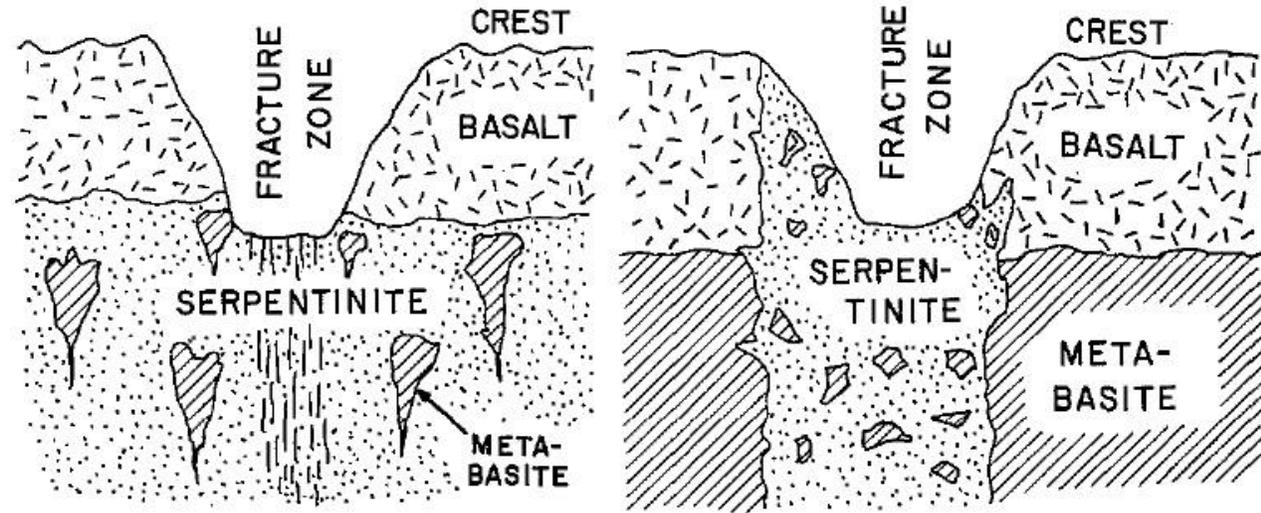
Anomalous Oceanic Crust

Oceanic Plateaux

Large volumes of magma emplaced in a short time (2-3 Myr)

Anomalous crustal structure: large thickness and high seismic velocities (7.1 km/s)
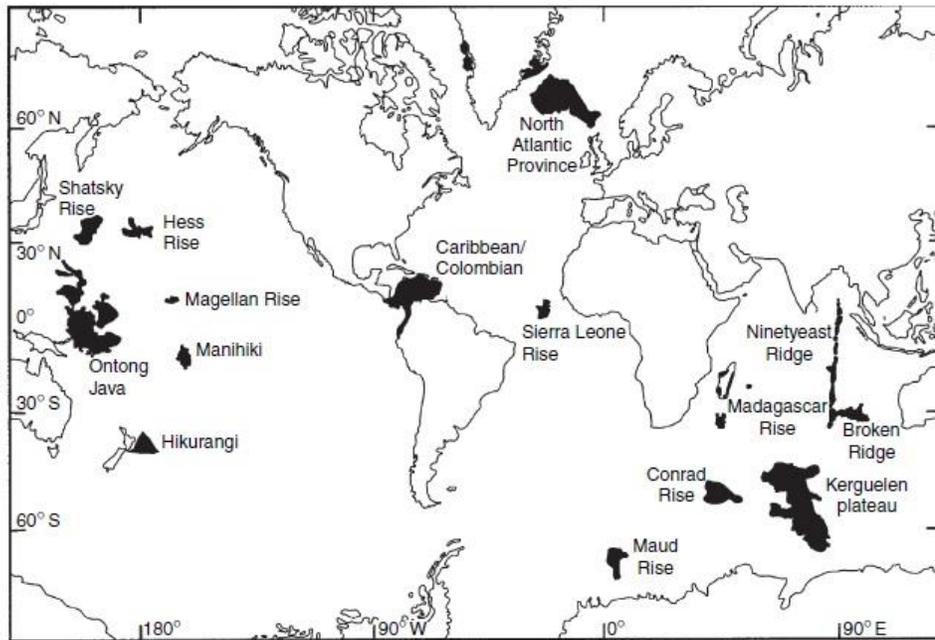
Oceanic plateau	Mean age (Ma)	Area (10⁶ km²)	Thickness range (km)	Volume (10⁶ km³)
Hikurangi	early-mid Cretaceous	0.7	10–15	2.7
Shatsky Rise	147	0.2	10–28	2.5
Magellan Rise	145	0.5	10	1.8
Manihiki	123	0.8	>20	8.8
Ontong Java	121(90)	1.9	15–32	44.4
Hess Rise	99	0.8	>15	9.1
Caribbean	88	1.1	8–20	4.4
South Kerguelen	110	1.0	~22	6.0
Central Kerguelen/Broken Ridge	86	1.0	19–21	9.1
Sierra Leone Rise	~73	0.9	>10	2.5
Maud Rise	~>73	0.2	>10	1.2

Mooney, 2007

Iceland
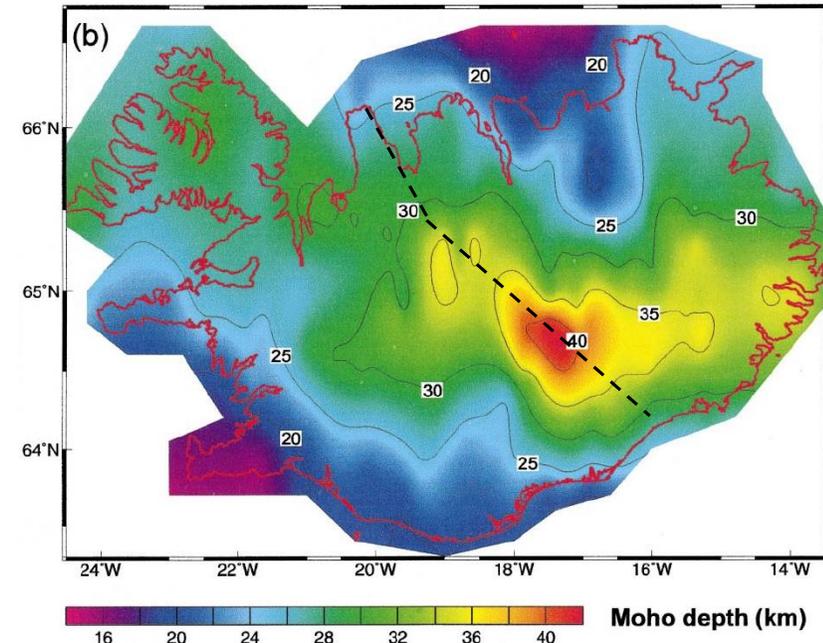
Darbyshire, 2000, EPSL, 181
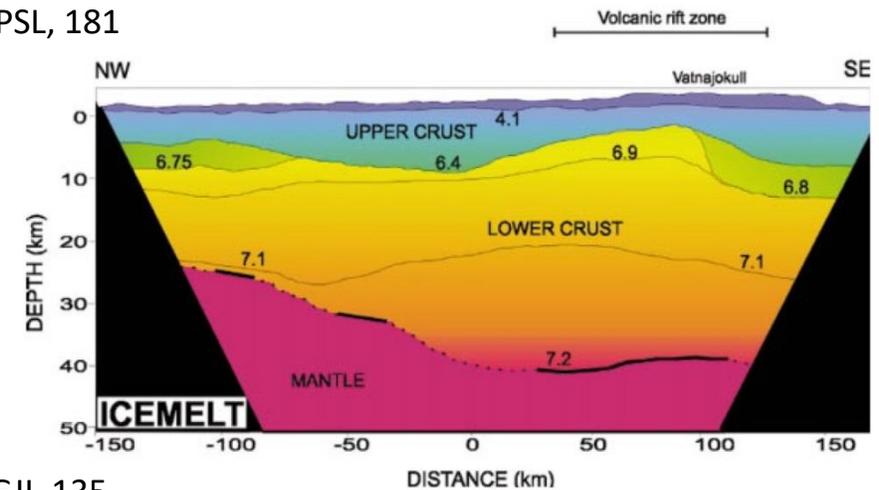
Darbyshire, 1998, GJI, 135

Anomalous Oceanic Crust

Ocean trench and subduction zone

Crustal model across Nankai Trough (Japan)
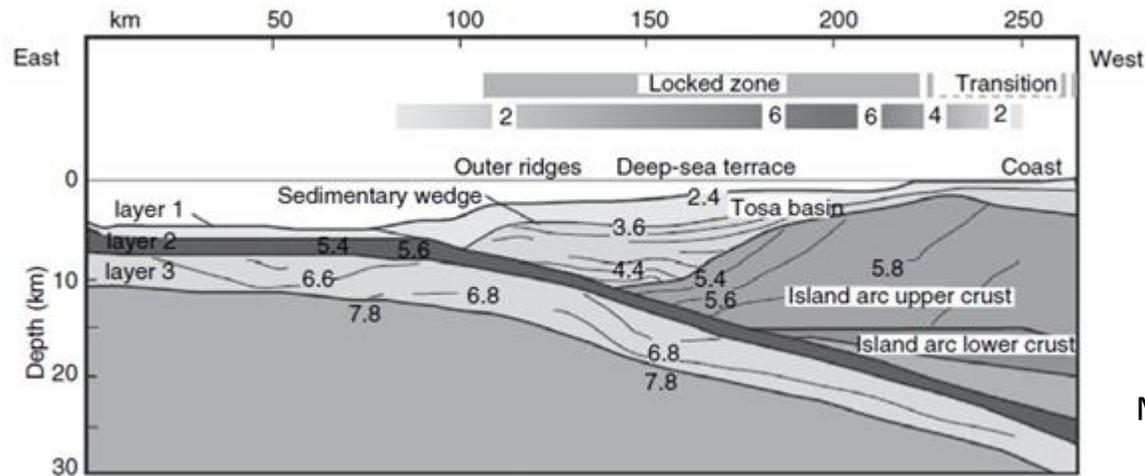
Mooney, 2007

Oceanic–continent transition zone (Ghana, West Africa)
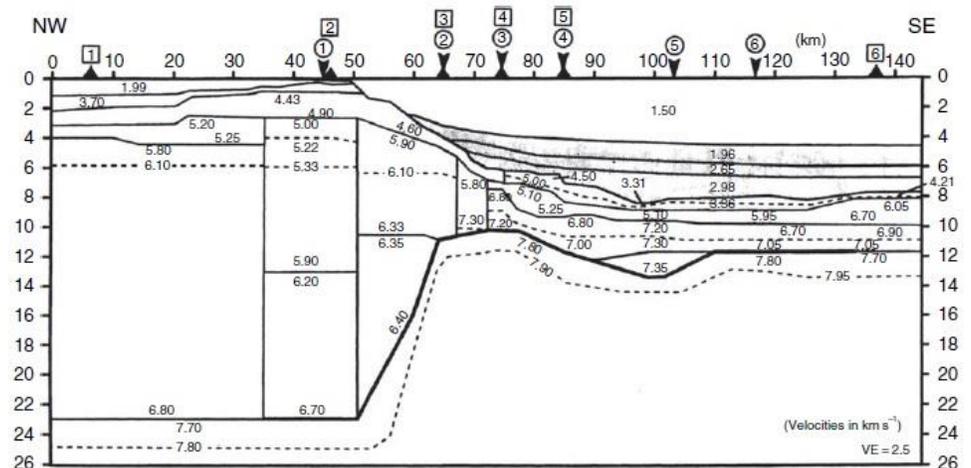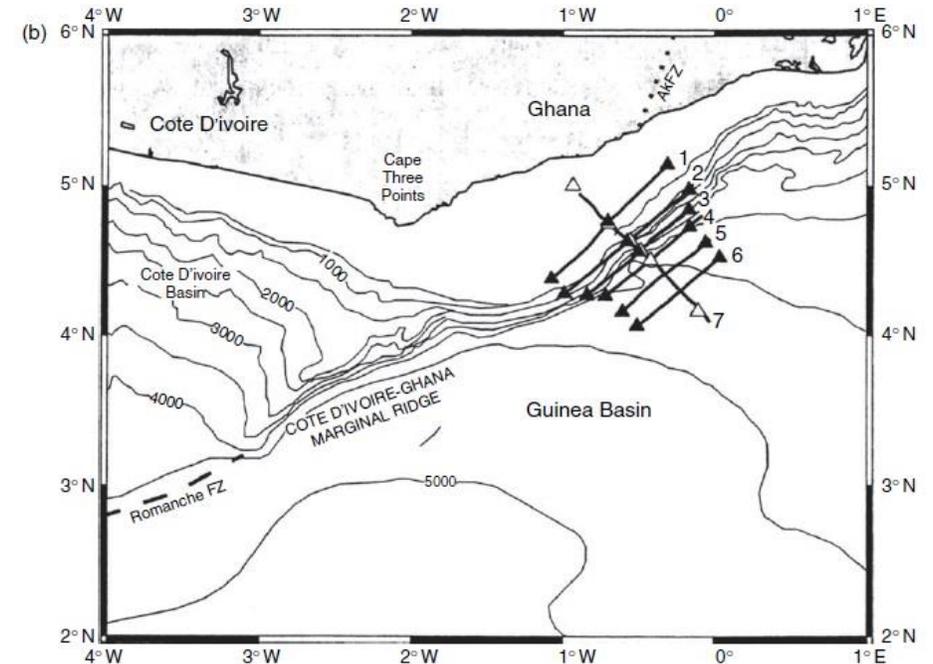
- The crustal structure in typical subduction-zone includes a prominent low-seismic-velocity sedimentary wedge and the higher velocity igneous crust of the island arc.
- The passive margin between continental and oceanic lithosphere is sometimes characterized by a sharp drop in elevation and 20–30 km of crustal thinning over horizontal distances less than 30km.

Mooney, 2007, Treatise of Geophysics, Vol. 1, 361-417

Basement age of continental crust

Mooney, 2007, Treatise of Geophysics, Vol. 1, 361-417

Continental crustal type

OCEANIC CRUST
0 - 20 Ma   20 - 65 Ma   > 65 Ma

GEOLOGIC PROVINCE
Shield
Platform
Orogen
Basin
Large Igneous Province
Extended Crust

U.S. Geological Survey
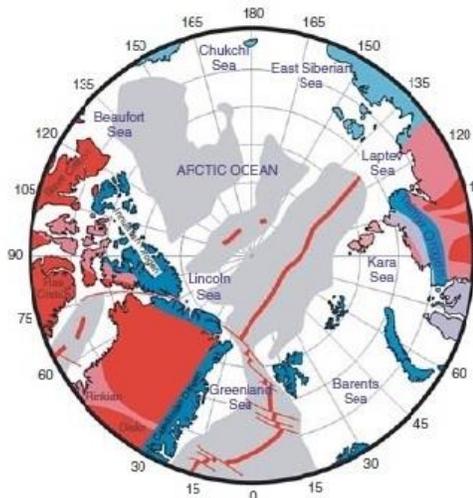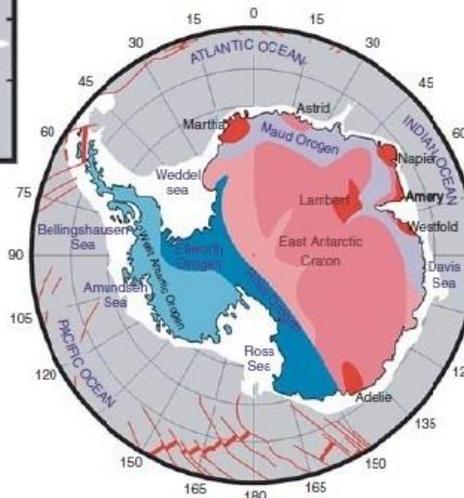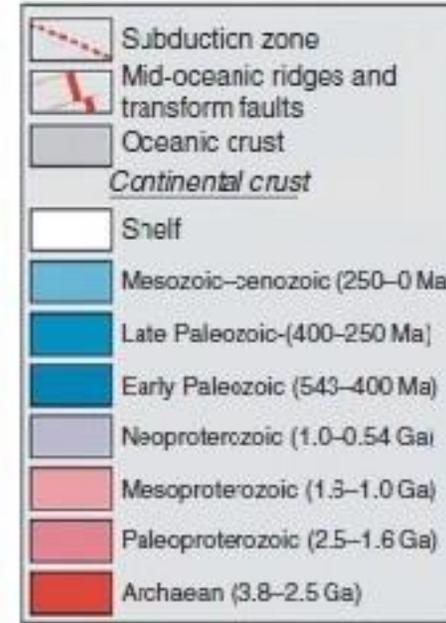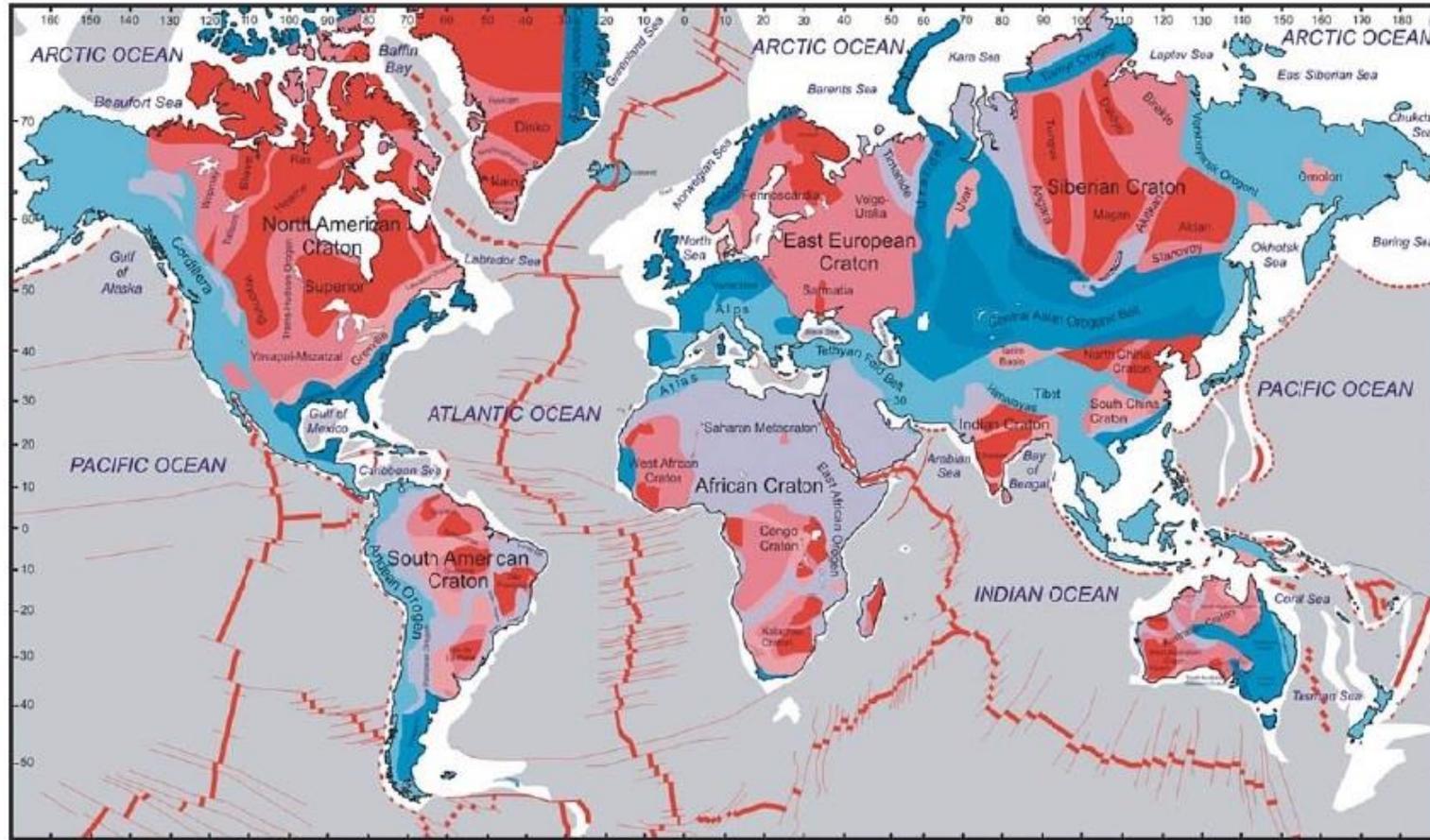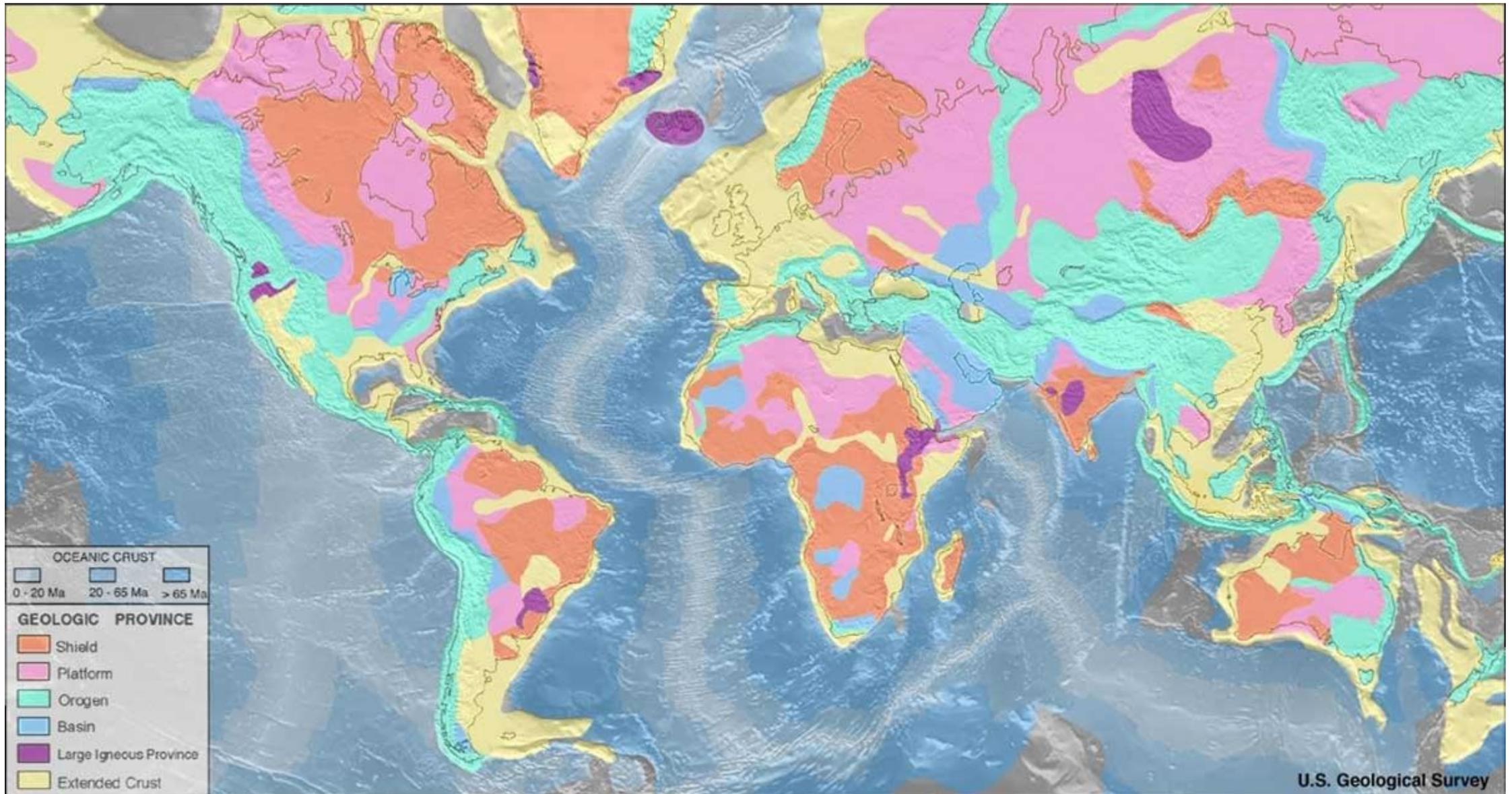
Continental and Oceanic crustal type

The Earth's crust constitutes about 0.7% of the total mass of the crust–mantle system
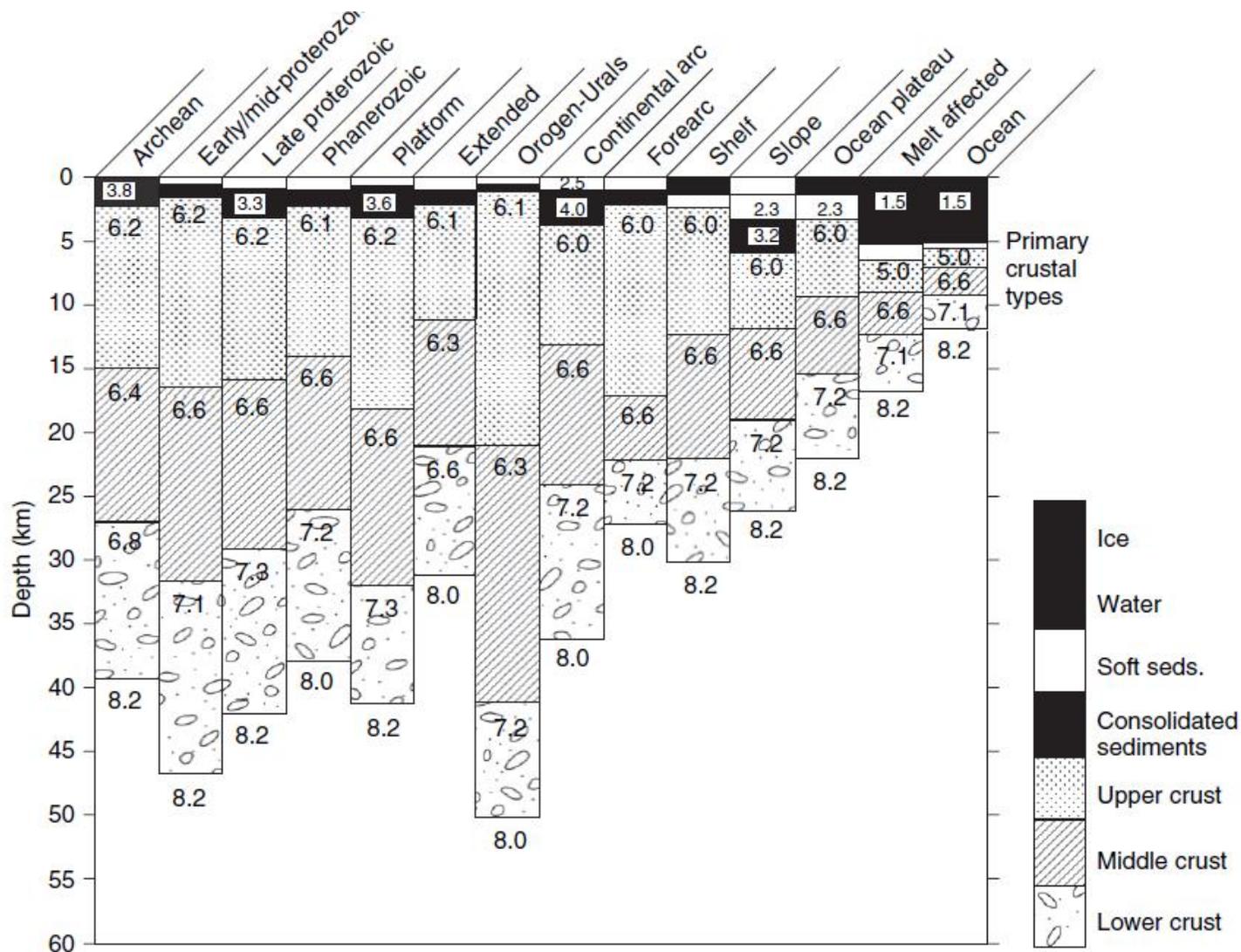
Proportion of continental crustal types:

69% shield and platform (cratons)
15% old and young orogens
9% extended crust
6% magmatic arc
1% rift

Continental crust (weighted average values):
Thickness = 41 km (SD=6.2 km)
$Vp=6.45$ km s^{-1} (SD=0.21 km/s)

Oceanic crust (average values):
Thickness = 7 km, $\rho=3$ g cm^{-3}, Age <=200 My

(Mooney et al., 1998)

Continental crust (average values):

Thickness = 39 km (range between 20 km and 80 km, 95% between 22 km and 56 km), Vp=6.45 km/s, ρ=2.84 g/cm^3, Age =1500 My

Worldwide Compilation
Average 39.17 km
Std. Dev. 8.52 km

Christensen and Mooney, 1995, JGR, 100

Worldwide Compilation
Average 6.45 km/s
Std. Dev. 0.23 km/s

Worldwide Compilation
Average 8.07 km/s
Std. Dev. 0.21 km/s
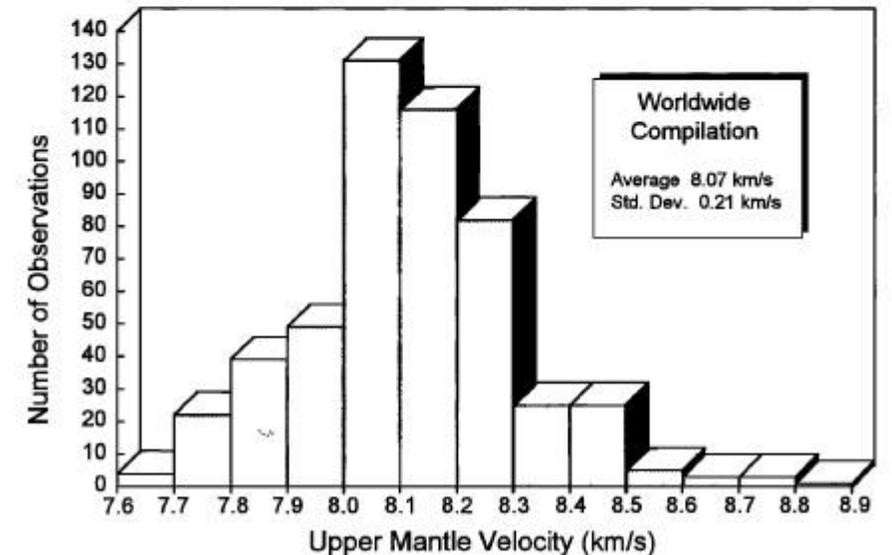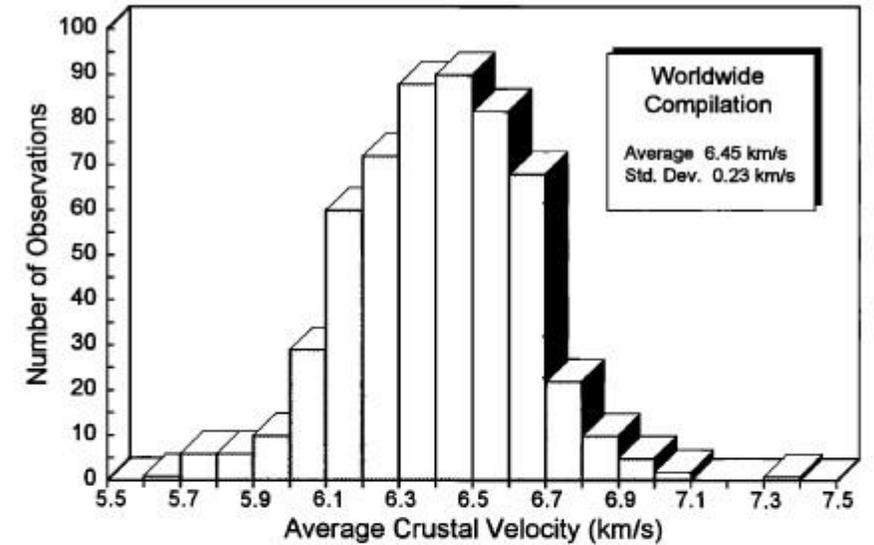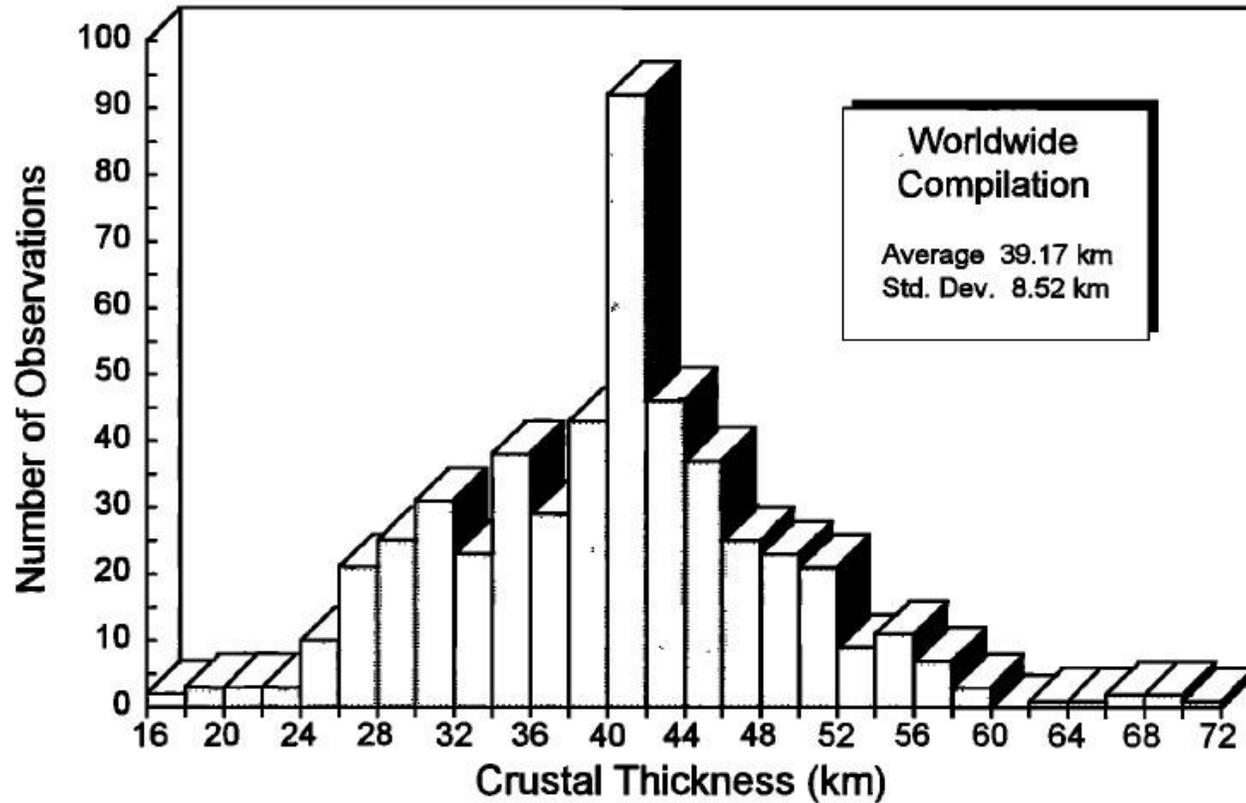
Crustal thickness distribution
(6 tectonic provinces)

World shields — No. of obs. — 249 data — Crustal thickness (km) (avg. 40.77, SD 7.04)

World orogens — No. of obs. — 352 data — Crustal thickness (km) (avg. 42.66, SD 10.56)

World platforms — No. of obs. — 445 data — Crustal thickness (km) (avg. 38.96, SD 7.03)

World forearcs — No. of obs. — 26 data — Crustal thickness (km) (avg. 26.78, SD 7.88)

World extended crust — No. of obs. — 266 data — Crustal thickness (km) (avg. 30.54, SD 6.03)

World arcs — No. of obs. — 29 data — Crustal thickness (km) (avg. 31.33, SD 8.27)

Table 3. Velocities and Crustal Thickness for Tectonic Provinces and Average Continental Crust

Crustal Property	Orogens	Shields and Platforms	Continental Arcs	Rifts	Extended Crust	Average* Crust
Vp at 5 km	5.69 ± 0.67	5.68 ± 0.81	5.80 ± 0.34	5.64 ± 0.64	5.59 ± 0.88	5.95 ± 0.73†
Vp at 10 km	6.06 ± 0.39	6.10 ± 0.40	6.17 ± 0.34	6.05 ± 0.18	6.02 ± 0.45	6.21 ± 0.27†
Vp at 15 km	6.22 ± 0.32	6.32 ± 0.26	6.38 ± 0.33	6.29 ± 0.19	6.31 ± 0.32	6.31 ± 0.27
Vp at 20 km	6.38 ± 0.34	6.48 ± 0.26	6.55 ± 0.28	6.51 ± 0.23	6.53 ± 0.34	6.47 ± 0.28
Vp at 25 km	6.53 ± 0.39	6.65 ± 0.27	6.69 ± 0.28	6.72 ± 0.35	6.69 ± 0.30	6.64 ± 0.29
Vp at 30 km	6.68 ± 0.43	6.80 ± 0.27	6.84 ± 0.30	6.94 ± 0.37	6.89 ± 0.40	6.78 ± 0.30
Vp at 35 km	6.81 ± 0.40	6.96 ± 0.30	6.99 ± 0.29	7.12 ± 0.33	6.93 ± 0.46	6.93 ± 0.32
Vp at 40 km	6.92 ± 0.44	7.11 ± 0.33	7.14 ± 0.25	7.12 ± 0.30	—	7.02 ± 0.32
Vp at 45 km	6.96 ± 0.43	7.22 ± 0.39	—	—	—	7.09 ± 0.35
Vp at 50 km	6.99 ± 0.52	—	—	—	—	7.14 ± 0.38
Crustal thickness	46.3 ± 9.5	41.5 ± 5.8	38.7 ± 9.6	36.2 ± 7.9	30.5 ± 5.3	41.0 ± 6.2
Average crustal velocity	6.39 ± 0.25	6.42 ± 0.20	6.44 ± 0.25	6.36 ± 0.23	6.21 ± 0.22	6.45 ± 0.21†
Pn velocity	8.01 ± 0.22	8.13 ± 0.19	7.95 ± 0.23	7.93 ± 0.15	8.02 ± 0.19	8.09 ± 0.20

Velocities in km/s and thickness in km.
*Weighted average (69% shields and platforms, 15% orogens, 9% extended crust, 6% continental arcs, 1% rifts).
†Sedimentary sections have been removed from upper 10 km.

Christensen and Mooney, 1995, JGR, 100

Seismic-depth measurements (1920-present)
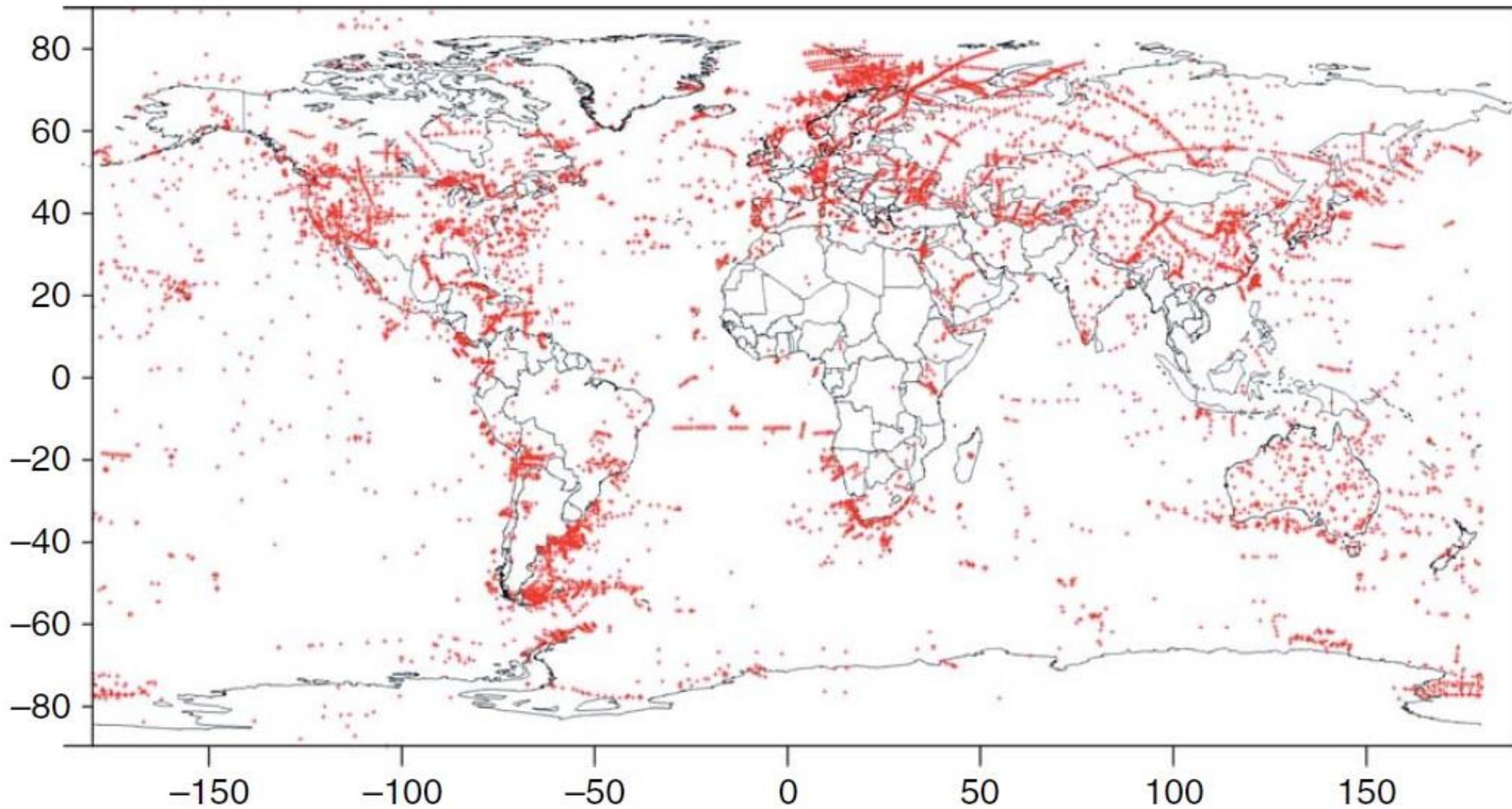
Moho depth

A compositional boundary formed during chemical differentiation within the lithosphere
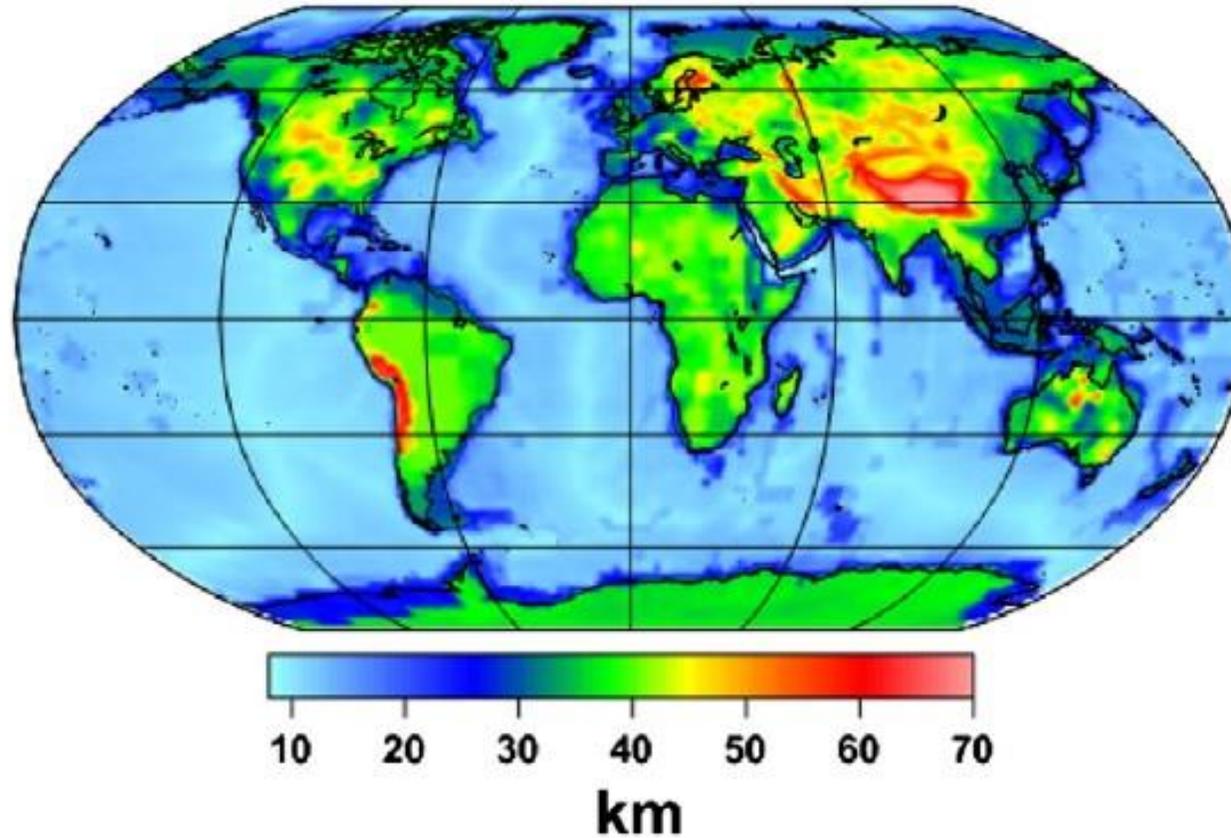
Tesauro et al., 2012, Global and Planetary Change, 90-91

Other Models

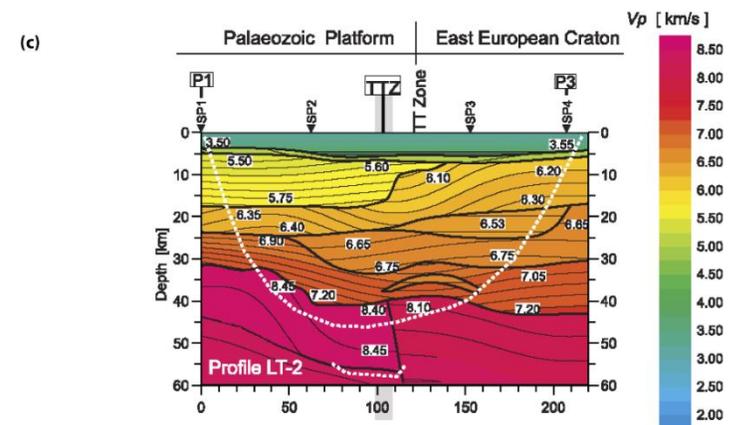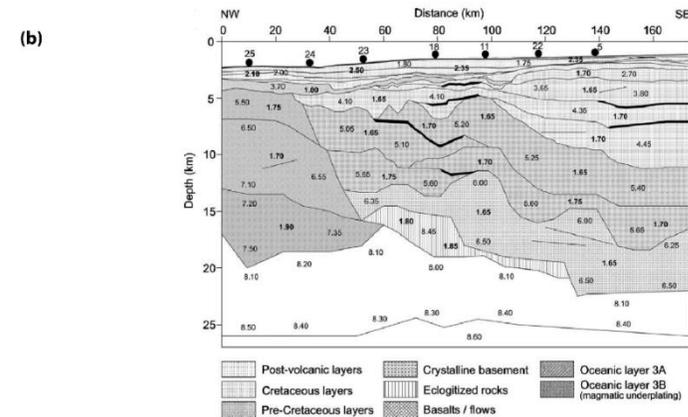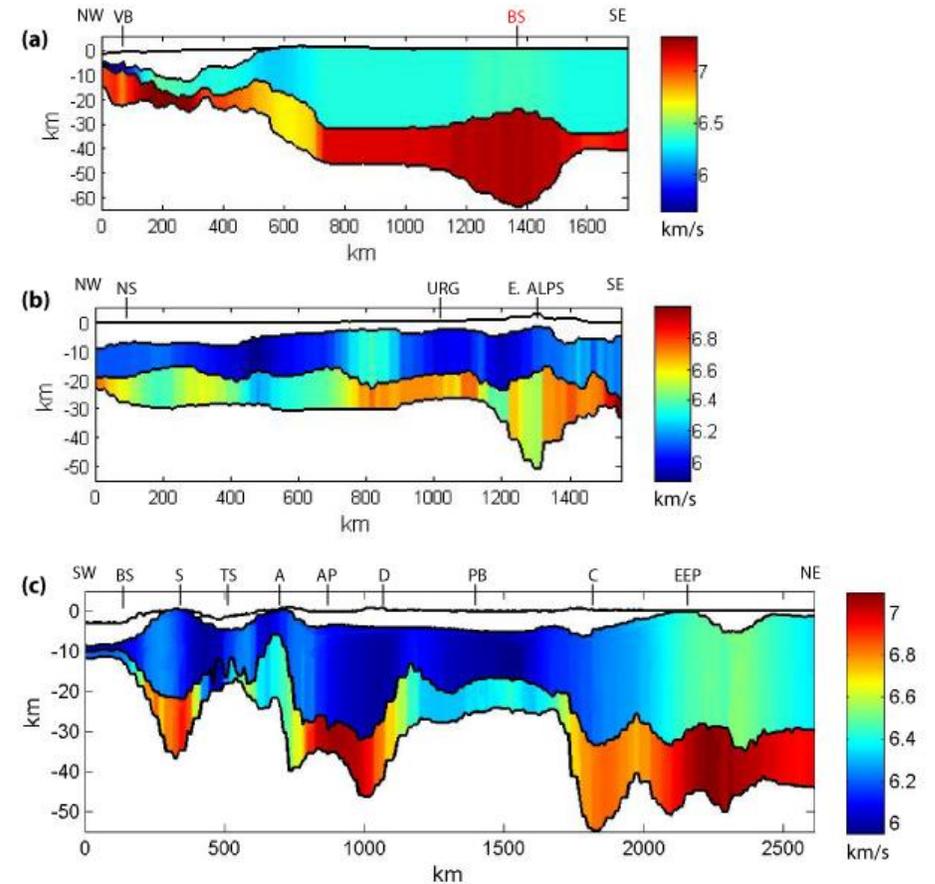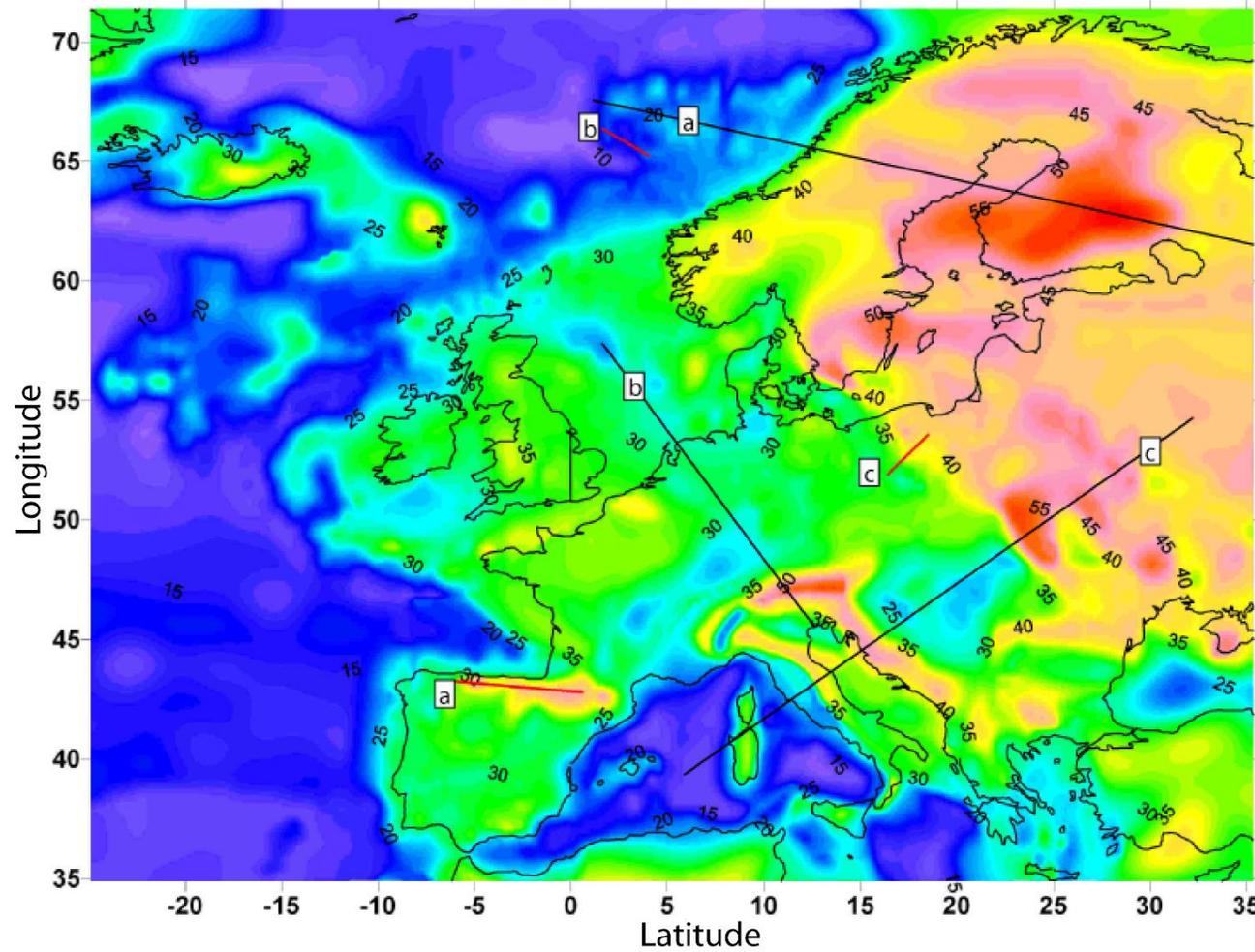CRUST 1.0: http://igppweb.ucsd.edu/~gabi/crust1.html (Laske et al., 2013)

Case Study: Europe
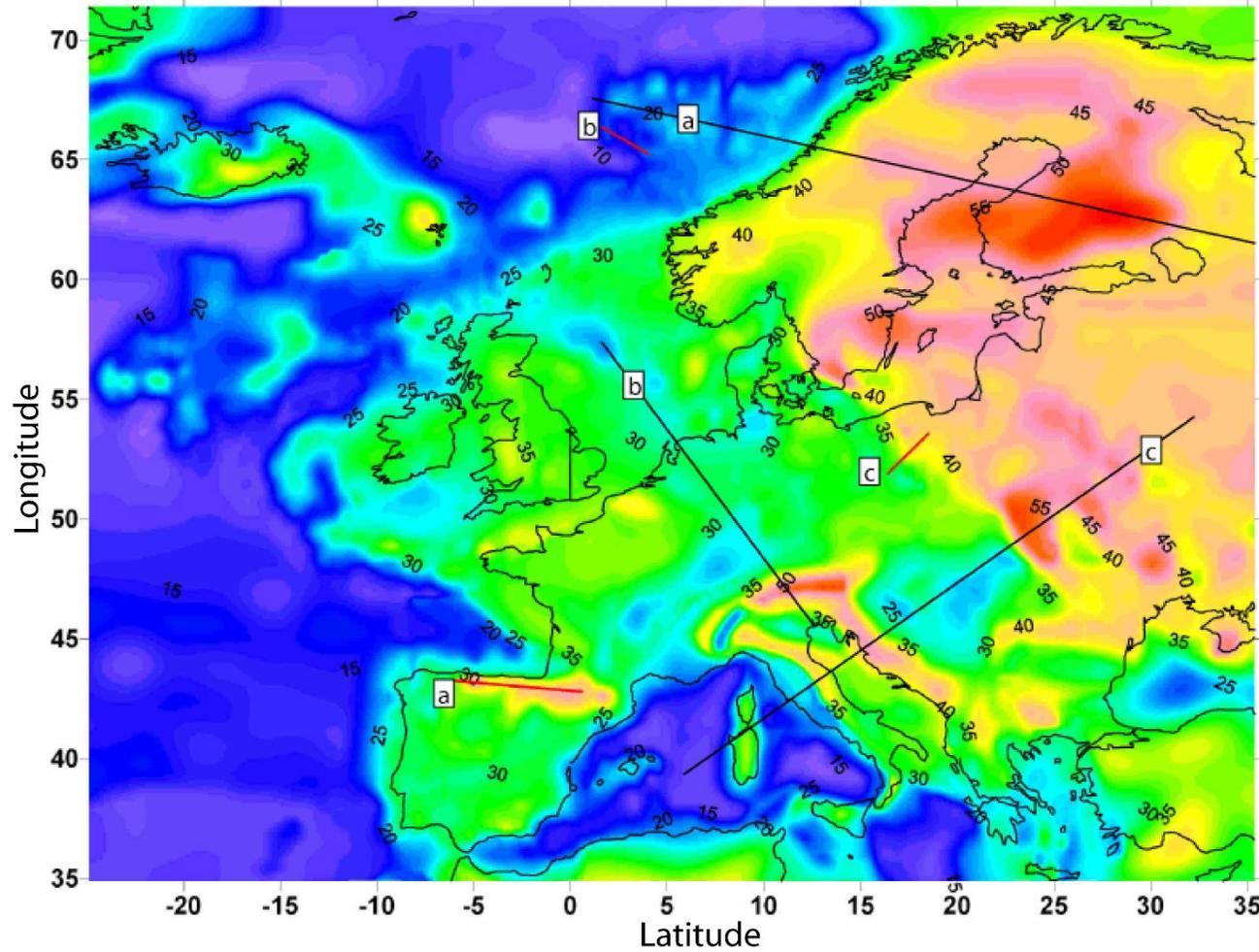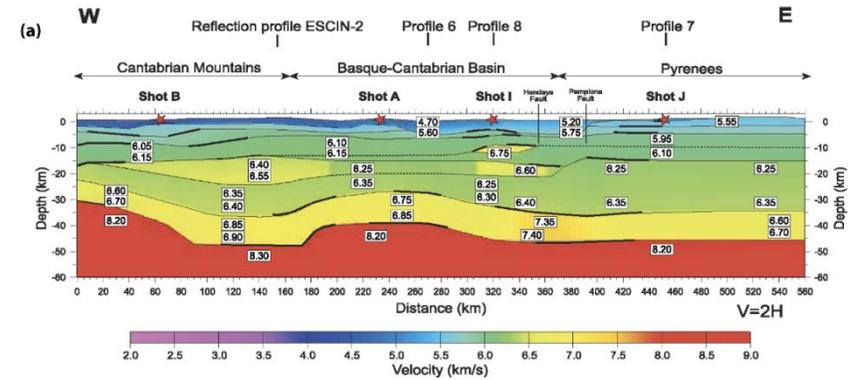
Crustal sections (a, b, c)

Moho depth

EuCrust07 (Tesauro et al., 2008, GRL)
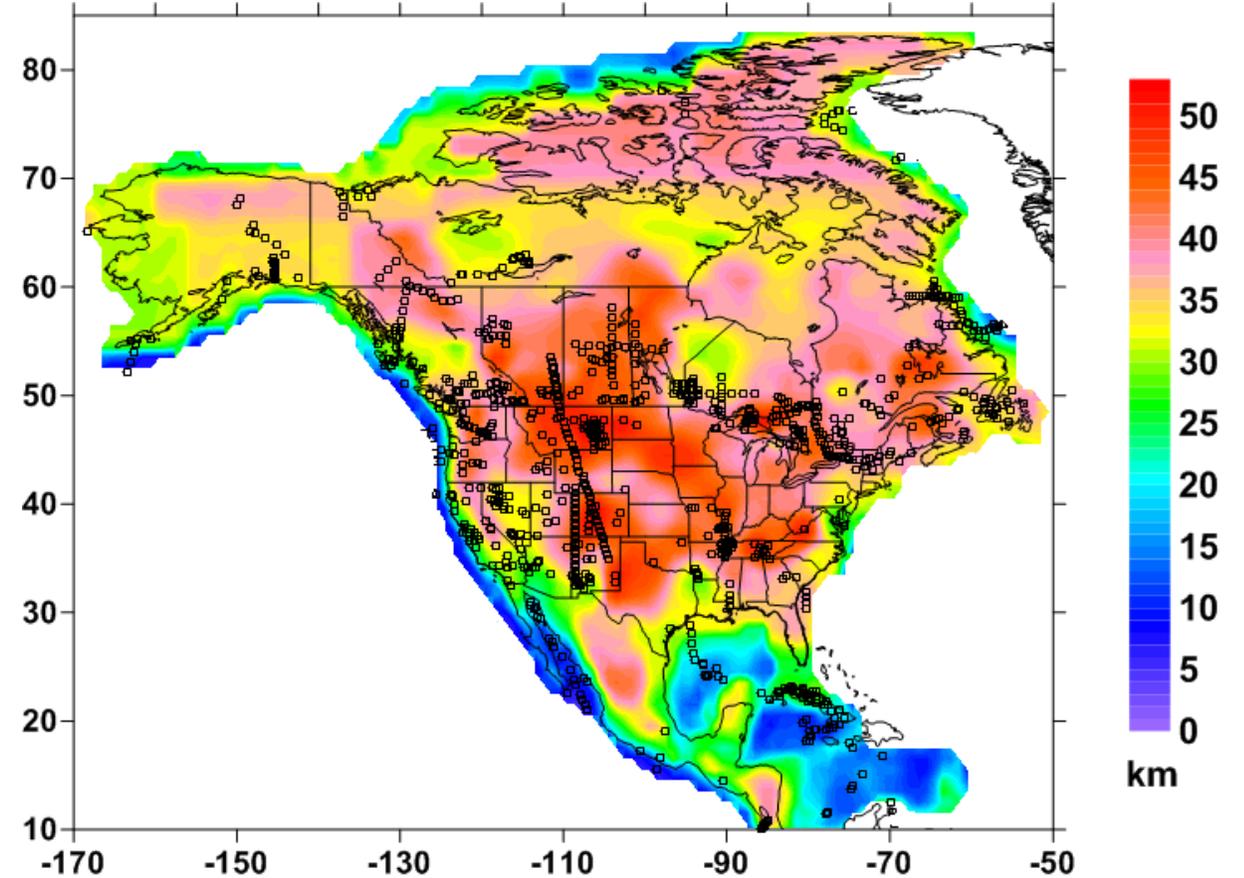
Case Study: Europe

Crustal sections (a, b, c)

Moho depth

EuCrust07 (Tesauro et al., 2008, GRL)

Case Study: North American continent

1. Depiction of the contours NA geological provinces

2. Selection and analysis of the seismic data
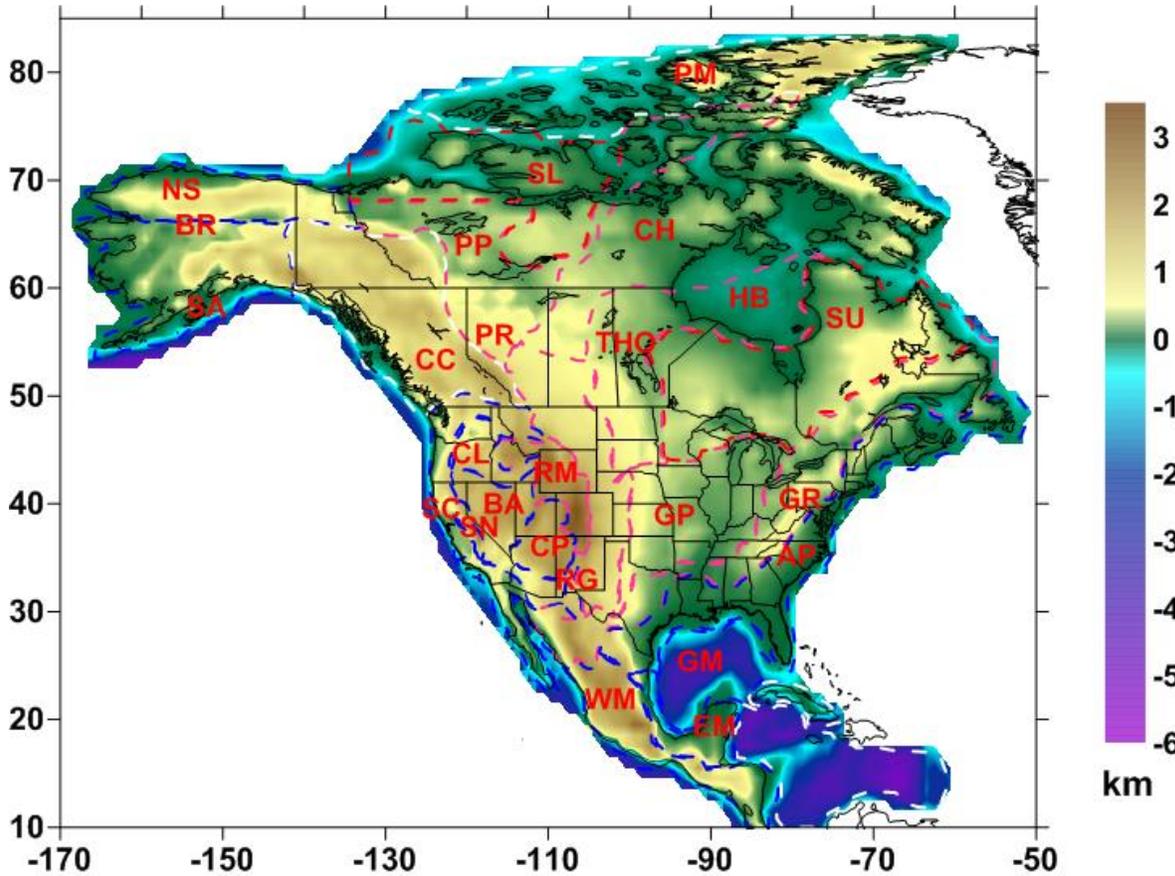
Topography, ETOPO2
(NOAA, 2010)

- - - - - **Archean**
- - - - - **Proterozoic**
- - - - - **Phanerozoic**

Crystalline crustal thickness
(Tesauro et al., 2014, Tectonophysics, 631)

AP, Appalachians; BA, Basin and Range; BR, Brooks Range; CC, Canadian Cordillera; CH, Churchill craton; CP, Colorado Plateau; CL, Columbia Plateau; EM, EasternMexico;GM, Gulf ofMexico; GP, Great Plain; GR, Grenville; HB, Hudson Basin; NS, North Slope; PM, Polar margin; PP, Paleoproterozoic platform; PR, Peace River arch; RG, Rio Grande rift; RM, Rocky Mountains; SA, Southern Alaska; SC, Southern Cordillera; SL, Slave craton; SN, Sierra Nevada; SR, Snake River Plain; SU, Superior craton; THO, Trans-Hudson Orogen; WB, Williston Basin; WM, Western Mexico.

Case Study: North American continent

2.   Selection and analysis of the seismic data

Crystalline Crust
usually composed of three layers
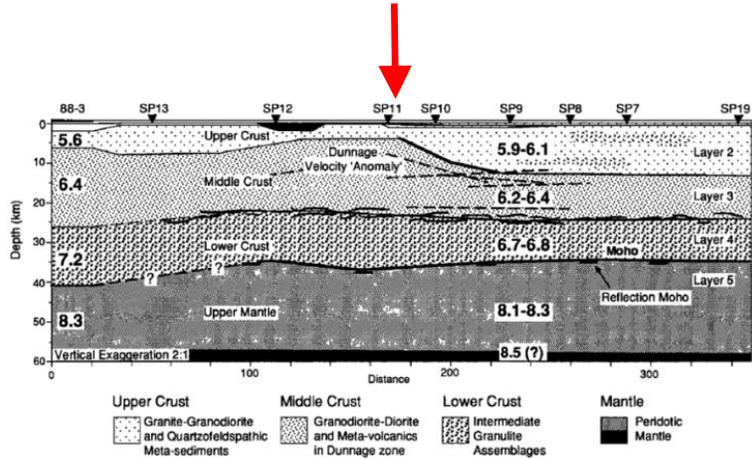
…or more

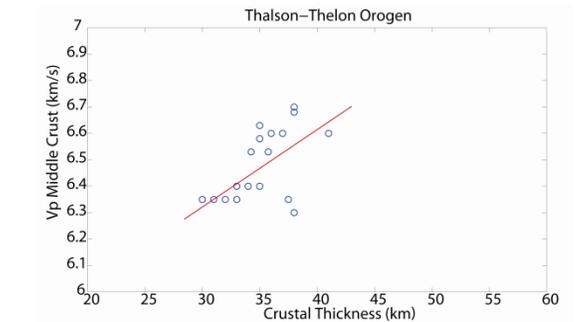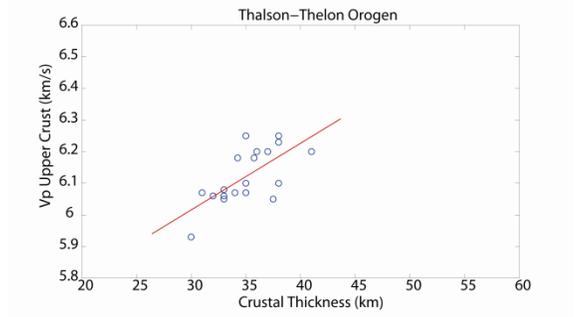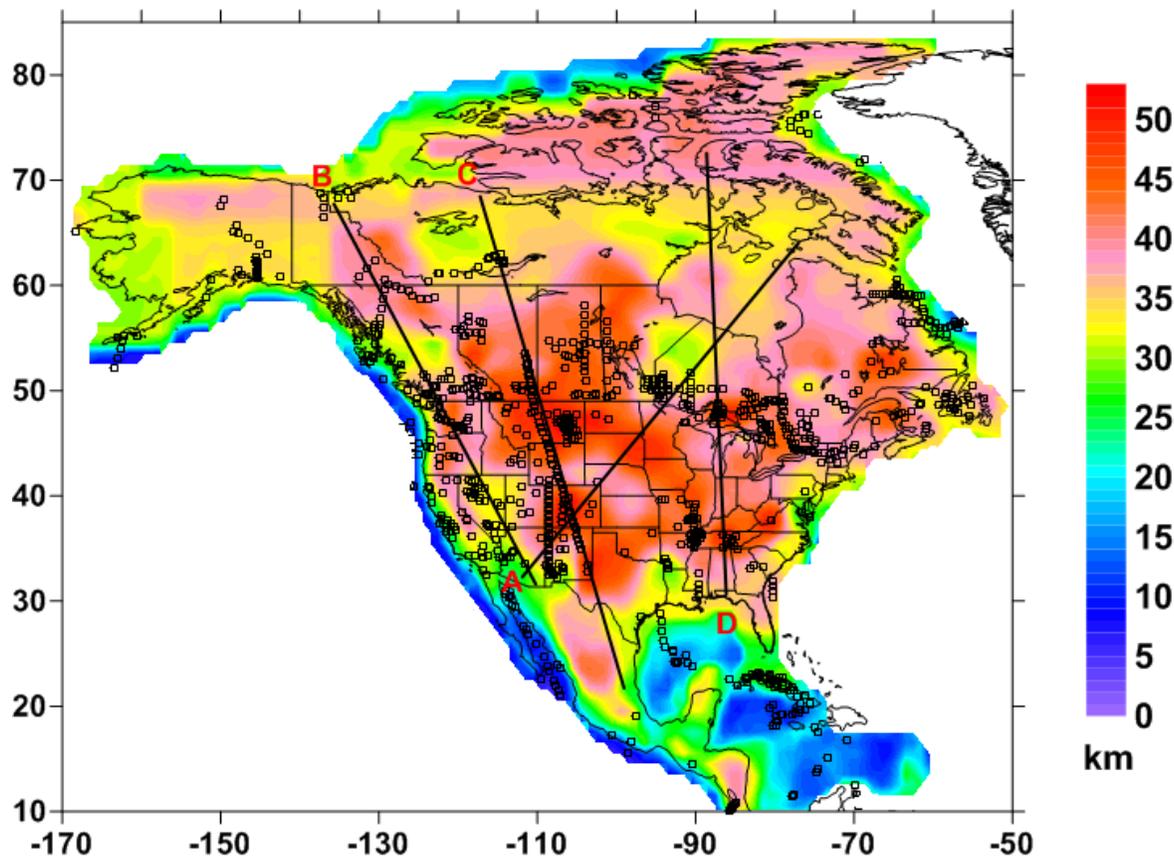Hughes and Hall (1994)
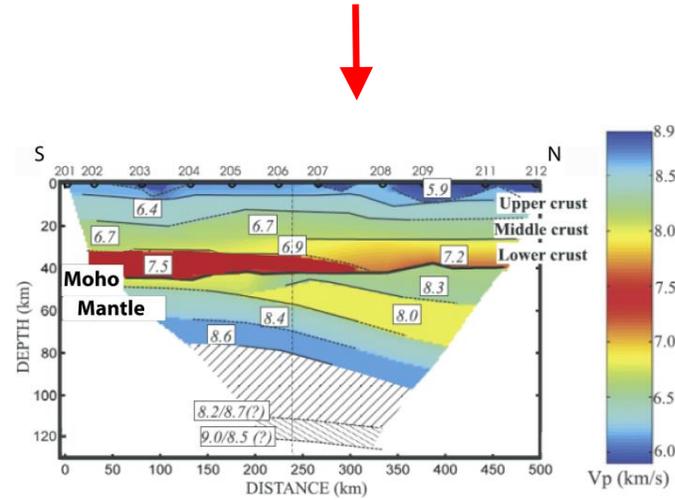
Musacchio et al. (2004)
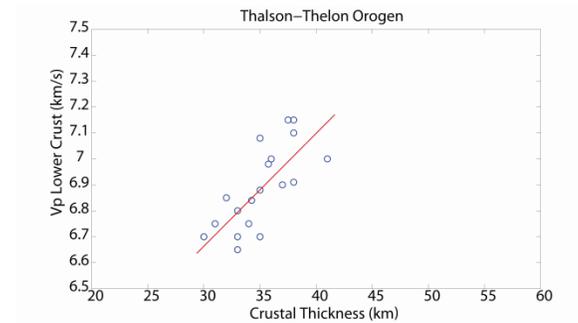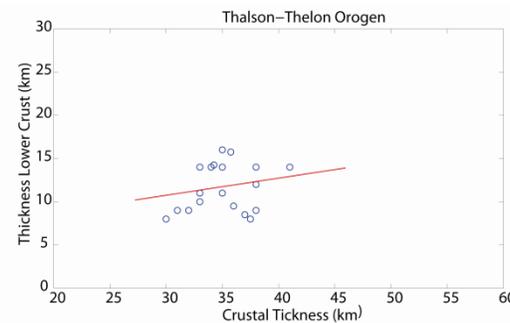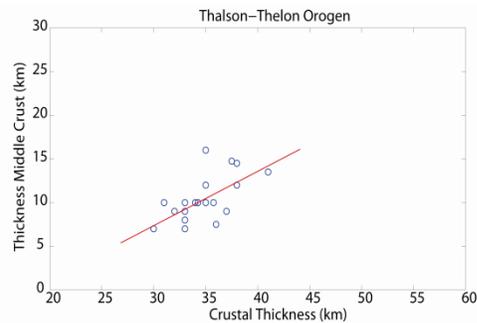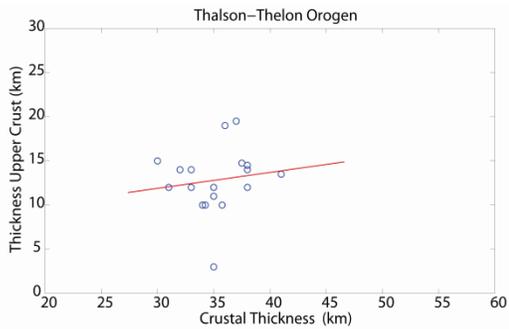
Positive correlation of velocity and thickness of the three layers with the thickness of the crystalline crust
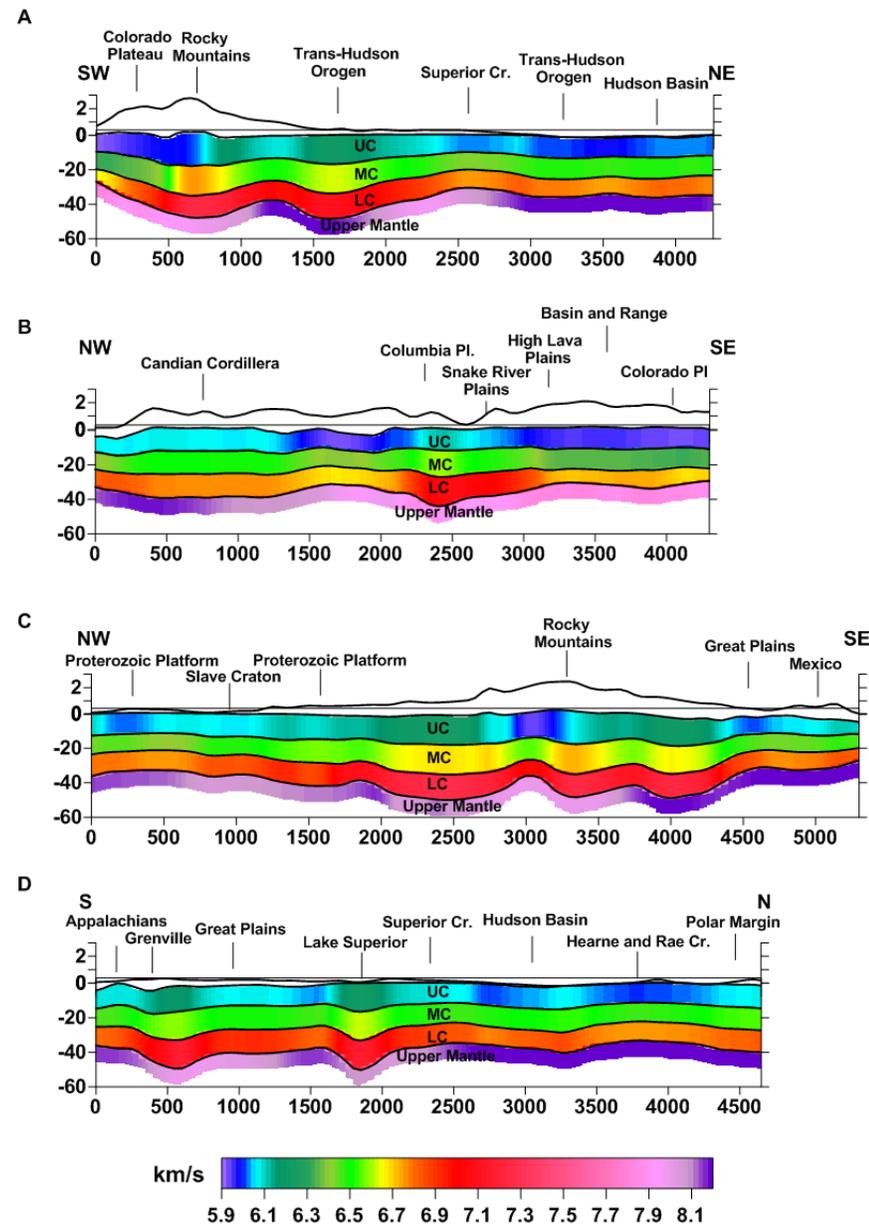(Tesauro et al., 2014, Tectonophysics, 631)

Case Study: North American continent
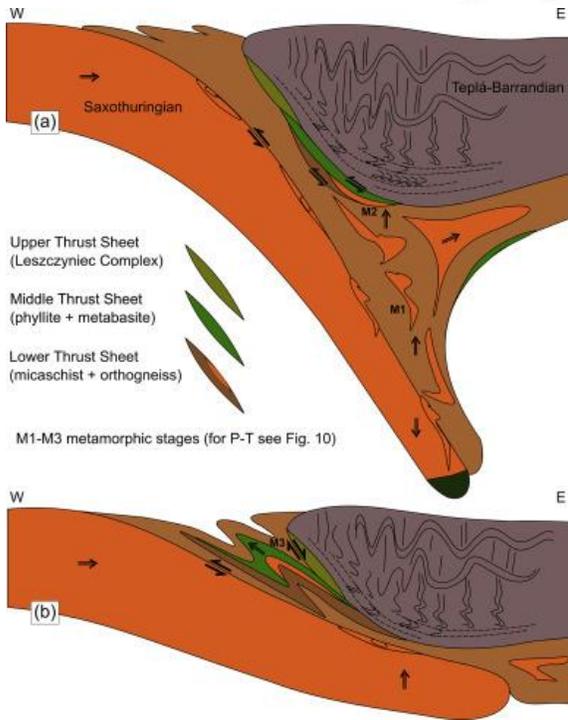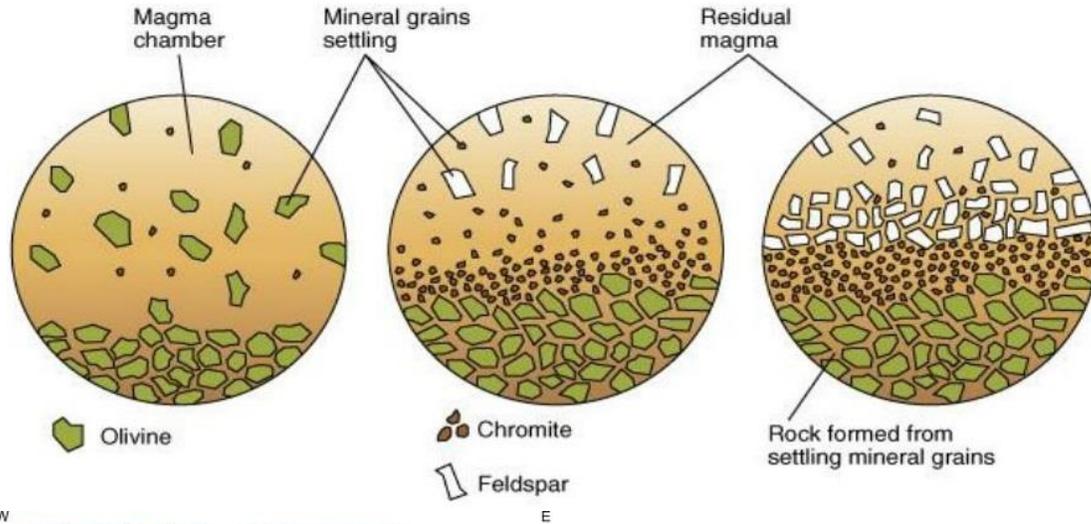
Crystalline crustal thickness

Crustal sections

Tesauro et al., 2014, Tectonophysics, 631
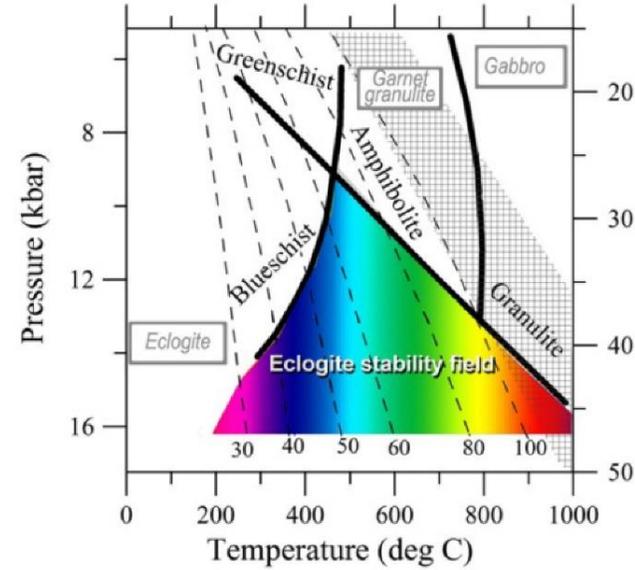
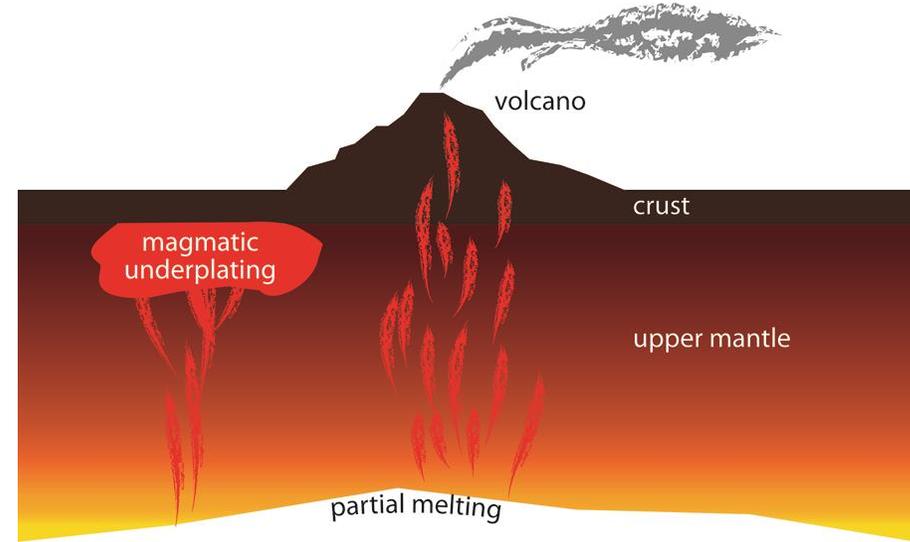# Origin of the lower crust high velocity layer (7x layer)

1. Magmatic Differentiation

Eclogite stability field

2. Eclogite formation

Eclogite:
Omphacite/Giadeite (CPX) +Garnet

3. Mechanical underplating
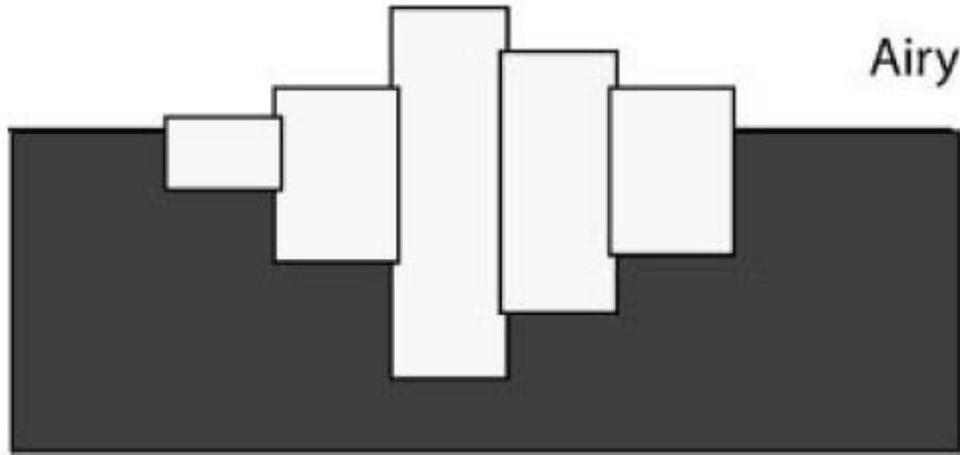

4. Magmatic underplating

Isostasy

The crustal heterogeneity in terms of thickness and density produces variation in the Earth's gravitational field over broad regions: Bouguer anomalies are generally negative over elevated continental areas (deficit of mass) and positive over ocean basins (excess of mass).
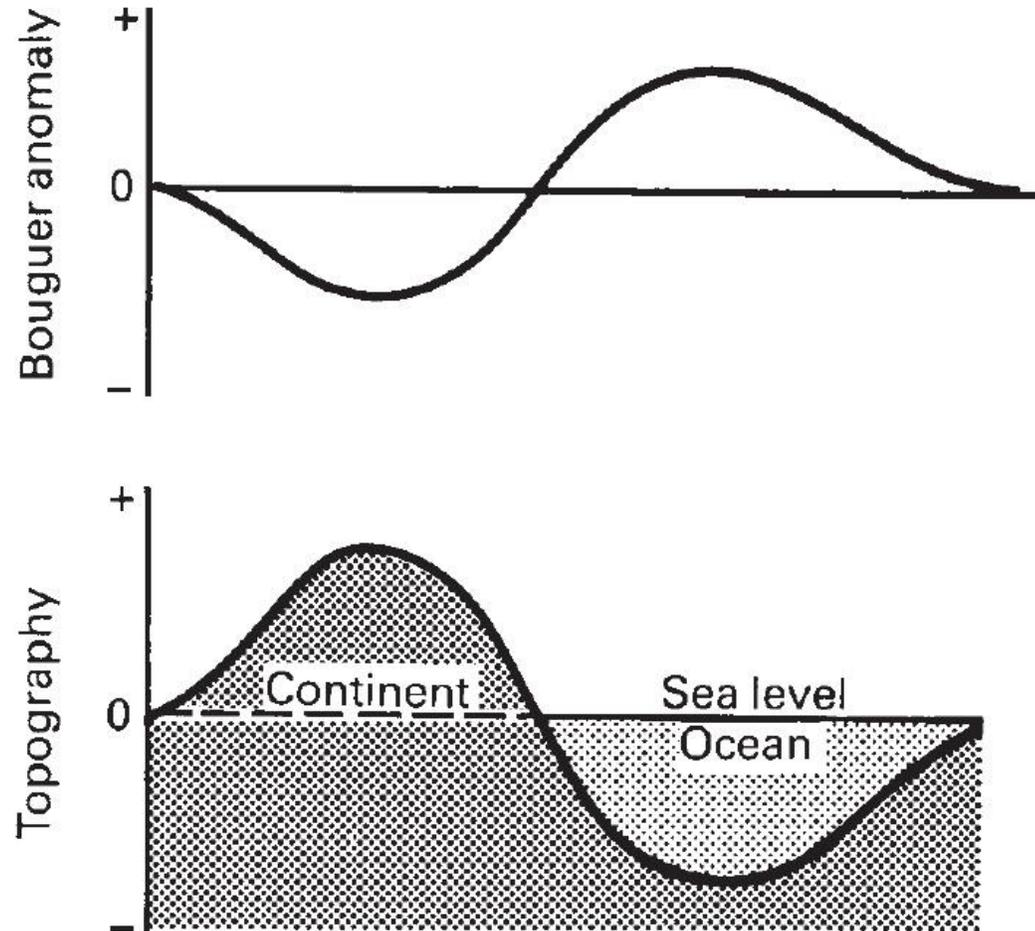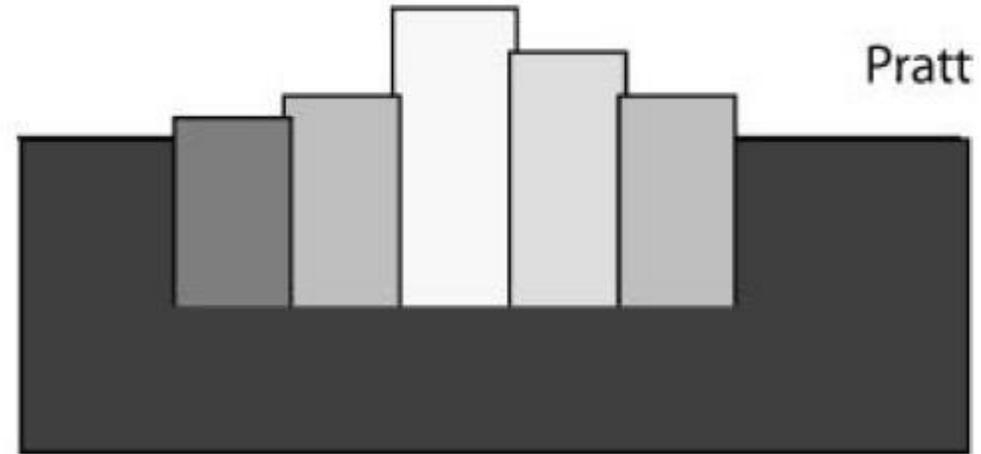
Isostasy

Isostatic compensation depth

Airy: Crustal density is roughly equal, compenstation is due to crustal roots (high topography compensated by thick crustal roots, low topography compensated by thin crustal roots).

Pratt: Continental crust extends to a common depth, while the density is variable (high topography compensated by low density and low topography compensated by high density).

Gravimetric data show that many orogens are not in isostatic equilibrium, but their topography is dynamically supported
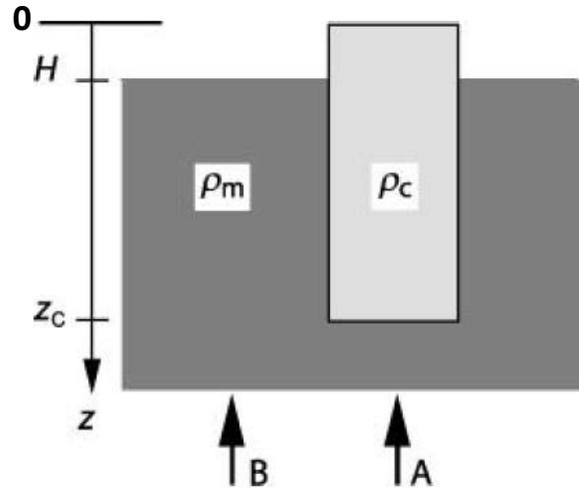
Airy Isostasy

- **Airy isostatic model**: all vertical profiles through the lithosphere may be considered indipendently of each other (shear stress are neglected). It is applicable only for features extended for few hundred km (hydrostatic isostasy).
- There is a depth (**isostatic compensation depth**) at which the vertical stresses of all vertical profiles are equal:

$\sigma_{zz}^{A}|_{z=z_{K}} = \sigma_{zz}^{B}|_{z=z_{K}}$ Downward force exerted by an entire vertical column:

$\int_{0}^{z_{K}} \rho_{A}(z)g dz = \int_{0}^{z_{K}} \rho_{B}(z)g dz$

Example:

$\rho_{c}gz|_{0}^{z_{c}} = g \int_{0}^{H_{mat}} \rho_{air} dz + g \int_{H_{mat}}^{z_{c}} \rho_{m} dz$ Since ρ_{air} is negligeble
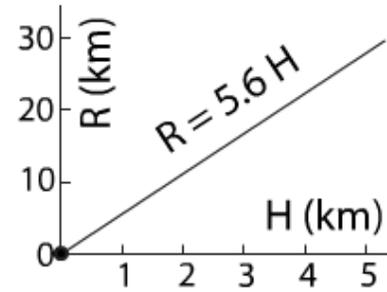
$\rho_{c}z_{c} = \rho_{m}z_{c} - \rho_{m}H_{mat}$ $H = H_{mat} = z_{c}\left(\dfrac{\rho_{m} - \rho_{c}}{\rho_{m}}\right)$

If $\rho_{c}=0$, H=z_{c}
If $\rho_{c}=\rho_{m}$, H=0

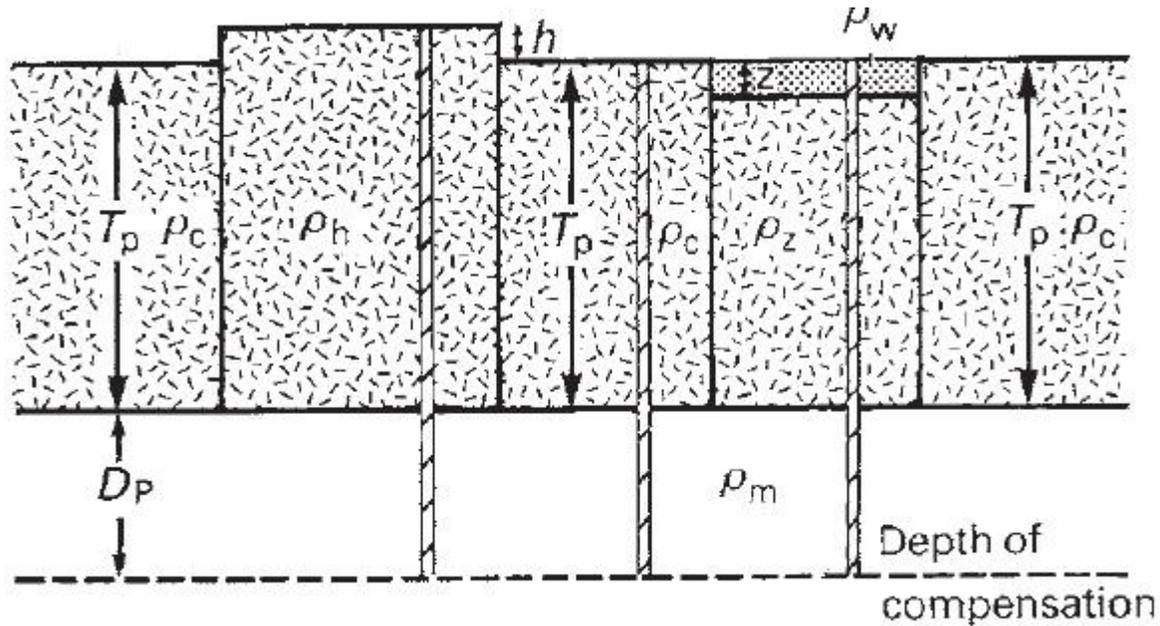# Airy Isostasy

Airy isostasy model for a thickening crust. The weight of Column 1, 2 and 3 are the same. Book Fig. 3.2.

Pratt Isostasy

According to Pratt's hypothesis, mountain ranges would be underlain by relatively low density material and ocean basins by relatively high density material:

Equating the weights of columns beneath a mountain range and a region of zero elevation we obtain:

$$g(T_p + h)\rho_h = gT_p\rho_c \quad \text{and} \quad \rho_h = \frac{T_p\rho_c}{(T_p + h)}$$

For oceanic basins:

$$\rho_z = \frac{(T_p\rho_c - z\rho_w)}{(T_p - z)}$$

References

Main Readings

Books:

- Fossen, Teyssier, 2024, Formation of Earth, Early Tectonics, and Continental Growth (Chapter 15), Plate Tectonics.
- Frisch, Meschede, Blakey, 2011, Early Precambrian plate tectonics, (Chapter 10), Plate Tectonics.
- Kearey, Klepeis, and Vine, 2015, The Interior of the Earth (Chapter 2), Global Tectonics.
- Kearey, Klepeis, and Vine, 2015, Precambrian tectonics and the supercontinent cycle (Chapter 11), Global Tectonics.
- Mooney, 2007, Crust and Lithospheric Structure – Global Crustal Structure, Treatise of Geophysics, Vol. 1, 361-417.

Articles:

- Cawood et al., 2022. Reviews of Geophysics, 60, e2022RG000789. https://doi.org/10.1029/2022RG000789.
- Christensen and Mooney, 1995. Seismic velocity structure and composition of the continental crust: A global view, JGR, 100, B7.
- Tesauro et al., 2008. EuCRUST-07: A new reference model for the European crust, GRL, Vol. 35.
- Tesauro et al., 2014. NACr14: A 3D model for the crustal structure of the North American Continent Tectonophysics, 631, 65-86.

Further Readings:

- Christensen, 1996, Poisson's ratio and crustal seismology JGR, 101, B2, 3139-3156.
- Darbyshire, 2000, Structure of the crust and uppermost mantle of Iceland from a combined seismic and gravity study, , EPSL, 181, 409-428.
- Darbyshire, et al., 1998, Crustal structure above the Iceland mantle plume imaged by the ICEMELT refraction profile, GJI, 135, 1131-1149.
- CRUST 1.0: http://igppweb.ucsd.edu/~gabi/crust1.html
- Rudnick and Gao, 2003, Composition of the continental Crust, Treatise on Geochemistry, vol. 3, pp. 1–64.
- Zhang et al., 2020, Crustal Composition and Moho Variations of the Central and Eastern United States: Improving Resolution and Geologic Interpretation of EarthScope USArray Seismic Images Using Gravity. JGR, 125, e2019JB018537.